

Measuring and Modelling the Dispersal of Pollen and Spores by Wind

Gail MacInnis

A Thesis

In the Department

of

Geography, Planning and Environment

Presented in Partial Fulfillment of the Requirements

For the Degree of

Master of Science (Geography, Planning and Environmental Studies)

At Concordia University

Montreal, Quebec, Canada

September 2012

© Gail MacInnis, 2012

CONCORDIA UNIVERSITY
School of Graduate Studies

This is to certify that the thesis prepared

By: Gail MacInnis

Entitled: Measuring and Modelling the Dispersal of Pollen and Spores by Wind

and submitted in partial fulfillment of the requirements for the degree of

Master of Science (Geography, Urban and Environmental Studies)

complies with the regulations of the University and meets the accepted standards with respect to originality and quality.

Signed by the final examining committee:

<hr/> Dr. Alan Nash	Chair
<hr/> Dr. Peter Kevan	Examiner
<hr/> Dr. Zavareh Kothavala	Examiner
<hr/> Dr. David Greene	Supervisor

Approved by: Dr. David Greene
Chair of Department or Graduate Program Director

Dr. Brian Lewis
Dean of Faculty of Arts and Science

Date: September 11, 2012

Abstract

Measuring and Modelling the Dispersal of Pollen and Spores by Wind

Gail MacInnis

Our present understanding of pollen dispersal by wind (anemophily) is quite limited. Due to the stochastic and complex nature of anemophily, modelling the dispersal patterns of the pollen and seeds of wind pollinated plants is not an easy task. The majority of the existing dispersal models are varied and have many conflicting predictions of pollen dispersal distances and concentrations from a source. These discrepancies between models reflect the lack of both short and long distance dispersal data, limiting the ability to seriously test the validity of these models. The main objective of this study was to measure ambient pollen concentrations of various tree and shrub species at both short and long distances from the source. A secondary objective was to measure the parameters involved in the dispersal process of anemophilous pollen and subsequently use these parameters and the empirical data collected to test the accuracy of three analytical mechanistic models of pollen and seed dispersal. The applications of such models are extensive; besides being of use to the allergy-suffering population, present-day issues such as climate change, pollen contamination in GMO crops, and landscape fragmentation raise concerns about whether plants will be able to adapt, disperse, and reproduce effectively in such rapidly changing environments.

Acknowledgements

First and foremost I thank my supervisor, Dr. David Greene, for guiding and supporting this project from beginning to end. I also thank Dr. Peter Kevan for his invaluable input and for providing us with the equipment required to complete this project.

Also to Nick and Kristina, without your hard work and help every day in the field, none of this would have been possible. I also thank Mr. Bob Hayes for providing us with extensive knowledge, supplies, maps, advice, laughs and rescues. Without him this project would most certainly be data-less and we would probably still be stranded in a leaky boat in the middle of the lake. Also to Kevin and Angie Wadelius, thank you for letting us take over your property, and for giving us a lake, a boat, a motor, and coffee every morning. Your kindness was above and beyond anything we could have expected. Also many thanks to Mike Paddock at the Pas office of Tolko Industries Inc, for providing detailed maps and information about the project site.

Contents

List of Figures	vii
List of Tables	xii
Chapter 1 Introduction	1
1.1 Research Objectives	5
Chapter 2 Literature Review - Anemophily	6
2.1 The Anemophilous Process	7
2.1.1 Pollen Production and Source Strength	7
2.1.2 Release Height	8
2.1.3 Pollen Abscission & Liberation	9
2.1.4 Terminal Velocity.	10
2.1.5 Wind Velocity and Direction	11
2.1.6 Deposition	12
2.2 Measuring Dispersal	13
2.3 Modelling Dispersal	16
2.3.1 Techniques	15
2.3.2 The Tilted Gaussian Plume Model	18
2.3.3 The Advection-Diffusion Model	20
2.3.4 The WALD Model	21
Chapter 3 Methodology	27
3.1 Area Source Experiment	27
3.1.1 Location and Field Methodology	27
3.1.2 Timing	31
3.2 Area Source Data Collection: Measuring Model Parameters	31
3.2.1 Estimating Release Height (x_r)	31
3.2.2 Estimating Source Strength (Q)	31
3.2.3 Wind Parameters	34
3.2.4 Horizontal Distance (x) – Rotorods	36
3.2.5 Terminal Velocity (v_t)	38
3.3 Point Source Experiment: <i>Lycopodium clavatum</i>	38

3.4 Using the Models	40
3.5 Statistical Methods & Sensitivity Analysis	43
Chapter 4 Results	44
4.1 General	44
4.2 Source Strength (Q) and Filtration Estimates	45
4.3 <i>Picea mariana</i>	46
4.4 <i>Abies balsamea</i>	53
4.5 <i>Pinus banksiana</i>	59
4.6 <i>Alnus rugosa</i>	65
4.7 <i>Lycopodium clavatum</i> (point source)	71
Chapter 5 Discussion	76
5.1 General	76
5.2 Model Performance – Area Source	76
5.2.1 The WALD Model	76
5.2.2 The Advection-Diffusion Model	77
5.2.3 The Tilted Gaussian Plume Model	78
5.3 Problems with Parameterizing Models for an Area Source	79
5.4 Model Performance - Point Source	82
5.5 Clumping	83
5.6 Filtration	84
5.7 Long-distance vs. Short-distance Dispersal	87
Chapter 6 Conclusion	89
References	90

List of figures

- Figure 2.1:** Percentage of ALS herbicide-resistant individuals in seed from non-resistant varieties in relation to distance from the source field. Samples pooled per field, with 63 fields sampled (Rieger et al. 2002) 14
- Figure 2.2:** (A) Schematic for Gaussian plume model, viewed from above. (B) Schematic for the tilted plume model. Here H denotes height of source, \bar{u} denotes mean wind speed, and W_s denotes settling velocity - Okubo & Levin (1989) 19
- Figure 2.3:** Measured (*circles*) and modeled (*lines*) kernels for the anemophilous seeds of *Cirsium dissectum* and *Hypochaeris radicata* as described in Soons et al. (2004). The solid line represents the fitted Wald analytical long-distance dispersal model obtained by first- and second-moment matching to the measured distances. The dashed lines represent the modeled kernels when release height and horizontal wind velocity are changed. Furthest measured data is at 100 m. (Katul, 2005) 23
- Figure 2.4** Wald analytical long-distance dispersal (solid lines), tilted Gaussian (dotted lines), advection-diffusion equation (dot-dashed lines), and the Gaussian plume (Dashed lines). Katul et al. (2005) 25
- Figure 3.1:** Rotorod raft design, modified from original image at: http://handbooks.btcv.org.uk/books/images/2467/11_8.jpg 27
- Figure 3.2** Transect and rotorod positions on (a) Clearwater and (b) Campbell Lake, Manitoba, Canada. 29
- Figure 3.3:** Sample species composition map at study site, alphanumeric coding indicates species type percentage composition of surrounding forest patches – e.g. BS6JP1TA3 = 60% black spruce, 10% jack pine and 30% trembling aspen. (Source: Tolko Industries Inc, 2010). 32
- Figure 3.4:** Forest composition for the province of Manitoba, a) by species b) by land use. The coniferous study species make up approximately 53% of the forest species in Manitoba – Black Spruce 29%, Jack Pine 21%, and Other Softwoods (Balsam Fir) 3%. *A. rugosa* was estimated to compose 10% of the Timber-unproductive land. (Source: Manitoba Conservation, 2001) 32
- Figure 3.5:** Wind rose depicting wind speed and directional profile for a typical sampling period. This particular example is for sampling period June 5 9:38am - 11:43am, Campbell lake site. Compiled using WRPLOT[®] 35

Figure 3.6: Study area (45.42 N, 74.62 W) and Rotorod arrangement for *Lycopodium* experiment. 38

Figure 3.7 Determining the contributing trees in the source forest using circular sector geometry (Weisstein, 2011). s is determined by using the standard deviation (σ_θ) of the recorded wind direction (θ) during the sampling period, R is the length of the contributing forest, d is the distance from each tree in the forest to the forest edge, $x+d$ is the distance from each tree to the Rotorod located at a distance x from the forest edge. The area-source program sums the theoretical pollen contributions from each tree located in the area encompassed by $\theta \pm \sigma_\theta$. 41

Figure 4.1: Observed (●) and Predicted grains/m³ for *Picea mariana*, $v_t=0.032\text{m/s}$, $h=7.84\text{m}$. Predictions based on the WALD(—) , advection-diffusion(– –) and tilted Gaussian plume(•••) models. 46

Figure 4.2: Linear regression of predicted versus observed pollen concentrations of *P. mariana*, with associated 95% confidence intervals. Predicted values based on a) WALD b) advection-diffusion c) tilted Gaussian plume models. 46

Figure 4.3: Observed *P. mariana* pollen concentrations from 0 to 10 km (●), and pollen concentrations as predicted by the WALD model. Predicted curves reflect the sensitivity analysis performed by modifying a) release height b) terminal velocity c) horizontal wind velocity d) variance in vertical wind velocity (turbulence). Solid line indicates average measured value (as used in Figure 4.1). 49

Figure 4.4: Observed *P. mariana* pollen concentrations from 0 to 10 km (●), and pollen concentrations as predicted by the Advection-Diffusion model. Predicted curves reflect the sensitivity analysis performed by modifying a) release height b) terminal velocity c) horizontal wind velocity. Solid line indicates average measured value (as used in Figure 4.1). 50

Figure 4.5: Observed *P. mariana* pollen concentrations from 0 to 10 km (●), and pollen concentrations as predicted by the tilted Gaussian plume model. Predicted curves reflect the sensitivity analysis performed by modifying a) release height b) terminal velocity c) horizontal wind velocity. Solid line indicates average measured value (as used in Figure 4.1). 51

Figure 4.6: Observed (●) and Predicted grains/m³ for *Abies balsamea*, $v_t=0.0984\text{m/s}$, $h=8.233\text{m}$. Predictions based on the WALD(—) , advection-diffusion(– –) and tilted Gaussian plume(•••) models. 52

Figure 4.7: Linear regression of predicted versus observed pollen concentrations of *A. balsamea*, with associated 95% confidence intervals. Predicted values based on a) WALD b) advection-diffusion c) tilted Gaussian plume models. 53

Figure 4.8: Observed *A. balsamea* pollen concentrations from 0 to 5 km (●), and pollen concentrations as predicted by the WALD model. Predicted curves reflect the sensitivity analysis performed by modifying a) release height b) terminal velocity c) horizontal wind velocity d) variance in vertical wind velocity (turbulence). Solid line indicates average measured value (as used in Figure 4.7). 55

Figure 4.9: Observed *A. balsamea* pollen concentrations from 0 to 5km (●), and pollen concentrations as predicted by the Advection-Diffusion model. Predicted curves reflect the sensitivity analysis performed by modifying a) release height b) terminal velocity c) horizontal wind velocity. Solid line indicates average measured value (as used in Figure 4.7). 57

Figure 4.10: Observed *A. balsamea* pollen concentrations from 0 to 5 km (●), and pollen concentrations as predicted by the tilted Gaussian plume model. Predicted curves reflect the sensitivity analysis performed by modifying a) release height b) terminal velocity c) horizontal wind velocity. Solid line indicates average measured value (as used in Figure 4.7). 58

Figure 4.11: Observed (●) and Predicted grains/m³ for *Pinus banksiana*, $v_t=0.0254\text{m/s}$, $h=7.23\text{m}$. Predictions based on the WALD(—) , advection-diffusion(– –) and tilted Gaussian plume(•••) models. 59

Figure 4.12: Linear regression of predicted versus observed pollen concentrations of *P. banksiana*, with associated 95% confidence intervals. Predicted values based on a) WALD b) advection-diffusion c) tilted Gaussian plume models. 59

Figure 4.13: Observed *P. banksiana* pollen concentrations from 0 to 10 km (●), and pollen concentrations as predicted by the WALD model. Predicted curves reflect the sensitivity analysis performed by modifying a) release height b) terminal velocity c) horizontal wind velocity d) variance in vertical wind velocity (turbulence). Solid line indicates average measured value (as used in Figure 4.12). 61

Figure 4.14: Observed *P. banksiana* pollen concentrations from 0 to 10 km (●), and pollen concentrations as predicted by the Advection-Diffusion model. Predicted curves reflect the sensitivity analysis performed by modifying a) release height b) terminal velocity c) horizontal wind velocity. Solid line indicates average measured value (as used in Figure 4.12). 62

Figure 4.15: Observed *P. banksiana* pollen concentrations from 0 to 10 km (●), and pollen concentrations as predicted by the tilted Gaussian plume model. Predicted curves reflect the sensitivity analysis performed by modifying a) release height b) terminal velocity c) horizontal wind velocity. Solid line indicates average measured value (as used in Figure 4.12). 64

Figure 4.16: Observed (●) and Predicted grains/m³ for *Alnus rugosa*, $v_t=0.0195\text{m/s}$, $h=3.86\text{m}$. Predictions based on the WALD(—), advection-diffusion(--) and tilted Gaussian plume(••) models 65

Figure 4.17: Linear regression of predicted versus observed pollen concentrations of *A. rugosa*, with associated 95% confidence intervals. Predicted values based on a) WALD b) advection-diffusion c) tilted Gaussian plume models. 65

Figure 4.18: Observed *A. rugosa* pollen concentrations from 0 to 2 km (●), and pollen concentrations as predicted by the WALD model. Predicted curves reflect the sensitivity analysis performed by modifying a) release height b) terminal velocity c) horizontal wind velocity d) variance in vertical wind velocity (turbulence). Solid line indicates average measured value (as used in Figure 4.17). 67

Figure 4.19: Observed *A. rugosa* pollen concentrations from 0 to 2 km (●), and pollen concentrations as predicted by the Advection-Diffusion model. Predicted curves reflect the sensitivity analysis performed by modifying a) release height b) terminal velocity c) horizontal wind velocity. Solid line indicates average measured value (as used in Figure 4.17). 68

Figure 4.20: Observed *A. rugosa* pollen concentrations from 0 to 2 km (●), and pollen concentrations as predicted by the tilted Gaussian plume model. Predicted curves reflect the sensitivity analysis performed by modifying a) release height b) terminal velocity c) horizontal wind velocity. Solid line indicates average measured value (as used in Figure 4.17). 69

Figure 4.21: Observed (●) and Predicted grains/m³ for *Lycopodium clavatum*, $v_t=0.0195\text{m/s}$, $h=2.0\text{m}$. Predictions based on the WALD(—), advection-diffusion(--) and tilted Gaussian plume(••) models. 70

Figure 4.22: Linear regression of predicted versus observed pollen concentrations of *L. clavatum*, with associated 95% confidence intervals. Predicted values based on a) WALD b) advection-diffusion c) tilted Gaussian plume models. 71

Figure 4.23: Observed *L. clavatum* pollen concentrations from 0 to 2 km (●), and pollen concentrations as predicted by the WALD model. Predicted curves reflect the sensitivity analysis performed by modifying a) release height b) terminal velocity c) horizontal wind velocity d) variance in vertical wind velocity (turbulence). Solid line indicates average measured value (as used in Figure 4.22). 72

Figure 4.24: Observed *L. clavatum* pollen concentrations from 0 to 2 km (●), and pollen concentrations as predicted by the Advection-Diffusion model. Predicted curves reflect the sensitivity analysis performed by modifying a) release height b) terminal velocity c) horizontal wind velocity d) variance in vertical wind velocity (turbulence). Solid line indicates average measured value (as used in Figure 4.22). 73

Figure 4.25: Observed *L. clavatum* pollen concentrations from 0 to 2 km (●), and pollen concentrations as predicted by the tilted Gaussian plume model. Predicted curves reflect the sensitivity analysis performed by modifying a) release height b) terminal velocity c) horizontal wind velocity d) variance in vertical wind velocity (turbulence). Solid line indicates average measured value (as used in Figure 4.22). 74

List of Tables

- Table 4.1:** Duration of pollen release for each study species, averaged horizontal wind speed (u), standard deviation in vertical velocity wind component (σ_w), and the average variation in the wind direction (σ_θ), over the 30 selected samplings. 43
- Table 4.2:** Average of field-measured (with the exception of v_t) parameters required for model testing. Measured distance from lake shore (x), terminal velocity (v_t), average release height (x_r), observed concentration at $x=15\text{m}$ (N_{shore}), and estimated source strength in grains per m^3 (Q) needed for each model prediction to equal N_{shore} . v_t was averaged from the terminal velocities calculated by Williams et al. (2006) Jackson & Lyford (1999). 44
- Table 4.3:** Concentration of pollen measured on the shore (N_{shore}) at 15 metres from the edge of the forest, original source strength (Q_i) required to attain this shore concentration, and the modified source strength (Q_f) accounting for the average 7 day pollination dispersal period and the percentage occupied by each species in the source forest. Point-source Q estimate is based on the actual number of grains released. 45
- Table 4.4:** Statistical testing of *P. Mariana* with the three models. R^2 , slope (β) and y-intercept (α) of the associated best-fit line of the model predictions vs. observed concentration. 95% confidence intervals and the significance in the slope and y-intercept of the regression are also listed. 47
- Table 4.5:** Statistical testing of *A. balsamea* with the three models. R^2 , slope (β) and y-intercept (α) of the associated best-fit line of the model predictions vs. observed concentration. 95% confidence intervals and the significance in the slope and y-intercept of the regression are also listed. 53
- Table 4.6:** Statistical testing of *P.banksiana* with the three models. R^2 , slope (β) and y-intercept (α) of the associated best-fit line of the model predictions vs. observed concentration. 95% confidence intervals and the significance in the slope and y-intercept of the regression are also listed. 60
- Table 4.7:** Statistical testing of *A.rugosa* with the three models. R^2 , slope (β) and y-intercept (α) of the associated best-fit line of the model predictions vs. observed concentration. 95% confidence intervals and the significance in the slope and y-intercept of the regression are also listed. 66
- Table 4.8:** Statistical testing of *L.clavatum* with the three models. R^2 , slope (β) and y-intercept (α) of the associated best-fit line of the model predictions vs. observed concentration. 95% confidence intervals and the significance in the slope and y-intercept of the regression are also listed. 71

Measuring and Modelling the Dispersal Distances Pollen and Spores by Wind

1 Introduction

Wind pollination (anemophily) is a common means of sexual reproduction for many species. About 18% (Ackerman, 2000) of angiosperm species are wind pollinated and 51% of gymnosperms, including all conifers, are solely anemophilous, with a few species retaining some degree of entomophily (Proctor et al. 1996; Owens et al. 1998). It is also the most common syndrome of deciduous trees of temperate climates and almost all grasses, sedges and rushes. As the name suggests, it is the form of pollination whereby the wind is the vector that transports the male reproductive cells to the female cells. Pollen grains are carried by the wind until they settle to the ground or impact on a wet or sticky object, ideally near a receptive ovule.

Anemophily has evolved into a highly complex syndrome, with specific morphological traits which respond to particular sets of environmental conditions (Whitehead, 1983). Pollen shedding mechanisms are highly dependent on the temperature, relative humidity (RH), and amount of precipitation during the flowering period (Sarvas, 1962); high relative humidity can temporarily suppress abscission and release of pollen, and a moderate shower can result in the total elimination of pollen particles from the air (Whitehead, 1969). Dispersal distances are also greatly influenced by wind parameters like turbulence, speed, and direction (Di Giovanni & Kevan, 1991).

Information on the dispersal distances of pollen and spores, especially long-distance dispersal (LDD), has many significant applications. In the forestry sector,

understanding the effect of landscape fragmentation on breeding mechanisms is poorly understood (Greene & Johnson, 1995; Koenig & Ashley, 2003). However, the rapid decrease in pollen concentration with distance from the source requires that conspecifics must not be located too far from each other in order to reproduce (Whitehead, 1969). Therefore, landscape fragmentation can effectively increase isolation and hence the reproductive ability of trees. If conspecific plants are too far apart, wind velocity and turbulence may be insufficient to keep the pollen grains airborne long enough for them to travel the distance required to reach the female sites (megastrobili or stigmas) (Whitehead, 1983). The flowers and seeds of trees also play key roles in the life histories of many herbivores and their predators (Koenig & Ashley, 2003).

Good empirical data sets of dispersal distances adequately expressed in consensual models are also of great importance to modern day silviculture, agriculture, and health sciences. Presently, seed-source plantations are one of the primary strategies for the improvement of commercially valuable tree species as they provide the bulk of seeds used by nurseries for plantation stock. Pollen contamination by wild pollen into the selectively bred orchard plants is one of the most serious obstructions to the production of high-quality seeds (Di Giovanni & Kevan, 1991). Knowing more about dispersal patterns and LDD would allow for more efficient designs and locations of seed orchards to minimize contamination (Di Giovanni & Kevan, 1991). Similarly in agriculture, pollen contamination of traditional crops by adjacent genetically modified (GMO) crops and vice versa, is a major issue that has been addressed without well-tested models (Arritt et al. 2007).

More detailed knowledge of long-distance dispersal could also help the allergy suffering portion (typically 10%) of the population. A better understanding of pollen abscission and dispersal in relation to forecasted weather conditions would allow for far more precise predictions of pollen concentrations; thus anti-histamines, which have unpleasant side effects for many allergy sufferers, could be used more intelligently.

Furthermore, the distribution of fossilized pollen grains is one of the primary sources of information on past vegetation patterns and locations (Jackson & Lyford, 1999). A better understanding of pollen transport can lead to more precise reconstructions of past climates and past vegetation responses to climate change which could then be used to predict future vegetation and tree migration rates as a result of present-day climate change (Jackson & Lyford, 1999; Davis, 2000; Moen et al. 2004).

Modelling anemophilous dispersal patterns has been approached analytically and mechanically, using a variety of techniques, theories and parameters. However, the lack of both short- and long-distance dispersal data has limited the ability to seriously test these models. Thus, there are presently a large number of competing models, with often quite different predictions, making it very hard to decide which models are best. The majority of the existing models that predict pollen concentration declines with distance from the source are merely curve fitting exercises, with most dispersal curves following power law or negative exponential shapes (Okubo & Levin, 1989). Process-based models predict less sedimentation near the source, with a peak in concentration being reached some distance away from the source, due mostly to effects of release height (Okubo & Levin, 1989; Jackson & Lyford, 1999). The models differ especially in their treatment of the far tail; some models argue that updrafts cause pollen to be entrained into

areas of higher horizontal wind speeds, carrying the pollen great distances, sometimes on the order of several hundred to a thousand kilometres (Katul, et al. 2006). However, most often pollen concentration measurements are only made out to a few tens of meters from the source (Bateman, 1947; Sreemula & Ramalingam, 1961; Raynoor et al. 1970; Aylor, 1987; Bullock & Clark, 2000; Rieger et al. 2002; Jarosz et al. 2003, Tackenberg et al. 2003c). Very rarely has it been attempted to measure ambient pollen concentrations further than a hundred meters from a source (Andersen, 1991; Giddings et al. 1997; Nathan et al. 2001; Messeguer, 2003; Tackenberg et al. 2003a,b). Only two studies were able to be found where measured dispersal data exceeded a distance of 400 meters from a pollen source - Reiger et al.'s 2002 study, and Sharma & Khanduris 2007 study, both are discussed below.

The quantification of LDD is exceedingly difficult, so data on long-distance pollen (and seed) dispersal is severely limited (Cain et al. 2000, Nathan et al. 2003, Levin et al. 2003.) Due to the general inability to obtain data out to far distances, there are many models which use the few existing near-source datasets to predict dispersal out to further distances. Pollen concentration measurements at a range of source distances, coupled with meteorological and environmental measurements, are needed to validate the dispersal models already in existence (Kuparinen, 2006). The research described here assesses whether several existing models accurately depict pollen dispersal patterns from a source, both at near and far distances.

1.1 Research Objectives

The main goal of this project was to develop reliable data sets of pollen dispersal from 1 to 10,000 metres for a number of conifer, herb, and shrub species on the boreal plains of north-western Manitoba. This was accomplished by measuring pollen concentration levels and atmospheric data over long distances and time scales. The field data was then used to test the accuracy of Katul et al.'s (2005) WALD model of pollen and seed dispersal, and two other analytical mechanistic models: Okubo & Levin's (1989) Advection-Diffusion and tilted Gaussian models. The data collected could also be used to test any of the other existing models which utilize the parameters measured: pollen release height, three-dimensional wind velocities, source strength (pollen per m³), and pollen concentrations at numerous horizontal distances from the pollen source.

2 Literature Review - Anemophily

Anemophilous plants are frequently characterized by the vast production of small, dry pollen grains, which have low settling rates (Whitehead, 1983; Ackerman, 2000). Such pollen grains are often retained in the male strobili or anther until atmospheric conditions are suitable for optimal dispersal (Dafni et al., 2005). This is assumed to be an efficient strategy that has evolved as a response to environmental stimuli such as availability of potential animal pollinators, long term weather averages (especially RH), species diversity (and thus mean inter-mate distance), and vegetation structure (Whitehead, 1969). Anemophily is assumed to dominate in species-poor environments and in areas where the insect and animal populations are less abundant (Proctor et al. 1996). Generally, the percentage of trees (angiosperms included) pollinated by wind increases steadily from the equator toward the poles. By contrast, many shrub and herbaceous species are animal-pollinated, the major exception being grasses and sedges (Proctor et al. 1996; Owens et al. 1998; Whitehead, 1969). It has been suggested that the latitudinal patterns are the evolutionary result of (1) the high frequency of rainfall and high prevailing RH in the lower latitudes, and (2) the feeble wind speeds in the lower portion of forests dominated by herbs and shrubs (Whitehead, 1969; Niklas, 1985). A third possibility is that the main driver is species diversity; when diversity is high, and thus inter-mate distances are greater, perhaps wind pollination is too inefficient or unreliable relative to animal pollination. Although it has recently been postulated that wind may be important in bringing about pollination and increasing seed-set in some tropical species (Kevan 1993; Ashburn et al., 2001; Melendez et al. 2004).

2.1 The Anemophilous Process

The parameters to be included in any serious mechanistic model of the anemophilous process include: pollen abscission, source strength, distance, release height, wind velocity, atmospheric turbulence, terminal (settling) velocity, filtering rates, and aerodynamic properties of the pollen grains (Di Giovanni & Kevan, 1991; Dafni et al. 2005). I will discuss each in turn.

2.1.1 Pollen Production and Source Strength

Effective wind pollination for most species requires the copious production of pollen. The average pollen grain is about 65 μm in diameter (Niklas, 1985) and it has to reach a stigma or pollination droplet with an average diameter of about 200 μm (Owens et al. 1998), hence the probability of a lone pollen grain reaching an ovule is small. To compensate for that disadvantage, every square metre of the plants habitat must receive around a million pollen grains (Proctor et al. 1996). Faegri & van der Pijl (1979) cite pollen to ovule ratios of greater than 10^6 in various species of conifers, although on average (including many herbaceous angiosperm species) the ratio is less than 10^5 . However, some angiosperms such as *Ambrosia* have ratios greater than 10^{15} (Akerman, 2000). Katul et al. (2006) estimated that on average a *Pinus taeda* tree at 16 metres tall produces 113.9 grams of pollen over a 14-day period, amounting to about 113.4×10^6 pollen grains per tree per day. Using a tree density of a typical southern pine plantation, this rounds out to about 2×10^{11} grains per hectare per day (1750 trees per ha).

Pollen source strength is a measure of the amount of pollen produced per unit area and is typically calculated as the mean production of a plant multiplied by the number of such plants per area (Jackson & Wong, 1994).

2.1.2 Release Height

Many species of trees place the male organs high within the canopy. Likewise, herbaceous anemophiles in grasslands place the anthers high in the canopy (Burd & Allen, 1988; Whitehead, 1983). The height at which pollen is released has been shown to be an important determinant of the distance the abscised grain can travel (Burd & Allen, 1988; Okubo & Levin, 1989; Tackenburg et al. 2003a,b). This makes sense for several reasons; firstly, there is more time for the pollen to travel further horizontally before gravitational settling brings it to the ground (Niklas, 1985). Secondly, horizontal wind speeds and turbulence generally increase with increasing height. Third, the increase in turbulence also results in a decrease in the density of vegetation elements (leaves, shoots), and thus wind speeds are greater (less drag) and there is less of a chance for filtration of the pollen grains by leaves, etc (Burd & Allen, 1988). In regards to the dispersal curve, ground or near-ground level release of pollen will result in a dispersal curve that has a peak at the source and then falls off with distance (Aylor, 1989). By contrast, an elevated creates a gap between the source tree and the peak deposition point (Silen, 1962; Boyer, 1966; Raynor et al., 1975; Okubo & Levin, 1989; Nathan et al. 2005).

2.1.3 Pollen Abscission & Liberation

The abscission and subsequent liberation of these pollen grains from the anther depends on many parameters, the effects of which are still not fully understood. Pollen liberation has been shown to depend upon temperature, RH, precipitation, solar radiation, topography and wind direction and velocity (Hjelmroos, 1991). There is also an argument that there is a threshold wind velocity required for grains to be released, and below which, pollen fails to be entrained into the airflow (Greene & Johnson, 1989; Katul et al. 2005). Jackson & Lyford (1999) term this the ‘paradox of pollen liberation’ and quantify the threshold wind velocity with an equation depending on particle mass, radius, density, acceleration of gravity, the viscosity of air, and the orientation of the grain with respect to the contact surface. However, this theory remains experimentally unproven and there is actually very little known about the aerodynamics of abscission processes. Further studies of anther or microstrobilus morphology combined with meteorological data are needed to fully understand the conditions responsible for pollen release (Jackson & Lyford, 1999).

The timing of the release of pollen grains also plays an important role in dispersal distances and the ultimate fertilization of ovules. For some species, date and time of abscission can be predicted with a calendar (e.g. *Ambrosia*) or through monitoring atmospheric conditions and growing degree days (Di Giovanni *et al*, 1996). In order for thecae (pollen sacs) to open and release the pollen grains, conditions must be relatively dry, i.e. low RH (Jackson & Lyford, 1999; Niklas, 1985). Interestingly, on average the early afternoon, when RH is minimal, is also when horizontal wind speed, turbulence, and temperature are maximal (Whitehead, 1969; Hjelmroos, 1991; Jackson & Lyford,

1999; Ackerman, 2000; Greene et al. 2008;). Another way in which anemophilous species capitalize on periods of maximal wind speed is by having anthesis occur prior to leaf deployment in the spring in deciduous forests. About half of all anemophilous tree species produce pollen in the spring (Whitehead, 1969).

2.1.4 Terminal Velocity

Terminal velocity, also known as settling velocity, plays a major role in the distance a pollen grain travels. It is the downward movement of the grain in response to gravity; the denser the grain, the faster it falls, effectively decreasing the horizontal distance travelled. Therefore, the dispersal range of the pollen grains increases as the terminal settling velocity decreases (Niklas, 1985).

It has been shown that Stoke's law accurately determines the terminal velocity of pollen grains, having being verified by direct measurement of the rates of fall in long settling tubes (Di Giovanni et al. 1995). Vogel (1981) used Stoke's law to define terminal velocity (v_s) in terms of the size and density of a spherical particle:

$$v_s = \frac{2r^2g(\rho_o - \rho)}{9\mu} \quad (2.1)$$

where r is the radius of the particle, ρ_o is the particle density and ρ is the density of the fluid (for air = $1.27 \times 10^{-3} \text{g/cm}^3$), and μ is the viscosity of the fluid (for air at 18° C this is $1.8 \times 10^{-4} \text{g/cm/sec}$). For a non-spherical particle,

$$v_s = \frac{mg}{C_d\mu V^{1/3}} \quad (2.2)$$

where m is mass, g is the acceleration of gravity (981cm/sec^2), V is volume, and C_d is a dimensionless drag coefficient which changes depending on the shape and fall

orientation. Settling velocity decreases with decreasing particle size, mass, or density and irregularity of shape or deviation from spherical form (Jackson & Lyford, 1999). Settling velocities for pollen grains of a great variety of species have been calculated this way, yielding values comparable to measured terminal velocities found using fall chambers. A comprehensive list of terminal velocities as measured by various authors was compiled by Jackson & Lyford (1999), with species' mean values range from about 0.03 to 0.4 m s⁻¹.

There are some wind-pollinated plants in the families Pinaceae, Podocarpaceae, and Phyllocladaceae, which contain grains that have air-filled bladders called sacci. These sacci have been theorized to increase dispersal distance by increasing buoyancy and surface area of the grain (Schwendemann et al. 2007). Schwendemann et al.'s (2007) study of the dispersal differences between saccate and non-saccate pollen was the first of its kind to demonstrate that sacci do effectively decrease the settling velocity of most pollen grains which have them.

2.1.5 Wind Velocity and Direction

Atmospheric parameters such as turbulence, wind velocity and direction play a very important role in determining the dispersal of a pollen grain. Because the wind is the vector by which the pollen is transported, one would think the most influential parameter would be the horizontal wind velocity (Di Giovanni & Kevan, 1991). However, there have been few of studies done to try and quantify the correlation between distance travelled and horizontal wind velocity, and those that have focused on this topic have produced varying results. Greene & Johnson (1989) suggest horizontal wind speed

is a main controlling factor at short distances (say, within a distance equal to 5 release heights) but is much less important than updrafts at greater distances. Likewise, Tackenberg et al. (2003c) argued that, in open habitats, horizontal wind speed is much less important than updrafts for long-distance dispersal. Updrafts are so important because (1) they, in effect, extend the release height, and (2) they take the grain into the supra-canopy region where wind speeds and turbulence is much greater and filtration by vegetation elements is not possible (Bullock & Clark, 2000; Nathan *et al.* 2002a, b; Levin *et al.* 2003). Therefore, any study of long-distance dispersal must include a three-dimensional wind profile, and the variation in each of the horizontal, vertical and crosswind directions. That being said, there is almost no empirical work relating vertical turbulence to distance traveled or uplift; the majority of work is strictly in theoretical modelling (Portnoy & Wilson 1993; Tufto *et al.* 1997; Turchin, 1998). The measurement and modeling of dispersing pollen is discussed below.

2.1.6 Deposition

The last stage of the anemophilous process is the deposition of the pollen grain. Ideally this occurs on the stigmas of angiosperms or on the pollen drop at the base of the scale of megastrobili, but of course the vast majority of grains are deposited elsewhere.

Most pollen grains that are successfully entrained into turbulent airflows, tend to (1) settle to the ground, especially at night when wind speeds decline, (2) deposit on sticky or wet vegetation elements or spider webs, or (3) become absorbed within water drops (rain or fog or cloud) (Proctor *et al.* 1996; Jackson & Lyford, 1999). The

proportion of grains allocated to each of these preponderate ends is simply not understood.

Besides producing copious amounts of pollen, to compensate for the disadvantages of the stochastic nature of the environment, the male and female plant structures have evolved to increase the chance of fertilization. The pistils of wind pollinated angiosperms are often protruding beyond the corolla (ensemble of petals and sepals) to maximize exposure to wind flows. For conifers, female cones, the megastrobili, tend to be located towards the top of the tree, maximizing exposure to wind (Roussy & Kevan, 2000; Katul *et al.* 2005). Further, the pollination droplet is a small amount of liquid secreted by the cone at the base of each scale, which helps to trap pollen. (The drop evaporates after a few days leaving grains at the micropylar entrance to the ovule.)

Since the purpose of my study is to measure the distances of airborne pollen grains over lakes, there is more focus on the deposition of pollen grains onto the impaction samplers rather than on the effective deposition onto female reproductive structures.

2.2 Measuring Dispersal

Presently, most of the limited dispersal data available is focused on commercially important agricultural crops; field data regarding dispersal distances of wild plant pollen is almost non-existent. Studies like those done by Hoyle & Cresswell (2007), Aylor *et al.* (2003), and Timmons *et al.* (1995) focus on the distance genetically modified *Zea mays* and *Brassica napus* pollen can travel. This is because of the commercially important

issue of gene flow from the GM crops to non-GM crops. Even though the literature has been heavily focused on agricultural crops, those data sets are problematic as they do not often measure pollen concentrations further than 100 meters from the source fields.

There have been few attempts at measuring aerial pollen concentrations at long distances. The more common method is to use genetic markers to determine the paternal distance from the seed (Xie & Knowles, 1994; Schuster & Mitton 2000; Rieger et al.'s 2002). One of the most cited is the Rieger et al. (2002) study of canola (*Brassica napus*) dispersal, where dispersal distance was measured by tracking a herbicide resistant strain of canola over a very large area (one-third of Australia). The authors found that the use of such large pollen sources yielded a maximum dispersal distance of 3 kilometres from the source field, with no leptokurtic or exponential decline as is often seen in the common smaller-scale studies, see Figure 1.1 (Rieger et al. 2002). Notice that this study was not based on direct measurement of pollen. Notice also that the scatter in Figure 1 shows no distance decay relationship out to a distance of 3 km. In studies using genetic indicators, they are only sampling adult plants containing the gene of interest rather than pollen itself. Dispersal is thus defined on the basis of dispersal and establishment, instead of dispersal alone. It would be near impossible to measure the all potential parent plants within a 3 km radius to define a complete dispersal curve.

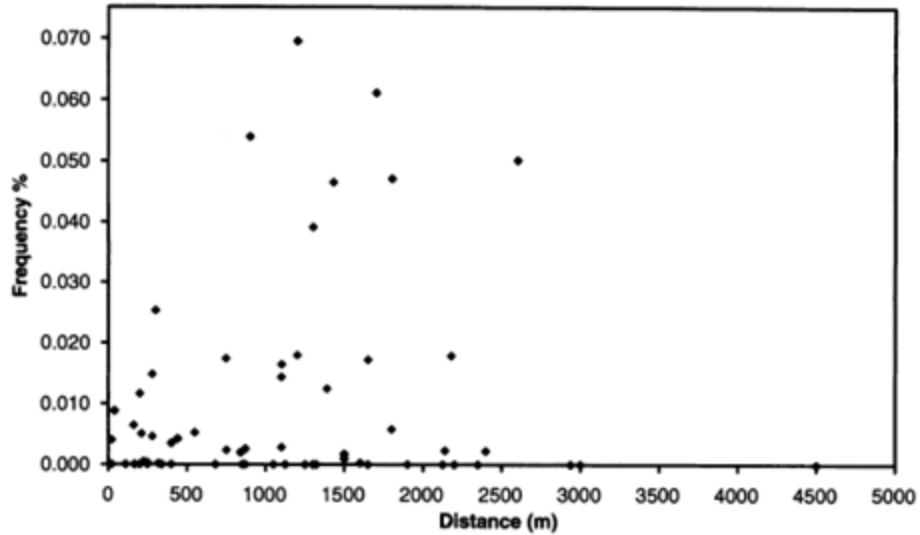


Figure 2.1: Percentage of ALS herbicide-resistant individuals in seed from non-resistant varieties in relation to distance from the source field. Samples pooled per field, with 63 fields sampled (Rieger *et al.* 2002).

The only other study I could find that measured actual ambient pollen concentrations was that of Sharma & Khanduri (2007). Pollen concentrations seem to be measured out to 2 km from the source, however the actual source distance is not clearly defined. The distance to the nearest conspecific forest is not listed and it is questionable whether or not the two singly isolated *P. roxburghii* trees were actually isolated.

The common conclusion in each of the studies cited above was that the results were highly variable. Undoubtedly much of the variability could be alleviated by more intensive sampling at each distance. Further, each of the studies expressed the critical need for large-scale studies where pollen concentrations are measured further away than the commonly used 100 meter distance, at a site where the source distance is known with absolute certainty. This is not an easy task, even with the problems associated with using a large body of water as a study site; this seems to be the only way to know the minimum source distance with absolute certainty.

The main problem with studying LDD for seeds is that there is no reasonable field method for collecting data at several kilometres from the source because the seed density would be so low that an inordinate amount of trap area would be required (Greene & Calogeropoulos, 2003). By contrast, there is still a great deal of pollen several kilometres from the source but its measurement requires specialized and expensive equipment. No one to date has had sufficient numbers of these devices to sample pollen at a large number of stations over several kilometres and thus delineate the full dispersal kernel. Where dispersal kernel refers to the probability density function of locating a pollen grain on the ground with respect to a point source at a given height (Katul et al., 2005).

2.3 Modelling Dispersal

2.3.1 Techniques

Modeling the path of pollen grains, seeds and spores from source to deposition site has been approached in a variety of ways. The processes involved in the dispersal of each of these diaspores are fundamentally the same: gravitational settling, advective motion by horizontal wind gusts and diffusion caused by turbulence (Andersen, 1991). The Gaussian plume and Advection-Diffusion approaches (discussed below) have been applied many times, but lack empirical validation over long distances. Both of these models along with the WALD model are tested with the empirical data obtained in this study. Another common technique used for developing dispersal curves has been empirical fits in the form of negative exponential or power law distributions (Okubo & Levin, 1989; Bullock & Clarke, 2000). However, this approach has been found to be less than accurate, especially so for LDD and even for some short-distance studies. This

technique provides no way of assessing inter-environmental extrapolation, and does not account for distributional peaks displaced at some distance from the source, which is commonly seen in the literature for elevated sources (Okubo & Levin, 1989; Nathan et al. 2002b, 2005). Bullock and Clark (2000), suggested that these techniques should be used in combination and proceeded to develop a mixed model, where short-distance (local) dispersal is represented by the negative exponential and LDD takes the form of a power law distribution. This is because LDD is often governed by extreme turbulence or wind conditions and should be described by different parameters than local dispersal. In any case, these are clearly non-mechanistic approaches.

Fully mechanistic models use probability distributions to describe particle density with distance, and can incorporate the many dispersal parameters which can be estimated independently of dispersal data. Mechanistic modelling attempts to also recognize the different atmospheric conditions required for short and long-distance dispersal events (Kuparenin, 2006). Nathan et al.'s (2002) model predicts a bimodal distribution, with near-source distances being controlled by within canopy airflow, and LDD being controlled by higher wind speeds and turbulence, rapidly increasing with height above ground. Mechanistic models may be more useful than empirical models, but that is contingent on their accuracy; and like all models, this class has not been rigorously tested.

Mechanistic and analytic modelling techniques can more or less be grouped into two categories, Lagrangian or Eulerian. The Lagrangian approach models the movement of the individual particles based mainly on horizontal and vertical wind speeds and takes into account the wind conditions specific to small discrete steps in time. This approach

has been widely applied to the modelling of seed dispersal (Andersen, 1991; Nathan et al. 2001, 2002a; Soons et al. 2004; Boehm & Aylor, 2005) however pollen grains and spores can be regarded as merely seeds with very low terminal velocities (Di Giovanni & Kevan, 1999; Aylor & Flesh, 2001; Jarosz et al. 2004). Unlike other modelling techniques, the Lagrangian approach can account for variation in the wind profile across time and space, and even for variability in intrinsic properties of the pollen grains (i.e. terminal velocity which may vary due to clumping).

The Eulerian approach attempts to describe the random movement of particles while incorporating advection and diffusion equations, yielding analytical solutions (Kuparinen, 2006). The Eulerian modelling approach has been widely applied to pollen as well as seeds (Di-Giovanni et al. 1989, 1990; Okubo & Levin, 1989; McCartney & Lacey, 1991; Greene & Johnson, 1995, Loos et al. 2003). The Eulerian and Lagrangian approaches have also been combined to produce the promising Coupled Eulerian-Lagrangian closure (CELC) models (Nathan et al. 2002b, Katul et al. 2005, 2006). However, these models can be computationally intensive and require thousands of trajectory calculations, therefore restricting their use to simpler, smaller scale applications (Katul et al. 2002).

2.3.2 The Tilted Gaussian Plume Model

The initial breakthrough in modelling dispersal was in the form of the Gaussian plume models. They predict that the distribution of pollen grains from a point source takes the form of a bell-shaped plume, with most pollen being deposited in a straight line directed outward from the source and tapering off at distances perpendicular to this line,

see Figure 1.2 (Okubo and Levin, 1989). Gaussian plume models are most commonly used in air-pollution studies, to predict particle concentrations in terms of distance from a ground-level point source. This approach deals with light particles with a terminal velocity of zero, and ground level emission. Adding release height and gravitational effects (for “heavy” particles) brought about the next generation of Gaussian plume models, known as the tilted Gaussian plume (Okubo & Levin, 1989):

$$p(x_l) = \frac{V_t}{\sqrt{2\pi} \bar{u} \sigma} \exp \left\{ -\frac{[x_r - (V_t x_l / \bar{u})]^2}{2\sigma^2} \right\} \quad (2.3)$$

where $p(x_l)$ is the probability density function of locating a seed or pollen grain at a distance, x_l , on the ground with respect to a point source at a given height, x_r . V_t is the terminal velocity of the grain, \bar{u} is the time and depth averaged horizontal wind velocity, σ is the mean eddy diffusivity (for boundary rather than canopy layer flow) and is described as $2Ax_1/\bar{u}$, where A is the diffusion coefficient given by $ku_*x_r/2$. Where u_* is the frictional velocity, x_r is the release height, and k is the von Kármán constant, regularly used for describing the logarithmic velocity profile of a turbulent fluid flow near a boundary layer.

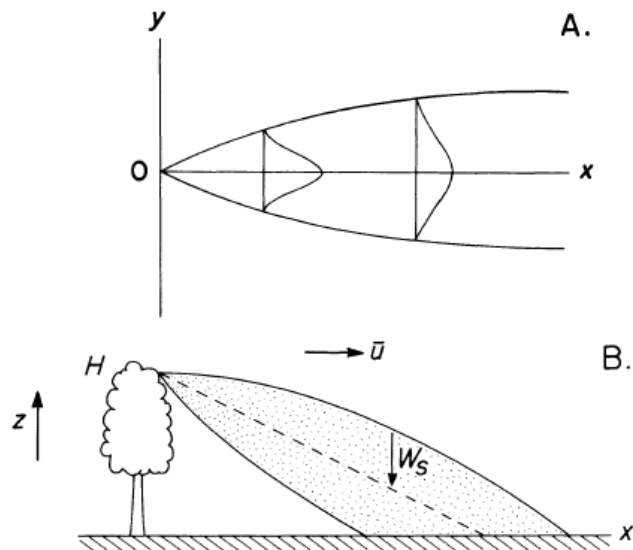


Figure 2.2: (A) Schematic for Gaussian plume model, viewed from above. (B) Schematic for the tilted plume model. Here, H denotes height of source, \bar{u} denotes mean wind speed, and W_s denotes settling velocity - Okubo & Levin (1989)

The tilted Gaussian plume models dispersal as a balance between gravity and friction (Greene & Johnson, 1989). It incorporates both the influences of wind advection and gravity on particle movement (Okubo & Levin, 1989). Advection refers to the effect of the one dimensional horizontal wind velocity (u) on dispersal, and the force of gravity determines the grain's terminal velocity (V_t). If pollen and seed movement were entirely deterministic, then it would be determined entirely by wind speed, the height of release, and terminal velocity (Nathan et al. 2001 and references therein).

This model is still problematic as they assume the dispersal kernel peaks at some distance x from the source and ignores vertical, and crosswind variation in wind speed. This tends to produce dispersal curves predicting less pollen in the far tail and no flattening of the curve is seen at far distances. In reality, stochastic effects due to fluctuations in wind speed and turbulence lead to much greater variation in dispersal distances.

2.3.3 The Advection-Diffusion Model

The tilted Gaussian plume model assumes that all particles reaching the ground bounced back, and that wind speed and vertical eddy diffusivity are constants (Okubo & Levin, 1989). To deal with this simplification, Okubo & Levin (1989) considered the dynamics of advective and diffusive movements of air flow in both the horizontal and vertical directions. The average wind speed takes into account the variation in wind speed with height, and the particle is assumed to be deposited at ground level without bouncing. The result was the Advection-Diffusion (A-D) model:

$$p(x_1) = \frac{V_t x_1^{-\beta_2-1}}{x_r \bar{u} \Gamma(1 + \beta_2)} \left(\frac{x_r^2 \bar{u}}{2(1 + \alpha_2)Ax_1} \right)^{1+\beta_2} \exp \left\{ -\frac{x_r^2 \bar{u}}{2(1 + \alpha_2)Ax_1} \right\} \quad (2.4)$$

The parameters are defined in the same way as the tilted plume model with the exception of β_2 and α_2 . $\beta_2 = V_t/W^*$, where W^* is the vertical mixing velocity - a measure of how fast particles at the release height x_r , would reach the ground by diffusion alone, and is defined as $2(1+\alpha)A/x_r$. α_2 is the power-law exponent of the mean wind velocity profile in a rough-wall boundary layer and varies between 0.14 - 0.17 (Katul et al. 2002), Γ is the gamma function and A is again the diffusion coefficient as used in the tilted Gaussian plume model equation.

2.3.4 The WALD Model

As identified by Katul et al. (2005) there are a number of problems with several of the modelling approaches. Phenomenological models are fitted to observed dispersal data, so can provide more accuracy but often they are too simplistic and are specific to

the environments where the data were collected. The CELC models can account for release processes, aerodynamics and turbulence, all of which are crucial to and provide accurate probabilities of LDD, but because they are so computationally intensive and require extensive wind statistics, they are often impractical for large-scale and long term studies (Katul et al. 2005). Since both analytic and mechanistic approaches have inherent strengths and weaknesses, Katul et al.'s (2005) model is one of the only models to date which attempts to combine the major advantages of both analytic and mechanistic modelling techniques, while avoiding their disadvantages. This model attempts to estimate long-distance dispersal from more commonly measured near-source data (Katul et al. 2005), even though it has been suggested that near-source data cannot be accurately extrapolated to model LDD because of the differences in the processes governing near and far-field dispersion (Bullock & Clarke, 2000).

The result of Katul et al.'s (2005) combinatory analytic-mechanistic technique was the Wald Analytical Long-distance Dispersal (WALD), or inverse Gaussian model. The objective of which was to estimate the long-distance dispersal (LDD) kernels of wind-dispersed pollen and seeds (where LDD is defined here as 100m from a seed source). Katul et al. (2006) suggests that there is much evidence that conifer pollen can readily exceed distances of several kilometres in less than an hour, based on the release height, wind speeds, and turbulent parameters of forested environments as opposed to agricultural crops (which often have lower release heights). Conifers increase in height annually, so with age, pollen has the potential to be carried further because it is released from a greater height (Katul *et al.*, 2005). Turbulent eddies, which also increase with height, can transport pollen to elevated regions of the atmosphere where wind speeds are

higher. This can increase dispersal ability, upwards of several hundred kilometres (Katul et al. 2006). However, the viability of this pollen when exposed to extreme temperatures and UV radiation is questionable, and grains reaching heights above 1 km or travelling for more than an hour were automatically discounted from the model.

The model focuses on a one-dimensional dispersal kernel, or the probability density function of locating a seed or pollen grain on the ground with respect to a point source at a given height (Katul et al. 2005). This kernel is found by analyzing a set of measurable parameters: release height, terminal velocity, source strength, time of release, location in Cartesian space, leaf area density (used to estimate the rate of change of air speed as a function of height within and above the canopy), and the averaged horizontal and vertical velocity components above the canopy. Formally:

$$p(x_1) = \frac{x_r}{\sigma\sqrt{2\pi x_1^3}} \exp\left[-\frac{(x_r - \gamma x_1)^2}{2\sigma^2 x_1}\right] \quad (2.5)$$

where x_1 is the horizontal distance from the source, x_r is the release height, σ incorporates the variance in the vertical wind velocity (σ_w), and the time and height averaged horizontal wind component; $\sigma^2 = kh\left(\frac{2\sigma_w}{u}\right)$. Where h denotes canopy height, k is again the von Kármán constant, and γ is the ratio of terminal velocity over horizontal wind speed ($\gamma = \frac{v_t}{u}$). For values of $\gamma \rightarrow 0$, $p(x_1)$ yields a power-law decay with an exponent of 3/2, and a finite γ causes a more an exponential decay of $p(x_1)$ (Katul et al. 2005).

To test their predicted dispersal distances, Katul et al. (2005) compared the predicted kernels to some of the existing dispersal data for a variety of grassland and

conifer species. The dispersal curve predicted by the model showed a good fit of the measured dispersal distances up to the 100 metre mark (see Figure 2.3). However, the maximum observed distance in the data is 100 m, i.e. none of the measured data includes any LDD events, as no mechanistic or analytical model has been tested against measured LDD data exceeding 2 km to date.

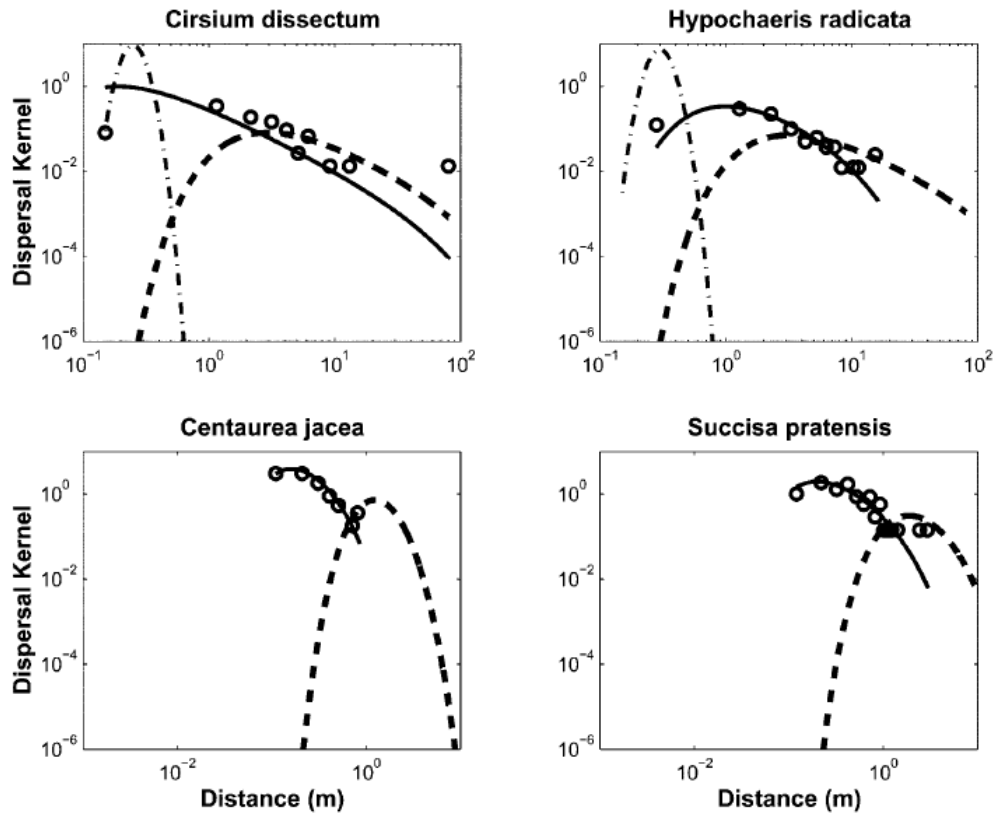


Figure 2.3: Measured (*circles*) and modeled (*lines*) kernels for the anemophilous seeds of *Cirsium dissectum* and *Hypochaeris radicata* as described in Soons et al. (2004). The solid line represents the fitted Wald analytical long-distance dispersal model obtained by first- and second-moment matching to the measured distances. The dashed lines represent the modeled kernels when release height and horizontal wind velocity are changed. Furthest measured data is at 100 m. (Katul, 2005)

A separate study was also done by Katul et al. 2006 using the WALD model to predict dispersal distances of pollen instead of seeds, on the basis that pollen can be considered seeds of low terminal velocity. The 2006 model operates on the same CELC

principles as the 2005 WALD seed dispersal model, but attempts to model long-distance dispersal of pollen up to 100 kilometres instead of 100 meters. The only comparison done for this model was done by estimating model parameters from a study of *Pinus taeda*. Pollen release height was estimated by observing the location of the majority of male cones on a *Pinus taeda* tree. Terminal velocity was obtained from typical terminal velocities for pines in the literature. Time of release was estimated using a heat sum model for the Duke Forest Plantation, while amount and location of pollen release were based on estimations of pollen yield per tree per day, and not on direct measurements of ambient pollen concentrations. The wind velocity data needed were obtained from the sonic anemometer measurements taken at the Duke Forest, while the leaf area measurements were collected by detailed observational analysis of the canopy (Katul et al. 2006). Based on these estimated, the model predicts that long-distance dispersal can range from 26-60 km and is one of the few studies to predict dispersal distances of greater than 100 m, but they had no empirical data to test the predictions.

Thus, the main objective of my thesis was to develop long-distance empirical data sets. A secondary objective was to use this data to test the WALD model of dispersal (Katul et al. 2005), along with the pioneering models of Okubo & Levin (1989) – the tilted Gaussian plume and Advection- Diffusion models. These three models were previously tested by Katul et al. 2005, but only up to a maximum of 60 meters as can be seen in figure 2.4. The parameters used in each of the three model equations (Eq. 2.1, 2.2, 2.3) are described in detail in section 3.3 below.

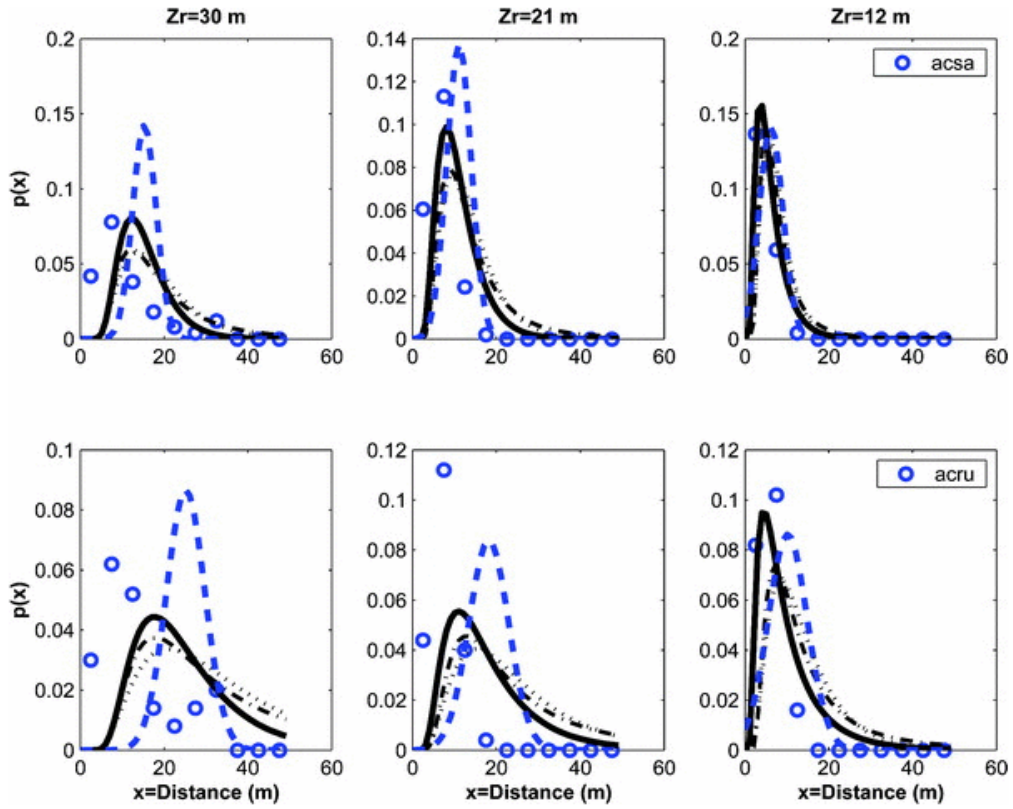


Figure 2.4: Wald analytical long-distance dispersal (solid lines), tilted Gaussian (dotted lines), advection-diffusion equation (dot-dashed lines), and the Gaussian plume (Dashed lines). Observed data (circles) based on five manual seed release experiments described in Nathan et al. 2002b. (Katul et al. 2005)

3 Methodology

3.1 Area Source Experiment

3.1.1 Location and Field Methodology

To study of dispersal from an area source I used a large lake lacking islands because that would permit me to (1) identify the pollen source area (i.e. the lake edge vegetation) with certainty, (2) have a more homogenous wind regime (at least over the lake), and (3) have less impact of moving pollen by vegetation elements (again, only over the lake portion of the grain's transport). Using Google Earth[®] to examine potential sites across Canada, I finally chose Clearwater Lake, Manitoba. It is located at 54.05° N and 101.06 ° W, and is 289 km² in area. This lake was chosen because it met all of the criteria:

- at least 10 km in diameter;
- no islands (and thus the source pollen must be from the mainland)
- a depth conducive to smaller waves; the mean depth of Clearwater Lake is 13 m, with the maximum depth being 39 m in the northern region. (Sampling was done only in the southern half)
- accessible by car
- surrounded by a variety of wind-pollinated species (*Picea mariana*, *Abies balsamea*, *Pinus banksiana*, and *Alnus rugosa* were the most common anemophilous species surrounding Clearwater)

A smaller lake, Campbell Lake, adjacent to Clearwater met all criteria except the size requirement, and so was used only to measure dispersal distances up to 2 km. It is located at 54.96° N and 101.15 ° W, and is 4 km² in area . It was even shallower than Clearwater and tended to be much calmer.

The pollen sampling was done using 22 Rotorod Samplers (Model 95), which are described in more detail below. The Rotorods were affixed to wooden rafts which were

anchored at specific intervals along the lake transects. The rafts were designed to each hold one rotorod sampler plus a 12 volt battery to power the sampler. A strip of buoyancy foam was used to support a 2 x 4 ft piece of plywood. The Rotorod was attached to the center of the plywood on top of a PVC pipe, and the battery for the Rotorod was held in a water resistant container (see Figure 3.1).

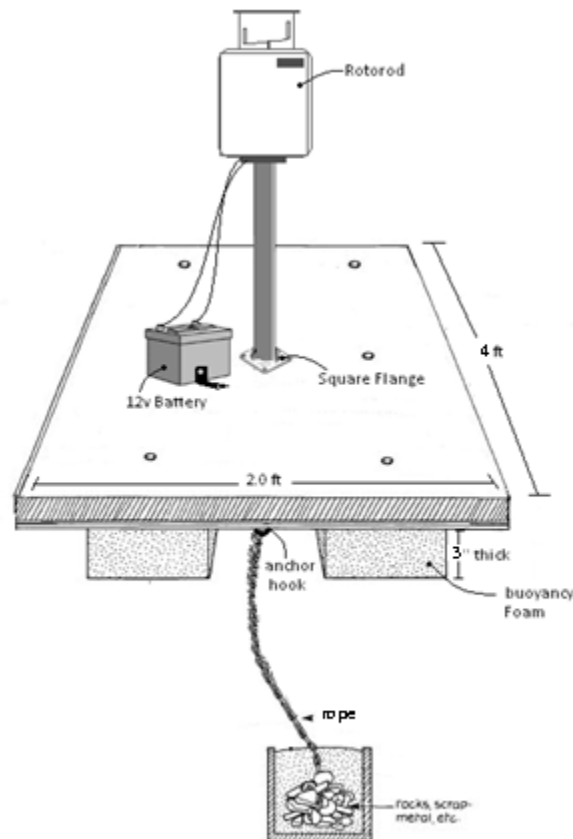


Figure 3.1: Rotorod raft design, modified from original image at: http://handbooks.btcv.org.uk/books/images/2467/11_8.jpg

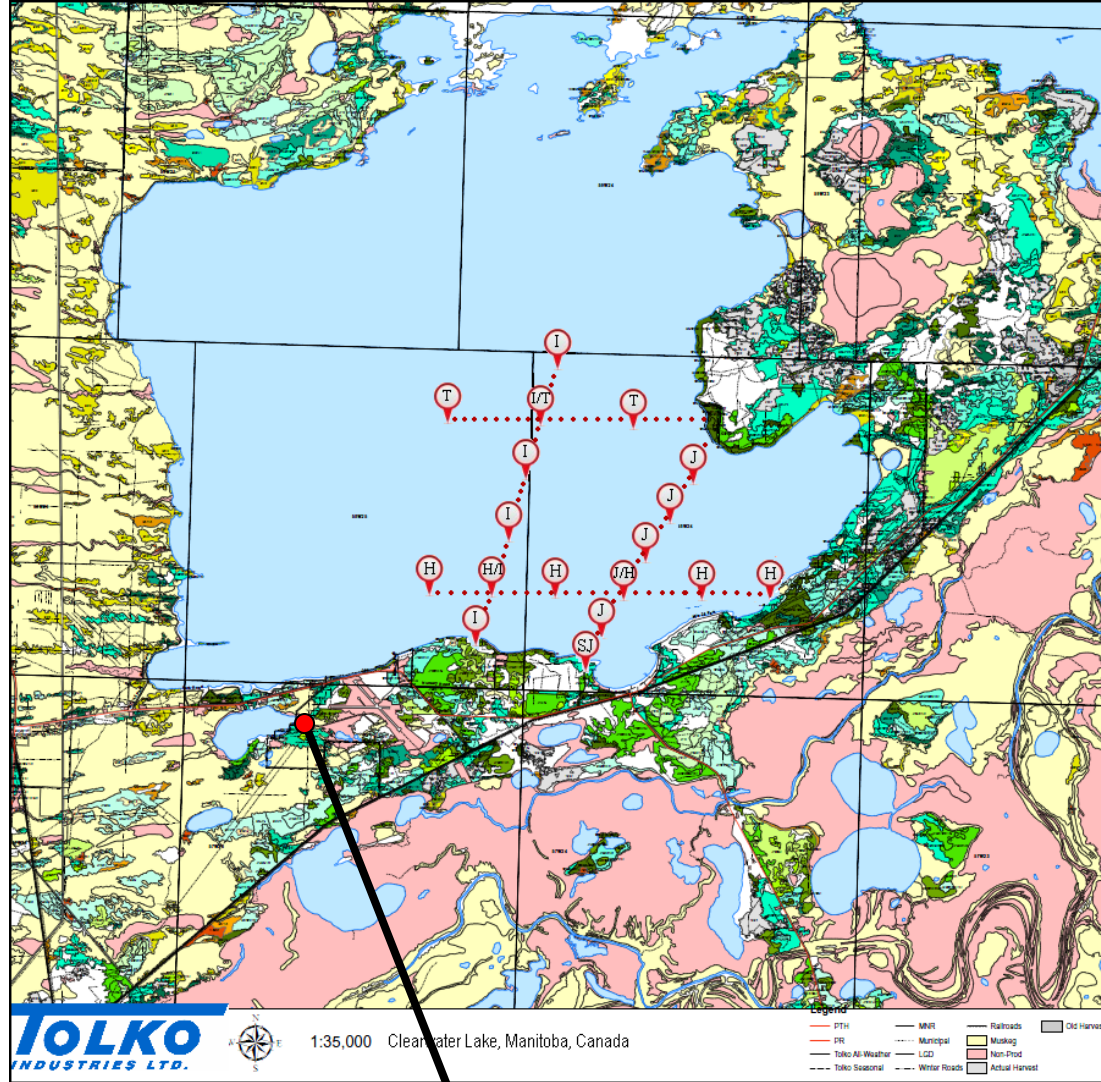
On Clearwater Lake, four transects were set up in the southern half of the lake, most extending out ten kilometres from the lake shore. Transects H and I consisted of six wooden rafts spaced every 2.04 km, extending out to 10.2 km, and Transect T consisted of 3 rafts separated by 3.3 km. Transect J was unique in that it covered an 8.3 km

transect extending from one shore to another, and so could be used for trials in which the wind was coming from the northeast or the southwest without having to reposition the rafts (see Figure 3.2). It was only feasible to transport six Rotorods at once on Clearwater Lake, but the placidity of Campbell Lake allowed more rafts to be used and anchored at shorter intervals along the transects. The transects on Campbell Lake consisted of ten rafts in the northeast-southwest direction (Transect A) and seven in the northwest-southeast direction (Transect B). Two Rotorods were also located on the mainland at Campbell (SB and SA in Figure 3.2a) and one at Clearwater (SJ in Figure 3.2b) to measure local concentrations at the edge of the area source.

The positions of the transects used for sampling depended upon the direction of the wind during the sampling period. If the wind was blowing along one of the line of transects then measurements were carried out. Wind direction was measured by the sonic anemometer at the beginning, and for the duration of, each sampling period.

The species studied are typical of the southern boreal forest (Lands Directorate, 1986). The three coniferous tree species I studied were *Picea mariana* (black spruce), *Pinus banksiana* (jack pine), and *Abies balsamea* (balsam fir). *Picea glauca* (white spruce), while abundant in the area had a poor year for reproduction and was therefore ignored. Two other common tree species, *Populus tremuloides* (aspen) and *Betula papyrifera* (paper birch) flowered before I finished building the rafts. I also sampled one shrub species, *Alnus rugosa* (speckled alder); the other common shrub species in this area had flowered before the rafts were completed.

a)



b)



Figure 3.2: Transect and rotorrod positions on (a) Clearwater and (b) Campbell Lake, Manitoba, Canada.

3.1.2 Timing

It was crucial to know the availability of pollen for each species within the source area during the brief period of abscission and release. The pollination season for the majority of the Pinaceae family (spruce, fir and pine) in the region typically starts mid-May and ends mid to late June (Farrar, 1995), but the exact schedule is highly dependent on the weather. Any single woody anemophilous species only flowers for about 10 days but pollen may remain airborne for longer. Male flowers (or staminate cones) of lake-edge trees and shrubs were monitored to determine the onset and end of the pollination season for each species. Alder was the first to begin pollination during the last two weeks of May, unfortunately a storm during that time damaged and displaced some of the rafts, so repairs and modifications meant that only the very end of the alder dispersal season was used. *P. mariana* and *A. balsamea* began pollination during the last week of May, and *P. banksiana* began during the first week of June.

3.2 Area Source Data Collection: Measuring Model Parameters

3.2.1 Estimating Release Height (x_r)

For each species, pollen release height was estimated by examining the height of the male flowers (alder) and staminate cones (conifers) on the study species. The mean male height was quantified using a laser range finder.

3.2.2 Estimating Source Strength (Q)

The Rotorod on the windward lakeshore edge (15 meters from the forest edge) was used to estimate the source strength, Q (mean pollen grains per m³ of air deep within

the source area). Each model prediction of grains/m³ at $x=0$ was assumed to be equal to that caught by the rotorod on shore (N_{shore}). Q was found by calculating the amount of pollen/m³ required to sum to N_{shore} at $x=15$ m. Q was then used as a multiplier in each model equation to account for the fact that there is more than 1 grain/m³ being emitted by the forest. This multiplier forced the origin of each model prediction to be equal to that of the observed pollen concentration at $x=15$ m.

To determine the proportion of study species present in the area surrounding the two lake sites, I surveyed the surrounding forests. Species composition maps (Figure 3.3) were also analyzed and the frequency of study species in the area surrounding the lake sites was determined. This was then used to calculate a weighted average based on frequency of the study species and the fraction of the species in each counted stand. This was done for all coniferous species; however, *A. rugosa* is a non-timber productive species and was not listed on the maps provided by Tolko[®]. According to Manitoba Conservation (2001) timber unproductive land makes up 17% of Manitoba (Figure 3.4). So the *A. rugosa* estimate was based on this figure and the frequency of *A. rugosa* seen around the lake site.

All the models assume that the grains stop when they reach the ground (or lake surface) and that the forest is composed entirely of the species it is modelling, so Q must be modified to account for the actual forest composition, the sampling period, and the approximate area occupied by one tree. For this study, a tree is assumed to disperse pollen for approximately 7 days, and one tree is assumed to occupy a more realistic 10m² (the typical crown area of a mature tree with a basal diameter of about 0.3 m) instead of 1m².

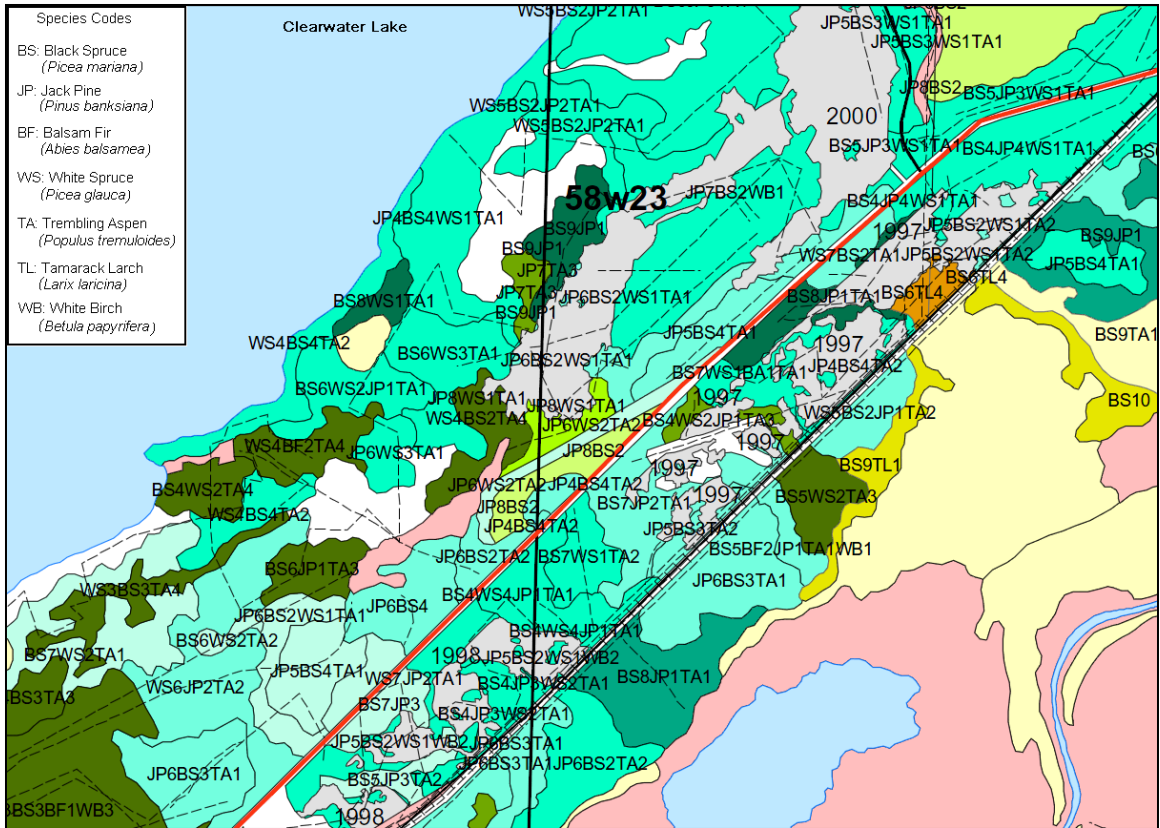


Figure 3.3: Sample species composition map at study site, alphanumeric coding indicates species type and percentage composition of surrounding forest patches – e.g. BS6JP1TA3 = 60% black spruce, 10% jack pine and 30% trembling aspen (Source: Tolko Industries Inc, 2010).

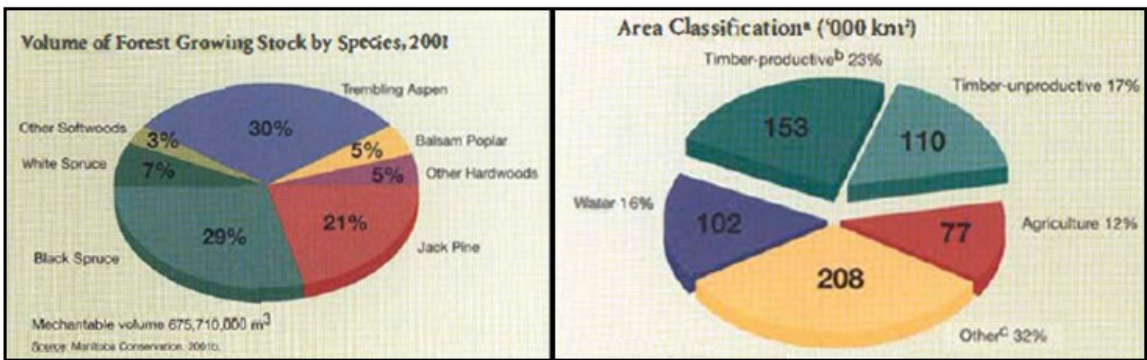


Figure 3.4: Forest composition for the province of Manitoba, a) by species b) by land use. The coniferous study species make up approximately 53% of the forest species in Manitoba – Black Spruce 29%, Jack Pine 21%, and Other Softwoods (Balsam Fir) 3%. *A. rugosa* was estimated to compose 10% of the 17% of Timber-unproductive land. (Source: Manitoba Conservation, 2001)

3.2.3 Wind Parameters

The wind parameters needed for the WALD, Advection-Diffusion, and tilted Gaussian models were the time- and height-averaged horizontal wind velocity (\bar{u}), the variation in the vertical component of the wind velocity (σ_w), the average wind direction (θ) during the sampling period, and the standard deviation in wind direction (σ_θ). These parameters were obtained with a RM Young 81000 sonic anemometer, which gives three dimensional wind measurements. The anemometer was programmed to output the wind velocity (m/s), direction($^\circ$), elevation (Radians), and temperature($^\circ\text{C}$) averaged over 12 second intervals. It was placed at the lake edge for the sampling period (typically 1-3 hours) of interest. Each measured wind parameter was then averaged over all the trials for a species.

Horizontal wind velocity (\bar{u}) changes in the fetch of the forest, as well as above the canopy, and outward toward the centre of the lake. The change in wind speed over the lake can be estimated using the protocol developed by Greene and Johnson (1996) for clearings in the lee of forests. Using this protocol, the anemometer measurements can be transformed into the spatially averaged horizontal wind speed for each measuring interval at the height of the Rotorods. The anemometer was located at the edge of the lake, and the edge of the forest was about 15 m away; so first the reference wind velocity (u_r) was found at the forest edge (which is a function of the distance to, and height of, the source forest). Then the wind speed above the canopy (u_{zh}) was calculated, and averaged with the wind speed in the upper and lower halves of the canopy. The wind speed will also increase with distance (x_p) over the lake, with the maximum velocity assumed to be achieved at the point along x in which u_{xp} reaches 100% of u_r . Beyond this point over the

lake, \bar{u} is assumed to be the same as u_r . The wind speed beneath the canopy in the source forest is much smaller than that over the lake and is understood to 12% of the reference speed (Greene and Johnson, 1996), and the forest is assumed to extend back to a maximum of 5000 meters. This results in three values for the horizontal wind profile:

- the mean velocity from the top of the canopy to the bottom
- the average velocity from the forest edge to the greatest distance examined on the lake
- the mean velocity within the source forest (12% of the reference wind velocity).

These three values are then turned into a distance-weighted average speed, calculated proportionally from the wind data collected at both lake sites.

The average wind direction and standard deviation of the wind direction over each sampling period was computed using the Yamartino Method (Yamartino, 1984), whereby the average wind direction is given by:

$$\theta = \tan^{-1} \frac{s_a}{c_a} \quad (3.1)$$

where s_a and c_a are the averages of the sines and cosines of all the measured wind direction angles in the sampling period. The standard deviation of θ is given by

$$\sigma_\theta = \sin^{-1}(\varepsilon) \left[1 + \left(\frac{2}{\sqrt{3}} - 1 \right) \varepsilon^3 \right] \quad (3.2)$$

where $\varepsilon = \sqrt{1 - (s_a^2 + c_a^2)}$. Wind direction could change in a sustained manner once a sampling trial had been begun. Given the typical shifting of direction with time, the rods were changed on the measuring devices every few hours so that I could define discrete periods when the wind was roughly unidirectional (see Figure 3.5). Only an interval with unidirectional winds was used for subsequent analysis.

The variation in wind direction (σ_θ) was used to determine the area of the forest actually contributing to the pollen load at each distance, x , along a transect during a trial interval. It was assumed that only those trees within two standard deviations of the angle would be contributors to the pollen load at x , as described below (Figure 3.7).

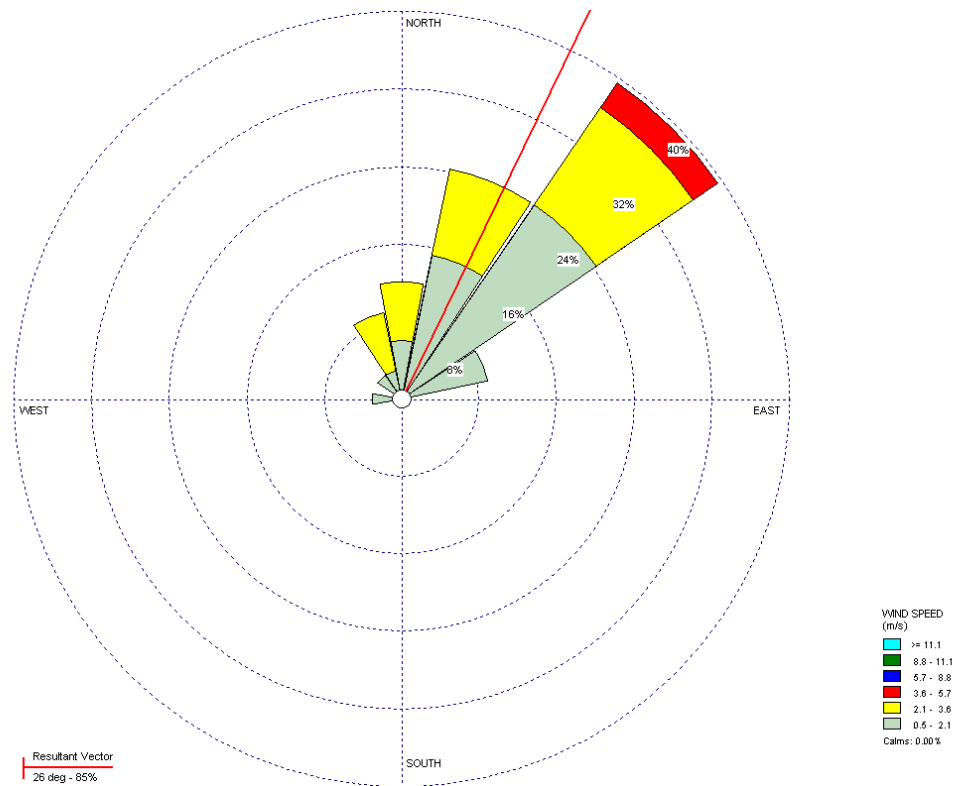


Figure 3.5: Wind rose depicting wind speed and directional profile for a typical sampling period. This particular example is for sampling period June 5, 9:38am -11:43am, Campbell lake site. Compiled using WRPLOT®

3.2.4 Horizontal Distance (x) – Rotorods

The distance travelled from the point of release to the point where the pollen grain reached the “ground” was measured using Model 95 Rotorod particle samplers. The Rotorod was sampling at a height about 0.5 meters above the lake surface, so it was assumed that at the scale of many kilometres, this height is roughly equal to the “ground level” deposition height of the Katul (2005) and Okubo & Levin (1989) models.

The Rotorod is a stationary, rotating-arm, impaction sampler that collects pollen grains on two plastic rods (I-rods). These I-rods are coated on one side (the collecting edge) with silicon grease, and are mounted on an armature which is rotated at 2400 rpm by an internal motor (Frenz & Lince, 1997). The Model 95 devices have timers which allow variable sampling from 1 to 100% of the operating time (Di Giovanni & Banks, 1994). For this study, they were run for two minutes out of every ten minutes for a time period of typically 1-2 hours before the wind changed direction. Increasing the duty cycle to anything above 20% caused the I-rods to become saturated with pollen, which makes for difficulties in counting the grains. Sampling took place variably from 8 am to 8 pm depending on wind and weather conditions. The amount of pollen collected on the I-rods was counted under a microscope according to the protocol outlined by the Rotorod Operating Manual (Sampling Technologies, Inc, 1989) to determine the pollen concentration in number of grains. This is then converted to grains per volume by using the Rotorods operating conditions, duty cycle and the sampling period. Under standard conditions the Rotorod samples 3.12m³ of air, standard conditions being 24 hour (1440 min) sampling period, 10% duty cycle. Since my sampling period and duty cycle changed from trial to trial, that number also changed, so volume became:

$$V = 3.12 \times \left(\frac{\text{sampling period}}{1440 \text{ mins}} \times \frac{\text{duty cycle}}{10\%} \right) \quad (3.3)$$

the number of particles is then divided by this new calculated volume to determine the actual grains per metre cubed of air.

3.2.5 Terminal Velocity (v_d)

Measurements of the terminal velocities of the pollen grains of many species have been collated by Jackson and Lyford (1999). Most of the measurements were based on fall-tower experiments in which pollen is released from the top of an evacuated cylinder and the time required to reach the bottom is measured (Jackson & Lyford, 1999).

3.3 Point Source Experiment: *Lycopodium clavatum*

To compare the difference in dispersal between area and point sources, the dispersal of the spores of *Lycopodium clavatum* was experimentally measured in two farmer's fields in Dalkeith, Ontario. One field measured 500 m in length, and the other 2000 m in length (Figure 3.6); both sites were located on previously harvested maize fields just after snowmelt; thus there could not be any naturally dispersing *Lycopodium* sources. It was not feasible to measure dispersal for distances longer than 2000 meters, because travel between consecutive Rotorods had to be done on foot. Furthermore, it was essential that all the Rotorods be turned on at roughly the same time and to change the I-rods quickly between sampling periods- in order to maximize the number of trials able to be done during consistent wind conditions. Also, because the Rotorods were aligned according to the line of action of the wind, these fields were chosen because there was ample area available for the sampler configuration to be changed whenever the wind direction shifted significantly.

L. clavatum was selected because large quantities of spores are easily obtained, the spores have low terminal velocities, and they do not clump (Sheeramulu & Ramalingam, 1961). Each spore is approximately 32 μm in diameter and has a terminal velocity of 1.9 cm/s (Chamberlain, 1967). With this diameter, each spore occupies a

volume of $1.72 \times 10^{-8} \text{ cm}^3$ or $1.78 \times 10^{-8} \text{ g}$, resulting in about 5.8×10^7 grains per gram. Based on these calculations and those of Sheeramulu and Ramalingam (1961), it was decided that in order to detect the spores at large distances (up to 2000 m), at least 100 grams of spore would have to be released at $x=0$ for each trial. However, the *lycopodium* powder purchased for this experiment was found to contain some ground leaf parts, and was estimated to only be composed of about 40% pure spores, and so the amount released was modified accordingly.



Figure 3.6: Study area (45.42 N, 74.62 W) and Rotorod arrangement for *Lycopodium* experiment.

The sonic anemometer was placed at the same location and height (2.0m) as the release location of the spores and run for the duration of each trial. The Rotorod

samplers were attached to pipes 0.75 m in length, positioned at regular intervals along two different configurations, each aligned with the wind direction during the sampling period. Configuration *r* was used for wind coming from the east/southeast, and configuration *n* (Figure 3.6) was used whenever the wind was coming from the northeast. After noticing a pronounced lateral dispersion of the spores at the release point, it was decided to place more Rotorods at each measurement interval (every 100 m) for configuration *n*, to ensure that enough spores were caught at each distance (*x*).

Over the next three days, ten trials were made with a weighed quantity (from 100g-300g) of spore slowly released into the wind at a height of two meters. The average release rate was 5 grams per minute (0.08g/sec), which was achieved by hand shaking the spores through a perforated container, and measuring the time it took to empty the container. This took between 20-60 minutes, and only the wind measurements during this time period were used. The sonic anemometer continually measured wind parameters throughout each trial over the three days of sampling.

3.4 Using the Models

The WALD model (Katul et al., 2005), the Advection-Diffusion model (A-D), and the tilted Gaussian model (Okubo & Levin, 1989) were tested by comparing the predicted grain density at each horizontal distance *x*, with the actual grain density measured with the Rotorods. For each species, the observed grain density at each distance (*x*) was converted into grains/m³ and averaged over all sampling periods. To obtain the predicted grains at *x*, the parameters of the WALD, Advection-Diffusion, and tilted Gaussian models (discussed above) were measured in the field (with the exception

of the terminal velocity, v_t) and input into the model equations (Eq. 2.3, 2.4, 2.5). The three model equations determine the probability that a grain reaches a Rotorod sampler at a distance x from a point source, $p(x)$. For the final determination of grains per volume at distance x , $p(x)$ was multiplied by the estimated source strength, Q .

The situation for the Manitoba data was also complicated by the fact that WALD, A-D and tilted Gaussian equations were designed to model the dispersal of a particle from a point source, so the models had to be modified to account for the fact that we are working with an area source. A program was created to calculate the number of grains deposited at x when the entire forest is taken into account. As in Greene & Johnson (1996), first the distance from the sampler to each individual tree is found:

$$x_p = \sqrt{(x + d)^2 + (a)^2} \quad (3.4)$$

where $(x + d)$ is the distance from each tree to the pollen sampler, and a is the distance to the tree along the chord length (Figure 3.7). The distance to each successive sampler (x_p) is found for each tree across the chord length from $R=0$ to R_{\max} , where the trees are assumed to be one meter apart, and R_{\max} was estimated to be 5000 meters, as at this distance there is vanishingly little contributed to the probability calculation. Each x_p is then input into the model equation, and then summed over the contributing forest to find $p(x)$. Where, the contributing forest consists only of those trees encompassed by two standard deviations of the angle of the wind direction.

Since $p(x)$ determines how many grains are contained in the entire annulus, and because here we have non-random wind direction, $p(x)$ must be divided by $2\pi x_p$ and then multiplied by the ratio $2\pi x_p/s$. Where s is the distance along the annuli given by the product of the radius (x_p) and θ ; where θ is the wind directional angle plus two standard

deviations (σ_θ) of the wind direction (Figure 3.7). This then gives the final number of grains which should be found in the arc (s) instead of the entire annulus. The annulus is also assumed to be unit width and height, to keep the dimension consistency of length cubed. This arc (s) is used because we are assuming that all grains are concentrated in this arc rather than the entire annuli due to the non-random wind direction. The resulting average probability of one grain reaching the rotorod at x is then multiplied by the estimated number of grains/m³ (Q), where each tree is assumed to occupy 1m³, see Table 4.2 for estimates of Q for each species. It is unimportant that no real tree or shrub is even approximately 1m³ in size. Working with the *Lycopodium* data was more straightforward, Q is simply the number of grains released and $p(x)$ only has to be divided by s , to convert the units into grains found per the arc s made by the standard deviation of the prevailing wind direction.

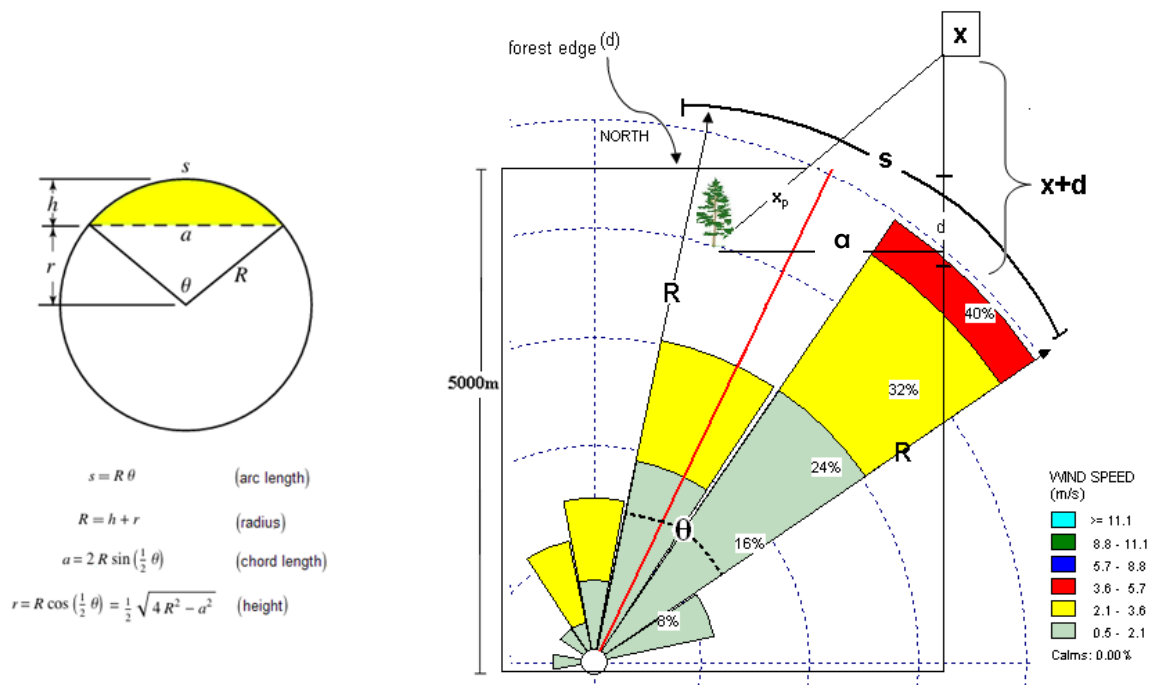


Figure 3.7: Determining the contributing trees in the source forest using circular sector geometry (Weisstein, 2011). s is determined by using the standard deviation (σ_θ) of the recorded wind direction (θ) during the sampling period, R is the length of the contributing forest, d is the distance from each tree in the forest to the forest edge, $x+d$ is the distance from each tree to the Rotorod located at a distance x from the forest edge. The area-source program sums the theoretical pollen contributions from each tree located in the area encompassed by $\theta \pm \sigma_\theta$.

3.5 Statistical Methods & Sensitivity Analysis

For the statistical testing of the three models, the observed pollen concentrations measured in the field were regressed against the model predictions $p(x)$ for each the three models. The goodness-of-fit of each model's predicted curve to the measured data was based on R^2 and the proximity of the slope and intercept of the regression line to 1 and 0 respectively. For the sensitivity analysis, the fundamental parameters in each model (Terminal velocity, horizontal wind velocity, release height and turbulence parameters) were either increased or decreased by multiples of the average field-measured value or to values near zero. Whether (and by how much) the parameters were increased or decreased depended on the level of over or under-prediction in the initial curve using the average field-measured values. If the initial model prediction was already over-predicting the observed data, only those variations when the curve would be shifted downward were used in the analysis, and vice versa. Because of the large difference in magnitude of the near and far source pollen concentration measurements and model predictions all regression and sensitivity analyses were performed on the logarithms (base 10) of the observed and predicted pollen concentrations. The variations which improved the R^2 and brought the slope closer to one, without causing too much of an over- or under-prediction at long distances were considered to improve the overall goodness-of-fit of the model.

4 Results

4.1 General

Duration of pollen release for each species was on average about 12 days (Table 4.1). Trial number varied by species from 4 to 11; since the entire pollination season was observed for *P. mariana* and *P. banksiana*, there were more useful trials for these species. The average time per trial was 150 minutes. The horizontal wind velocity was on average between 1.90 and 3.46m/s, with only the odd gust exceeding 4.0m/s. (Table 4.1) The variation in the vertical wind component (σ_w) averaged 0.2m/s to 0.5m/s for the species trials while the standard deviation in the wind direction (σ_θ) was always below 45°.

Table 4.1: Duration of pollen release for each study species, averaged horizontal wind speed (\bar{u}), standard deviation in vertical velocity wind component (σ_w), and the average variation in the wind direction (σ_θ), over the 30 selected samplings.

Species	Pollination Period Northern Manitoba (2010)	Trials per species	\bar{u} (m/s)	σ_w (m/s)	σ_θ (°)
<i>Alnus rugosa</i>	May 17-May 29	4	2.57	0.51	23.02
<i>Abies balsamea</i>	May 27-June 7	6	2.35	0.25	31.95
<i>Picea mariana</i>	May 30-June 14	11	1.90	0.32	41.4
<i>Pinus banksiana</i>	June 2-June 17	9	2.00	0.31	44.24
<i>Lycopodium clavatum</i> (point source)	n/a	10	3.46	0.20	19.03

The maximum distance over which data could be obtained was 10.1 km (Table 4.2). Data collection was attempted out to this distance for *A. balsamea*, but pollen was found only on those rotorods less than 4.3 km from the shore. The terminal velocity of *A. balsamea* also differed markedly from the other study species. The average v_t of the other species grains were roughly between 0.02m/s and 0.03m/s, while that of the larger grains of *A. balsamea* was almost 0.1m/s (Jackson & Lyford, 1999). The second-growth trees were relatively short; measured release height (x_r) was on average 7.8 m for the conifers,

and 3.9 m for *Alnus*. Table 4.3 also lists, N_{shore} - the number of grains/m³ captured on the shore 15 meters from the forest edge ($x=15$ m), and the final Q - the estimated number of grains/m³ for each model. Recall that the expected concentration at the forest edge was forced to be the same as the observed concentration at the shore ($x=15$ m).

Table 4.2: Average of field-measured parameters required for model testing. Measured distance from lake shore (x), terminal velocity (v_t), average release height (x_r), observed concentration at $x=15$ m (N_{shore}), and estimated source strength in grains per m³ (Q) needed for each model prediction to equal N_{shore} . v_t was averaged from the terminal velocities calculated by Jackson & Lyford (1999).

Species	x (km)	v_t (m/s)	x_r (m)	N_{shore} (grains/m ³)	Q (grains/tree)		
					WALD	A-D	Tilted
<i>P. mariana</i>	0-10.1	0.032	7.84	1208.53	8.27×10^8	9.49×10^8	6.70×10^8
<i>A. balsamea</i>	0 - 4.3	0.0985	8.23	28.04	3.39×10^8	3.01×10^8	2.92×10^8
<i>P. banksiana</i>	0-10.1	0.0254	7.23	396.87	6.42×10^8	8.38×10^8	5.46×10^8
<i>A. rugosa</i>	0 - 2.0	0.0195	3.86	116.18	3.23×10^8	3.66×10^8	2.17×10^8
<i>L. clavatum</i> (point source)	0 - 2.0	0.0195	2.0	242.45	Grains released : 2.24×10^9		

4.2 Source Strength (Q) and Filtration Estimates

Using the species composition maps and surveys of the study site (Section 3.2.2), the source forest was estimated to be composed of 45% *P. mariana*, 20% *P. banksiana*, 2% *A. balsamea*, and 10% *A. rugosa*. The remaining 23% of the forest surrounding the lake comprised non-study trees and shrubs.

In order for the observed and predicted pollen concentrations at the forest edge to be equal, the models initially showed that the amount of pollen produced per tree (Q) was between 58-4200 grains per tree, before accounting for the sampling period, forest species composition, and the approximate area occupied by one tree. This brought the Q estimate to a range of about 2.2×10^8 - 9.5×10^8 (see Table 4.3) grains per tree. Based on estimates for *Pinus taeda* (Katul, 2006), we expect about 113.4×10^6 pollen grains emitted per day for a tree occupying 10 m^2 . If a tree was dispersing for approximately 7 days, this translates into a theoretical estimate of about 7.9×10^8 grains per tree per

pollination period. The average Q estimates across models for each species, suggests about 62% of the *A. balsamea* and *A. rugosa* pollen was filtered out before reaching the lake, about 15% of *P. banksiana* pollen was filtered, and none of the *P. mariana* pollen was filtered.

Table 4.3: Concentration of pollen measured on the shore (N_{shore}) at 15 metres from the edge of the forest, original source strength (Q_i) required to attain this shore concentration, and the modified source strength (Q_f) accounting for the average 7 day pollination dispersal period and the percentage occupied by each species in the source forest. Point-source Q estimate is based on the actual number of grains released.

Species	N_{shore} (grains/m ³)	Q_{WALD} (grains/tree)		Q_{A-D} (grains/tree)		$Q_{tilted\ Gaussian}$ (grains/tree)	
		Q_i	Q_f	Q_i	Q_f	Q_i	Q_f
<i>P. mariana</i> forest comp: 45%	1208.53	3693.26	8.27×10^8	4237.28	9.49×10^8	2992.12	6.70×10^8
<i>A. balsamea</i> forest comp: 2%	28.04	67.23	3.39×10^8	59.64	3.01×10^8	57.98	2.92×10^8
<i>P. banksiana</i> forest comp: 20%	396.87	1273.15	6.42×10^8	1662.92	8.38×10^8	1084.07	5.46×10^8
<i>A. rugosa</i> forest comp: 10%	116.18	320.64	3.23×10^8	362.94	3.66×10^8	214.89	2.17×10^8
<i>Lycopodium clavatum</i> (point source)	242.45	2.24×10^9		2.24×10^9		2.24×10^9	

4.3 *Picea mariana*

The WALD model for *Picea mariana* under-predicted at all distances (Figures 4.1; 4.2a). The A-D model fit fairly well at distances less than 2 km but over-predicted the pollen concentrations at all distances beyond 2 km. The tilted Gaussian plume model predicted a steady decline over all distances which failed to express the flattening of the observed dispersal curve with distance.

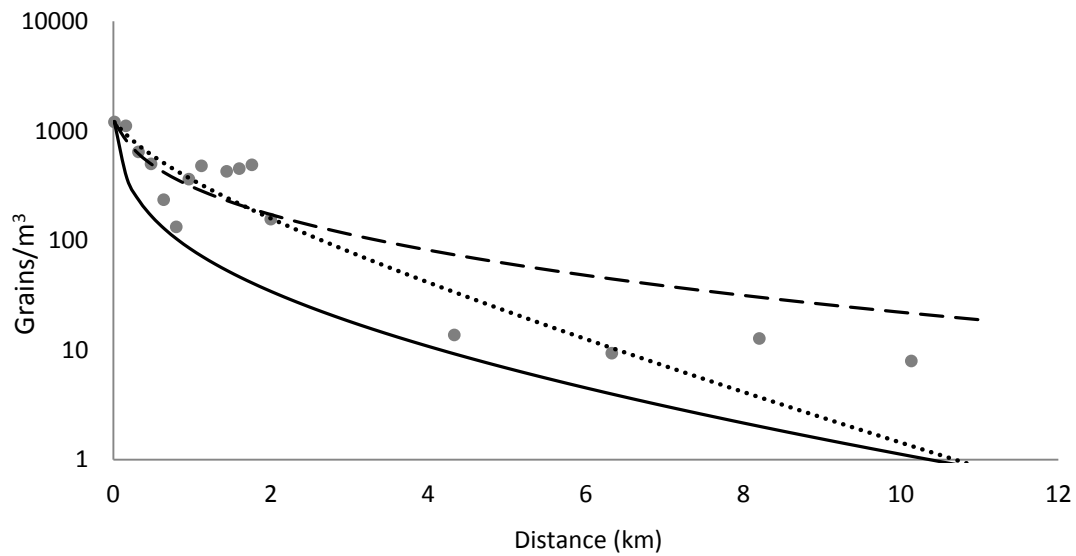


Figure 4.1: Observed (●) and Predicted grains/m³ for *Picea mariana*, $v_f=0.032\text{m/s}$, $h=7.84\text{m}$. Predictions based on the WALD(—), advection-diffusion(---) and tilted Gaussian plume(•••) models.

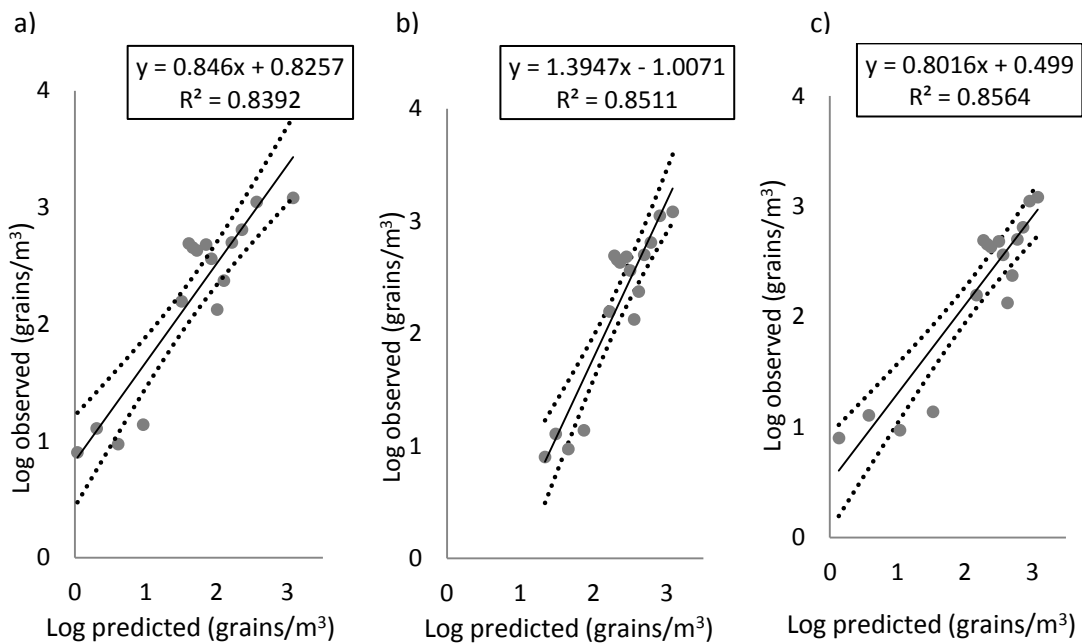


Figure 4.2: Linear regression of predicted versus observed pollen concentrations of *P. mariana*, with associated 95% confidence intervals. Predicted values based on a) WALD b) advection-diffusion c) tilted Gaussian plume models.

For the regression of the predicted versus observed values, only the WALD had a slope not significantly different from 1 (Table 4.4). The WALD model slope was also

the closest to 1, but it had a regression intercept significantly different from 0 ($p < 0.05$). I.e. the WALD model captured the observed change in concentration with distance fairly well but consistently underestimated the absolute magnitude of the concentration. Both the A-D and tilted Gaussian had intercepts significantly different from 0 and slopes significantly different from 1 (Table 4.4). Thus, none of the three models was clearly superior at fitting the data.

Table 4.4: Statistical testing of *P. Mariana* with the three models. R^2 , slope (β) and y-intercept (α) of the associated best-fit line of the model predictions vs. observed concentration. 95% confidence intervals and the significance in the slope and y-intercept of the regression are also listed.

<i>P.mariana</i>	R^2	β	α	95%		p(β)	p(α)
				(β)	(α)		
WALD	0.839	0.846	0.826	0.212	0.39	0.142	0.0005
A-D	0.851	1.395	-1.007	0.334	0.793	0.024	0.016
Tilted	0.856	0.802	0.499	0.188	0.437	0.040	0.028

In the sensitivity analysis, varying any one of the parameters within the WALD model shifted the curve up or down, reducing the under-prediction in some cases and increasing it in others (Figure 4.3). For the WALD model, reducing v_t by 50% of the measured value (0.016m/s) brought the slope of the regression closest to one ($\beta=1.03$, Figure 4.3b), but slightly decreased R^2 (0.83). Changing terminal velocity to near zero brought the regression intercept closer to zero and improved the prediction of the far tail, but was unable to increase R^2 and the majority of the WALD curve still greatly under-predicted the observed data.

The WALD model was more sensitive to changes in horizontal wind velocity (\bar{u}) and release height (x_r). Increasing x_r or \bar{u} to values 4 to 6 times that of the field-measured value resulted in a slight increase in R^2 (0.86) and reduced the under-prediction at all

distances. Increasing these two parameters more than 6 times the measured value still fit the near-source data well (Figure 4.3a,c), but caused a slight over-prediction of the far-source data and brought the regression slope and intercept further from 1 and 0.

Increasing the turbulence parameter (σ_w) by 10 times the measured parameter improved the regression slope ($\beta=1.03$), but was unable to improve R^2 , or reduce the overall under-prediction seen by the WALD model for *P. mariana* (Figure 4.3d). All improvements in the model fit made by the above parameter variations only improved the fit slightly, as fitting the near-source data tended to cause an over-prediction in the far source data. (But then again, with the R^2 value already so high, it is hard to make changes that can greatly improve it.) However, increasing the release height or horizontal wind velocity (by 4-6 times of the measured value) did reduce the tendency of the WALD model to under-predict the observed data.

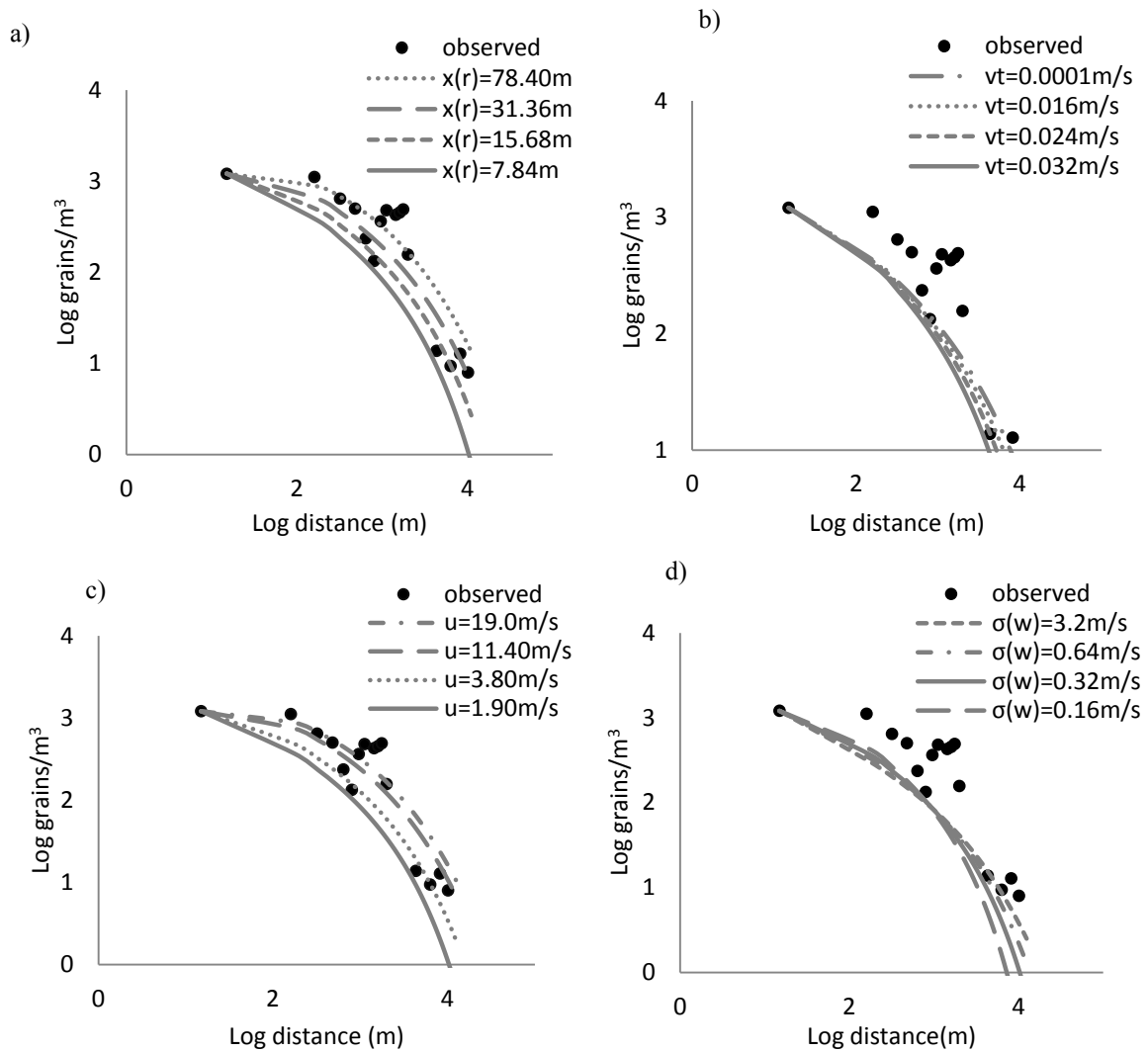


Figure 4.3: Observed *P. mariana* pollen concentrations from 0 to 10 km (●), and pollen concentrations as predicted by the WALD model. Predicted curves reflect the sensitivity analysis performed by modifying a) release height b) terminal velocity c) horizontal wind velocity d) variance in vertical wind velocity (turbulence). Solid line indicates average measured value (as used in Figure 4.1).

The Advection-Diffusion model already provided a relatively good fit of the observed data using the field-measured parameters. Most of the parameter modifications were not able to improve R^2 . Increasing horizontal wind velocity by 3-6 times that measured by the anemometer was the only parameter variation able to increase R^2 slightly (0.863), but this resulted in an over-prediction at almost all distances and brought the regression slope and intercept further from 1 and 0, respectively (Figure 4.4c).

Increasing v_t by 50% to 0.064 m/s (Figure 4.4b) reduced the over-prediction of the far tail and improved the regression slope and intercept ($\beta = 1.09$, $\alpha = 0.002$) but caused an under-prediction of the near-source data; decreasing release height to near zero had the same effect (Figure 4.4a). All improvements in the model fit made by the above parameter variations again only improved the fit slightly, as the model prediction using the measured data already resulted in a regression slope close to unity and an R^2 of 0.85.

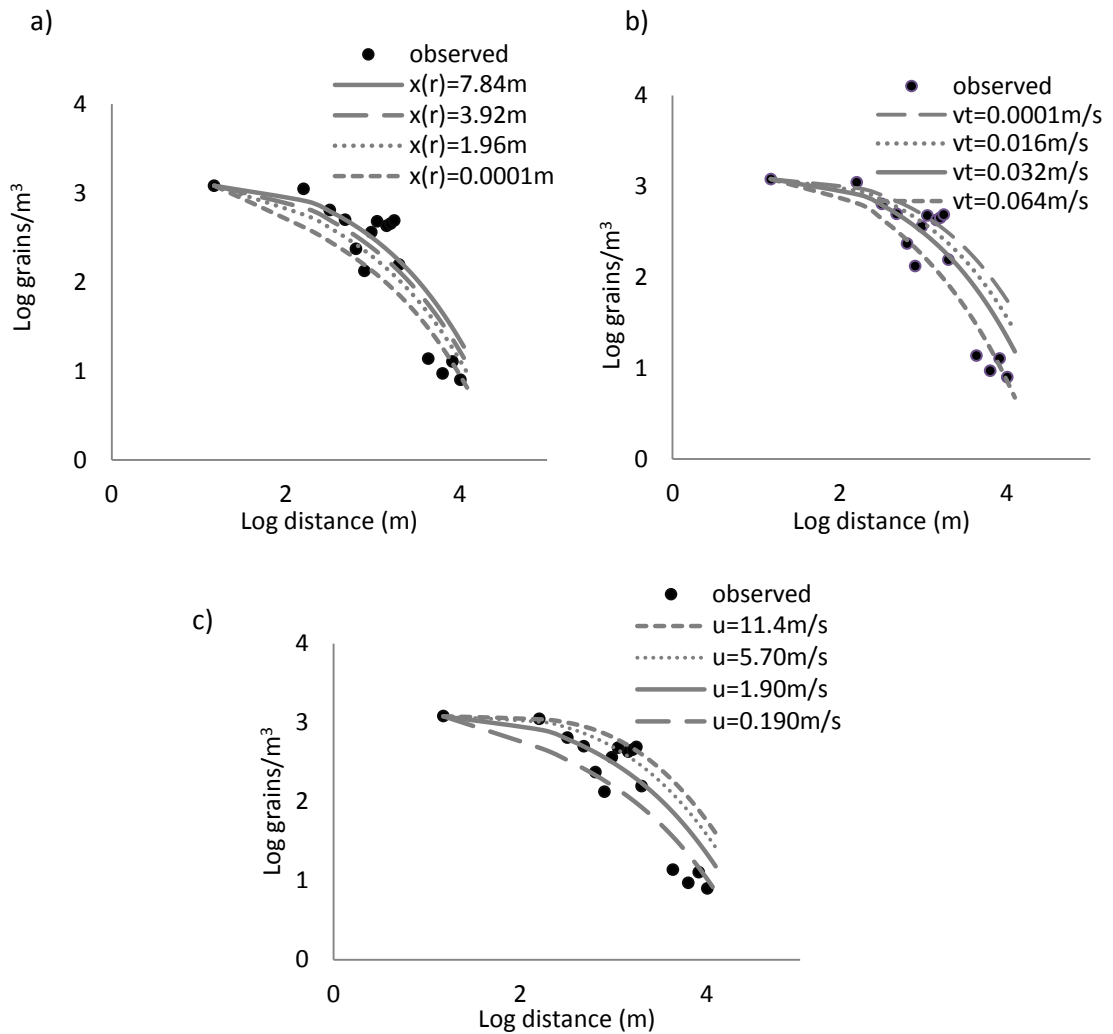


Figure 4.4: Observed *P. mariana* pollen concentrations from 0 to 10 km (●), and pollen concentrations as predicted by the Advection-Diffusion model. Predicted curves reflect the sensitivity analysis performed by modifying a) release height b) terminal velocity c) horizontal wind velocity. Solid line indicates average measured value (as used in Figure 4.1).

The tilted Gaussian model predicted a more rapid decline with distance than the previous two models, but still provided a relatively good fit (R^2 0.86) for both the near and far source data, under-predicting only in the last 2 km. The only parameter variation able to increase R^2 was decreasing v_t by 50% of the original value ($v_t=0.016\text{m/s}$), and even this only increased R^2 slightly (Figure 4.5b). The tilted Gaussian was much more sensitive to slight modifications than the other two models. Reducing the parameters by more than 50% of the measured values affected the curve dramatically, causing an over- or under-prediction at all distances. Using the field measured parameters provided the best fit of the observed data.

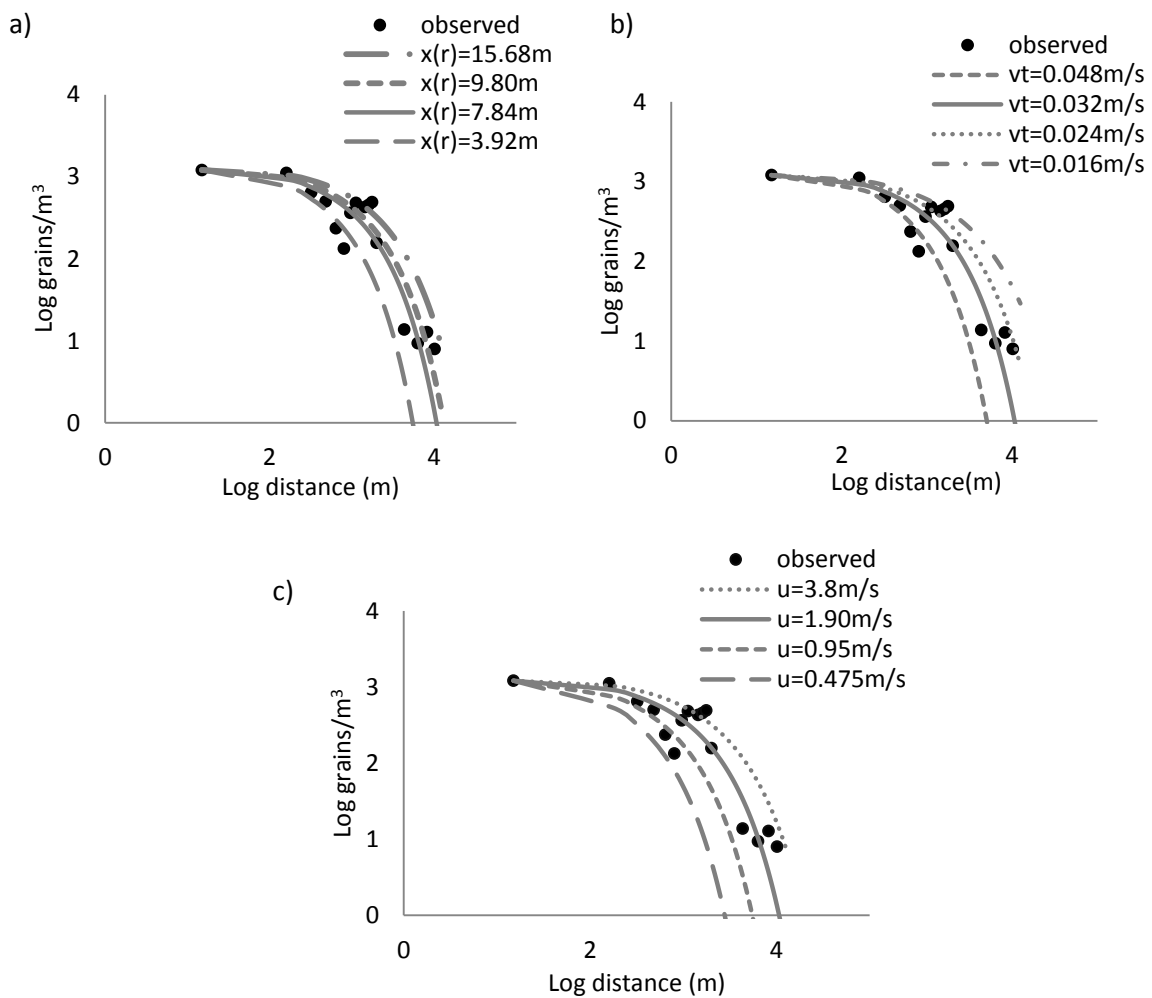


Figure 4.5: Observed *P. mariana* pollen concentrations from 0 to 10 km (●), and pollen concentrations as predicted by the tilted Gaussian plume model. Predicted curves reflect the sensitivity analysis performed by modifying a) release height b) terminal velocity c) horizontal wind velocity. Solid line indicates average measured value (as used in Figure 4.1).

4.4 *Abies balsamea*

For *Abies balsamea* the WALD, A-D and tilted Gaussian plume models all under-predicted the observed pollen concentrations at all distances. The A-D model exhibited the highest R^2 value (0.67), best regression line slope, and regression intercept closest to 0 of the three models (Table 4.5). However, all three models had a regression line slope that was significantly different from 1 and all intercepts were significantly different from 0 at the 95% confidence level (Table 4.5). Thus in sum for *Abies balsamea*, using slope, y-intercept, and R^2 of the regression as a measure of goodness-of-fit, the A-D model performed slightly better than the other two models, albeit still drastically under-predicted the measured data (Figure 4.6).

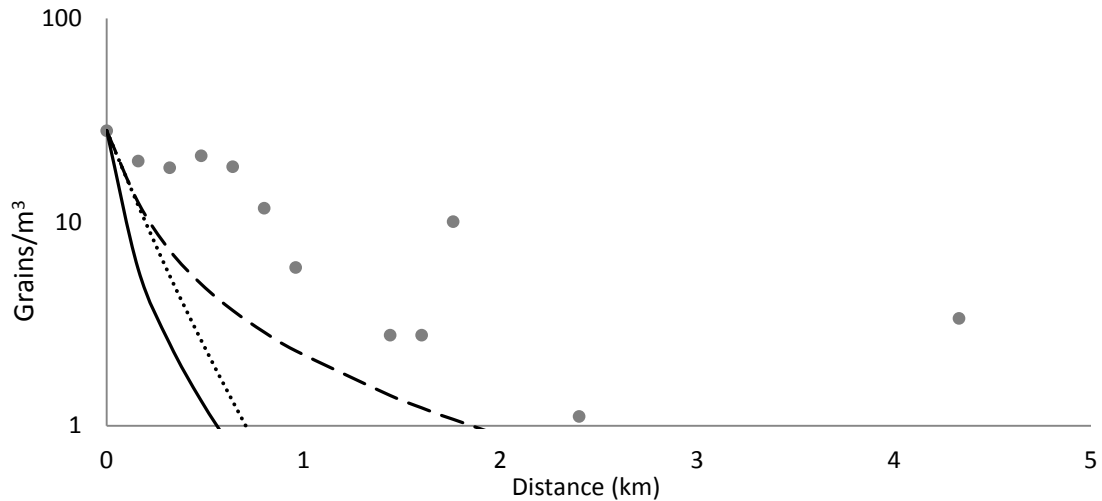


Figure 4.6: Observed (●) and Predicted grains/m³ for *Abies balsamea*, $v_t=0.0984\text{m/s}$, $h=8.233\text{m}$. Predictions based on the WALD(—), advection-diffusion(– –) and tilted Gaussian plume(•••) models.

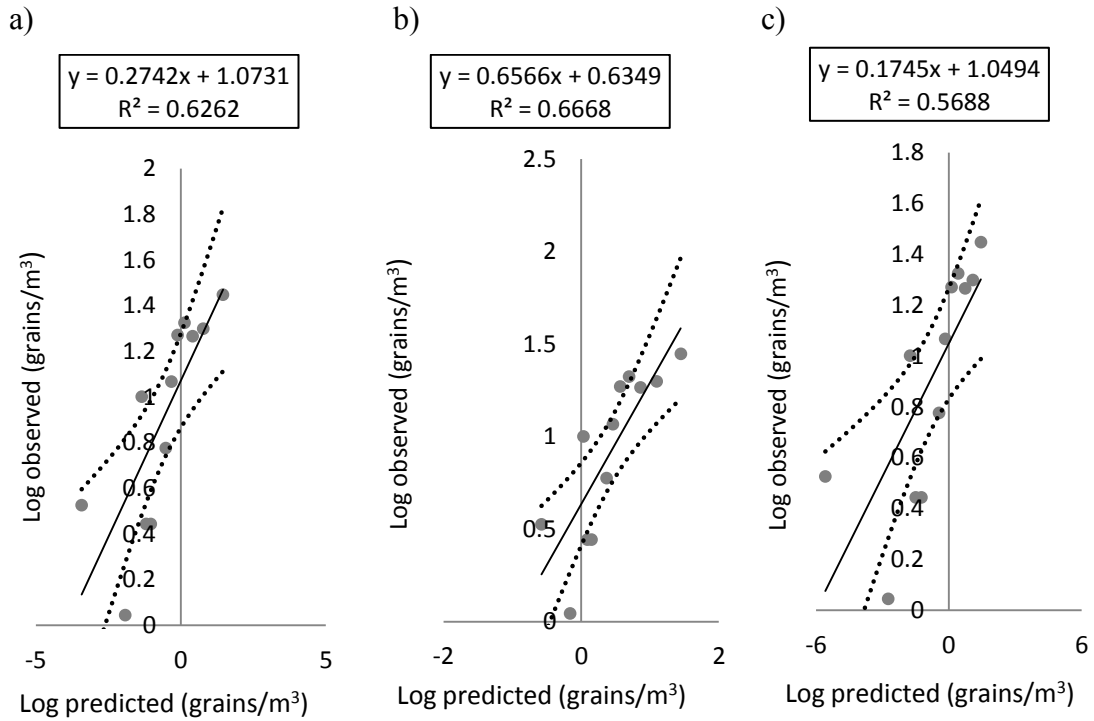


Figure 4.7: Linear regression of predicted versus observed pollen concentrations of *A. balsamea*, with associated 95% confidence intervals. Predicted values based on a) WALD b) advection-diffusion c) tilted Gaussian plume models.

Table 4.5: Statistical testing of *A. balsamea* with the three models. R^2 , slope (β) and y-intercept (α) of the associated best-fit line of the model predictions vs. observed concentration. 95% confidence intervals and the significance in the slope and y-intercept of the regression are also listed.

<i>A. balsamea</i>	R^2	β	α	95%		$p(\beta=1)$	$p(\alpha=0)$
				(β)	(α)		
WALD	0.626	0.274	1.073	0.149	0.207	7.58e-07	7.58e-07
A-D	0.667	0.657	0.635	0.327	0.223	0.0441	8.43e-05
Tilted	0.569	0.174	1.049	0.107	0.218	9.44e-09	8.32e-07

The WALD model exhibited the most drastic under-prediction of the three models and so the parameters had to be modified by a larger amount to improve the fit. All parameters had to be increased by unrealistic amounts to improve R^2 and attempt to shift the curve upwards and reduce the under-prediction. Doubling x_r , \bar{u} , or v_r still resulted in a great under-prediction at all distances, especially near the source forest. Increasing x_r ,

or \bar{u} by as much as four times the measured release height (32.93 m) improved the fit of the far-source data but still under-predicted all near-source dispersal points (Figure 4.8a,c). Increasing x_r or \bar{u} by 10 times the measured value were the only two parameter changes able improve the fit at both near and far distances. This dramatic increase in either parameter increased R^2 by 0.02, and brought the regression slope and intercept closer to 1 and 0, but a release height of 82.3 m or a wind speed of 23.5m/s is quite unrealistic. Also reducing v_t to 0.0001m/s (Figure 4.8b), brought the slope of the regression line much closer to 1.0 ($\beta=0.82$) and slightly improved the fit ($R^2=0.64$) but even with this near zero terminal velocity, the WALD model still under-predicted at most distances. Changing the variance in the vertical wind velocity component (σ_w) did not have much of an effect on the predicted curve; even modifying the turbulence parameter by 100 times the observed value could not shift the curve enough to seriously reduce the WALD under-prediction (Figure 4.8d). Summing up, the model was most sensitive to changes in x_r and \bar{u} , but even these two parameters had to be increased by a considerable amount to counteract the under-prediction.

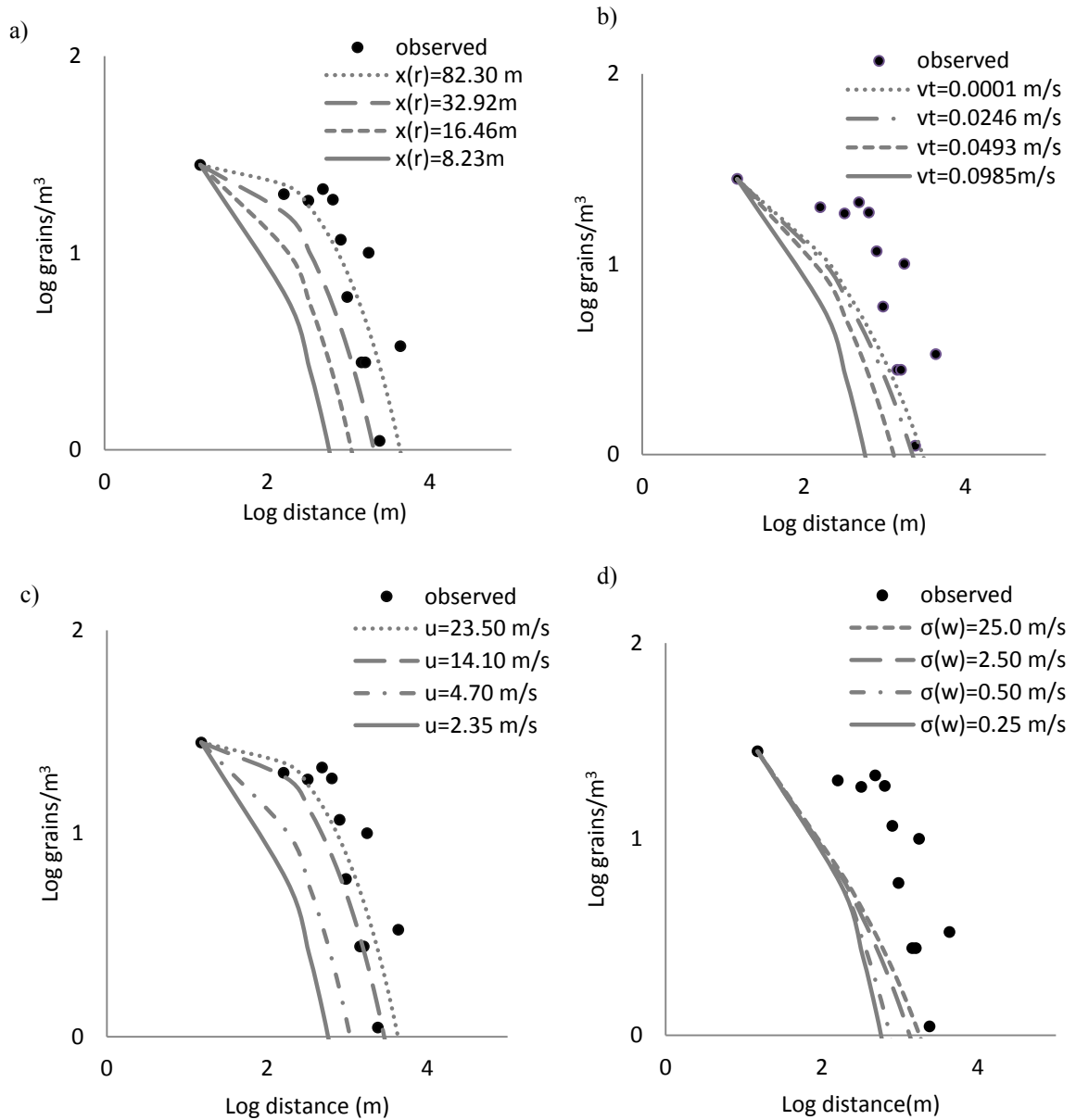


Figure 4.8: Observed *A. balsamea* pollen concentrations from 0 to 5 km (●), and pollen concentrations as predicted by the WALD model. Predicted curves reflect the sensitivity analysis performed by modifying a) release height b) terminal velocity c) horizontal wind velocity d) variance in vertical wind velocity (turbulence). Solid line indicates average measured value (as used in Figure 4.6).

Likewise, for the Advection-Diffusion model, doubling x_r or \bar{u} improved the regression slope ($\beta=0.76$) and improved R^2 slightly (by 0.01) but still under-predicted the majority of the observed data. Increasing these parameters by 4-6 times improved the

regression slope and intercept, and provided a better fit of both near- and far-source data. Terminal velocity had to be reduced by 50%-75% of the measured value to achieve the same effect. Fitting the long distance dispersal points (2-4 km for *Abies*) required changing x_r , \bar{u} or v_t by 10 or more times that of the measured values, but as before, fitting the far dispersal points tended to over-predict the near dispersal points (Figure 4.9a,b,c). The fit for *A. balsamea* using the A-D model was already better than the WALD or tilted Gaussian using field-measured parameters (dashed line - Figure 4.6), and all parameter variations were only able improve the R^2 of the regression by 0.01 at most.

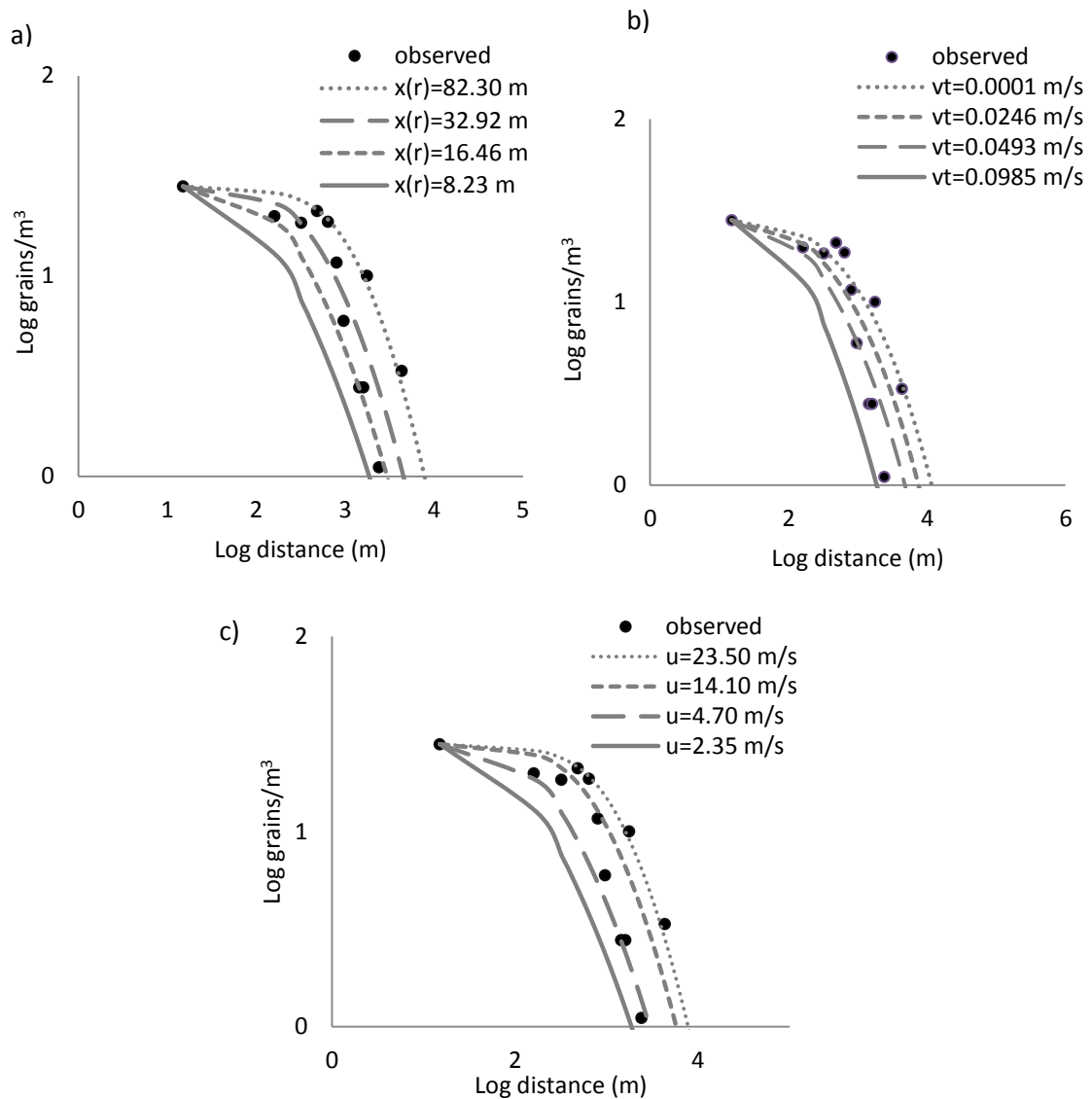


Figure 4.9: Observed *A. balsamea* pollen concentrations from 0 to 5km (●), and pollen concentrations as predicted by the Advection-Diffusion model. Predicted curves reflect the sensitivity analysis performed by modifying a) release height b) terminal velocity c) horizontal wind velocity. Solid line indicates average measured value (as used in Figure 4.6).

The tilted Gaussian plume model provided a fit intermediate between that of WALD and A-D models, hence still under-predicted at all distances. The tilted Gaussian model was more or less equally sensitive to changes in x_r , \bar{u} or v_t . Increasing x_r or \bar{u} to between 4 and 6 times the measured yielded the best fit; reducing v_t by 4 fold had the same effect (Figure 4.10a,b,c). The best R^2 (0.65) resulted from reducing v_t by 10 times

the measured value, but this caused an over-prediction at almost all dispersal points (Figure 4.10b).

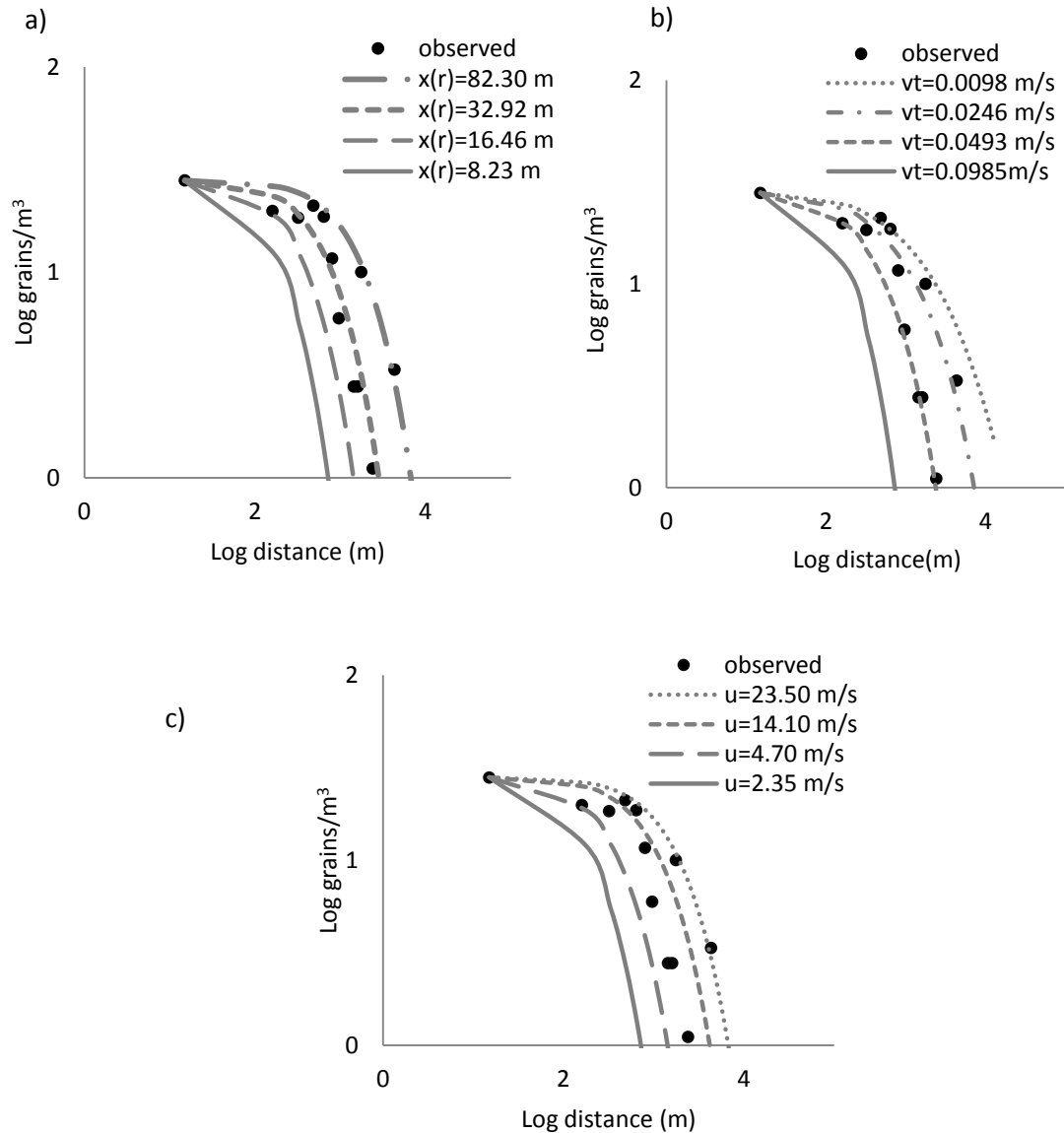


Figure 4.10: Observed *A. balsamea* pollen concentrations from 0 to 5 km (●), and pollen concentrations as predicted by the tilted Gaussian plume model. Predicted curves reflect the sensitivity analysis performed by modifying a) release height b) terminal velocity c) horizontal wind velocity. Solid line indicates average measured value (as used in Figure 4.6).

4.5 *Pinus banksiana*

For *Pinus banksiana*, all three models fit the observed data relatively well, although the A-D and tilted Gaussian plume models still over-predicted almost all of the

measured pollen concentrations, and the WALD model again under-predicted pollen concentrations at almost all distances. The A-D and WALD models had essentially the same R^2 (0.80) but the WALD model had a slope much closer to 1 and an intercept closer to 0 than the other two models (Table 4.6, Figure 4.12a). The tilted Gaussian had the lowest R^2 of the three models. The WALD and tilted Gaussian had regression line slopes not significantly different from 1, and regression intercepts not significantly different

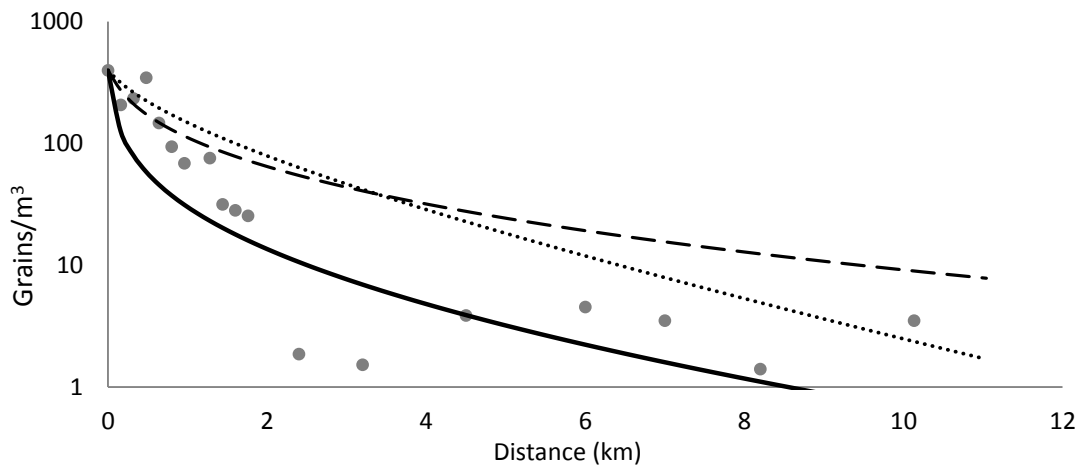


Figure 4.11: Observed (●) and Predicted grains/m³ for *Pinus banksiana*, $v_t=0.0254\text{m/s}$, $h=7.23\text{m}$. Predictions based on the WALD(—), advection-diffusion(– –) and tilted Gaussian plume(•••) models.

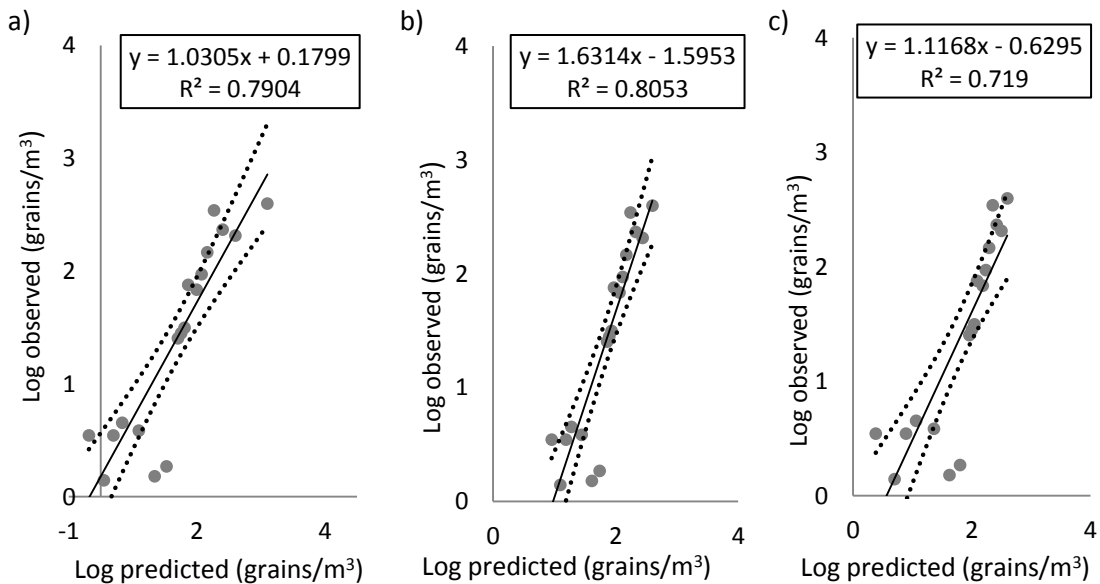


Figure 4.12: Linear regression of predicted versus observed pollen concentrations of *P. banksiana*, with associated 95% confidence intervals. Predicted values based on a) WALD b) advection-diffusion c) tilted Gaussian plume models.

from 0 at the 95% confidence level (Table 4.6). Both the slope and intercept of the A-D model regression were not significantly close to 1 or 0. Unlike the trials with the previous two species, the WALD model seemed to perform the better than the other two models, although still under-predicting the majority of the measured data.

Table 4.6: Statistical testing of *P.banksiana* with the three models. R^2 , slope (β) and y-intercept (α) of the associated best-fit line of the model predictions vs. observed concentration. 95% confidence intervals and the significance in the slope and y-intercept of the regression are also listed.

<i>P. banksiana</i>	R^2	β	α	95%		p($\beta=1$)	p($\alpha=0$)
				(β)	(α)		
WALD	0.790	1.030	0.180	0.281	0.388	0.821	0.340
A-D	0.805	1.631	-1.595	0.425	0.802	0.006	0.006
Tilted	0.719	1.117	-0.629	0.370	0.709	0.513	0.078

For the *P. banksiana* sensitivity analysis of the WALD model, changing v_t or σ_w did not improve the curve. Even when these parameters were modified by a considerable amount (Figure 4.13 b, d) the WALD model still under-predicted everywhere except at the far tail. The model was again more responsive to changes in release height or horizontal wind velocity. Increasing these two parameters by 4 times their measured values ($x_r=28.92\text{m}$, $\bar{u}=8.0\text{m/s}$) increased R^2 by 0.01 but moved the regression slope further from 1 (Figure 4.13a,c). The R^2 and regression slope were best when using the field-measured terminal velocity, release height, variance in vertical wind and horizontal wind velocity

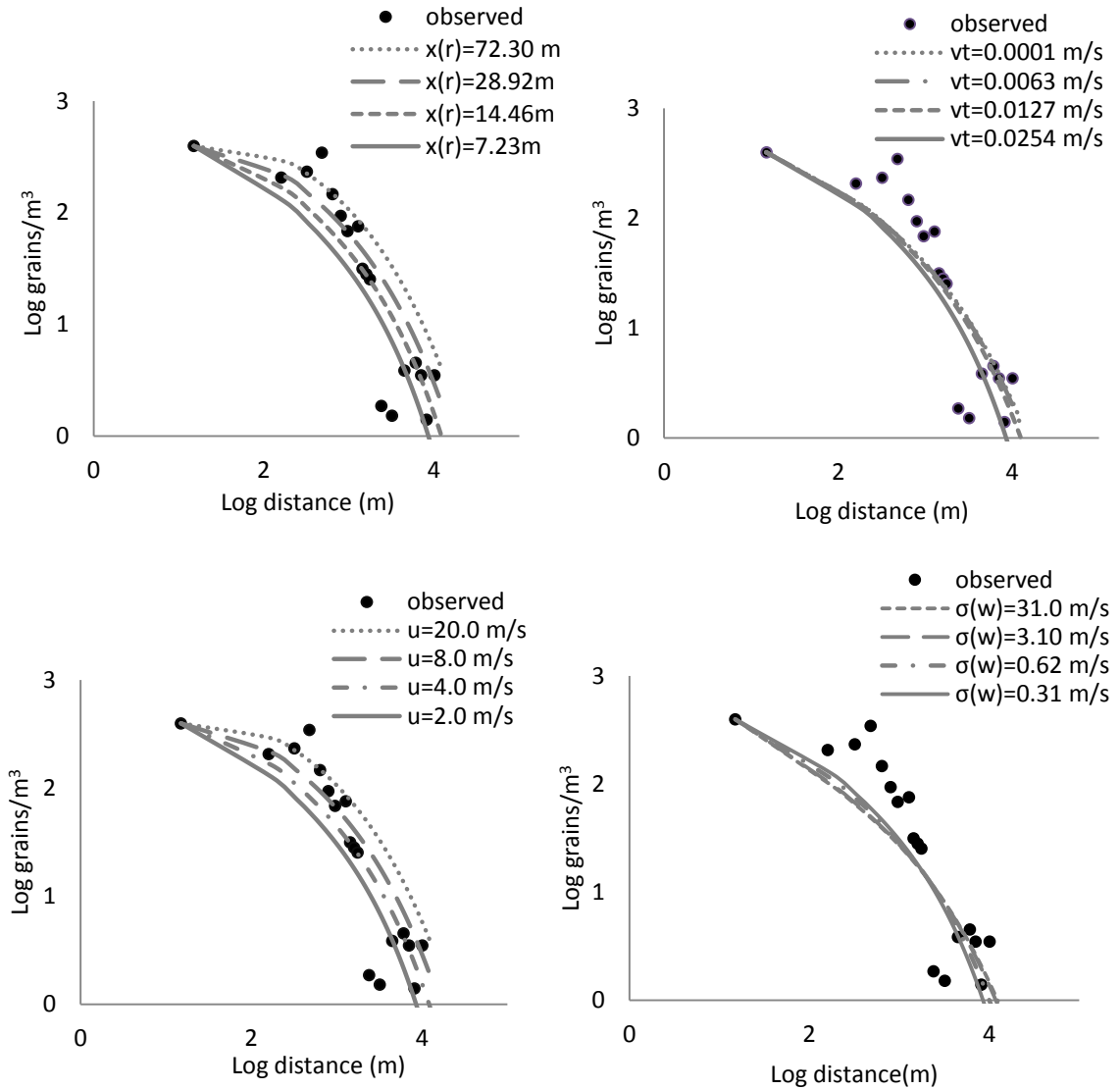


Figure 4.13: Observed *P.banksiana* pollen concentrations from 0 to 10 km (●), and pollen concentrations as predicted by the WALD model. Predicted curves reflect the sensitivity analysis performed by modifying a) release height b) terminal velocity c) horizontal wind velocity d) variance in vertical wind velocity (turbulence). Solid line indicates average measured value (as used in Figure 4.11).

For the A-D model reducing x_r or \bar{u} , was unable to improve the goodness-of-fit of the curve. Even reducing release height or horizontal wind to near zero could not affect the curve enough to reduce the over-prediction, especially at the far tail (Figure 4.14a,c). Terminal velocity was the only parameter able to cause significant changes to the predicted A-D dispersal curve, reducing the over-prediction at the far tail. Increasing v_t

by 3 times the measured amount, to 0.762 m/s, led to a better fit of the far-tail and increased R^2 to 0.813 but in turn caused an under-prediction at short-distances (Figure 4.14b).

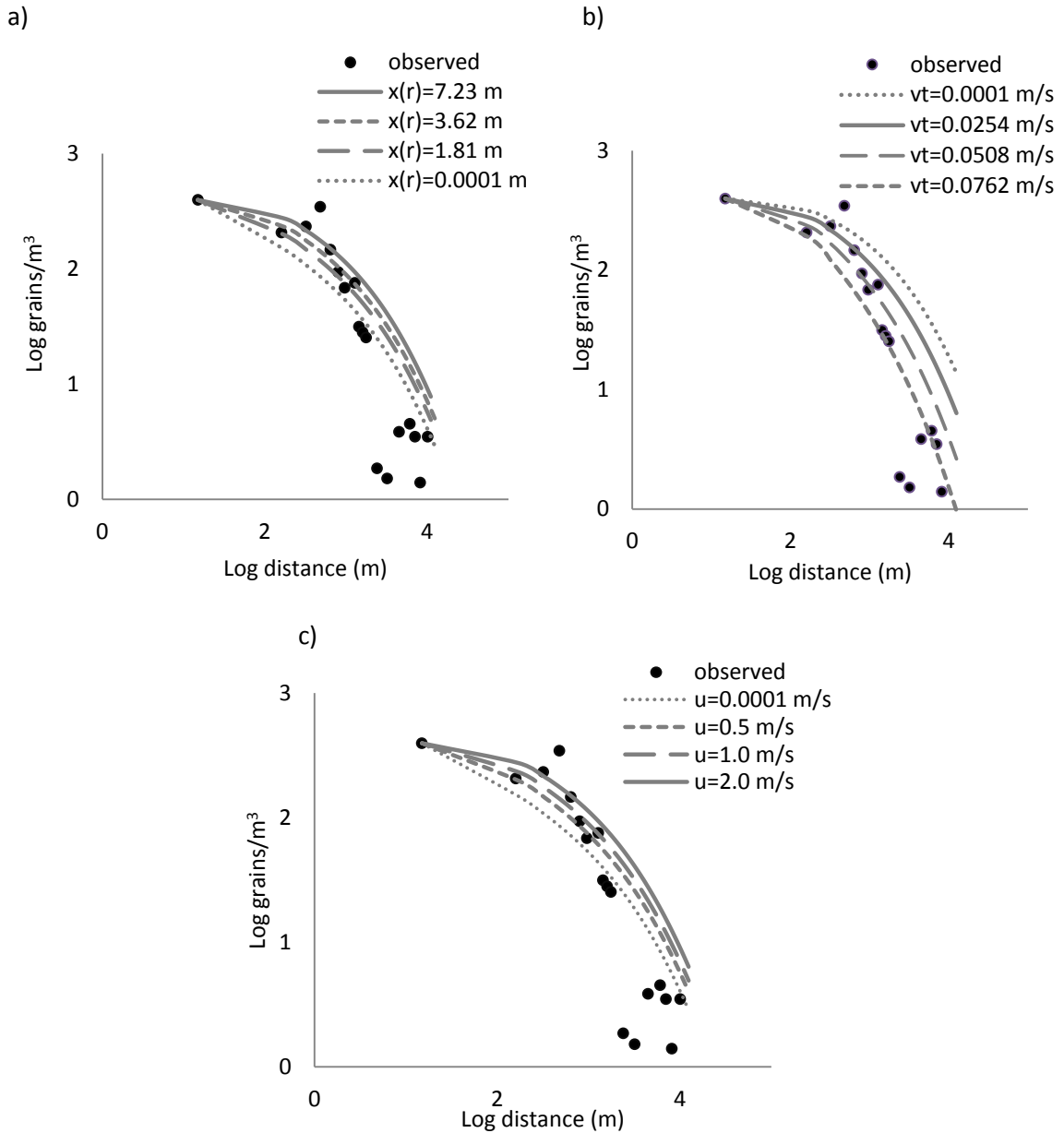


Figure 4.14: Observed *P.banksiana* pollen concentrations from 0 to 10 km (●), and pollen concentrations as predicted by the Advection-Diffusion model. Predicted curves reflect the sensitivity analysis performed by modifying a) release height b) terminal velocity c) horizontal wind velocity. Solid line indicates average measured value (as used in Figure 4.11).

For the tilted Gaussian plume, changing any one of the parameters was unable to greatly improve the R^2 or regression coefficients. Whatever improvements were possible occurred only with smaller increments of change in x_r , v_t or \bar{u} . Reducing x_r or \bar{u} by half was able to shift the curve down significantly, reducing the over-prediction, without causing too much of an under-prediction at short-distances (Figure 4.15a,c). Increasing v_t by 25% of the original terminal velocity had the same effect without causing too much of an under-prediction at long-distances (Figure 4.15b). Decreasing x_r , \bar{u} , by more than 50% or increasing v_t by more than 25% of the original value started to degrade the fit and only further augmented the under-prediction. Nonetheless, using the field-measured parameters yielded the best R^2 and the regression coefficients for the tilted Gaussian, as was the case with the previous two models.

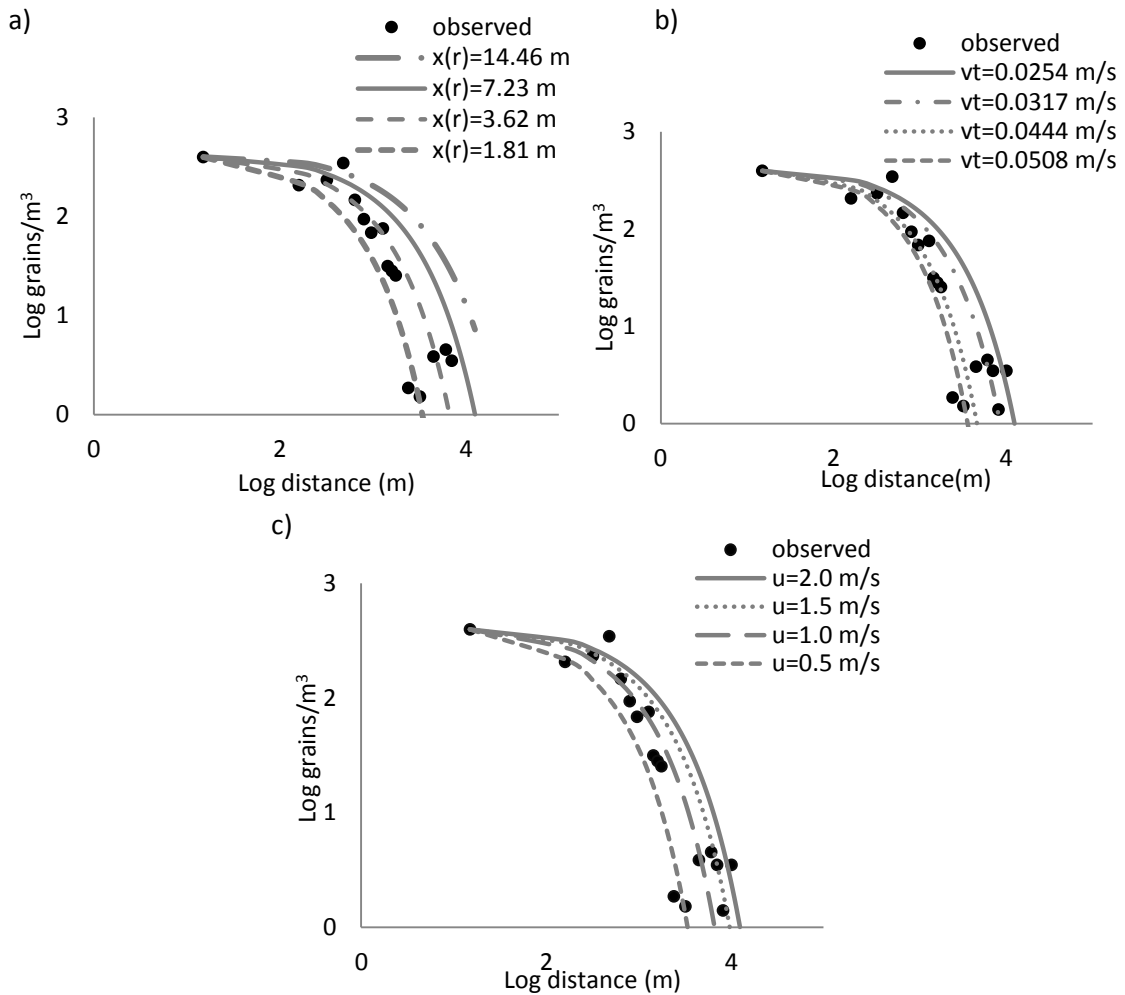


Figure 4.15: Observed *P. banksiana* pollen concentrations from 0 to 10 km (●), and pollen concentrations as predicted by the tilted Gaussian plume model. Predicted curves reflect the sensitivity analysis performed by modifying a) release height b) terminal velocity c) horizontal wind velocity. Solid line indicates average measured value (as used in Figure 4.11).

4.6 *Alnus rugosa*

For the shrub *Alnus rugosa* we only could examine dispersal out to 2 km. The fit was relatively good with all three models, especially for the A-D and tilted Gaussian plume models (Figure 4.16). The R^2 was highest for the WALD model (Figure 4.17), but both the slope and intercepts of the regression were significantly different from 1 and 0, respectively ($p < 0.05$; Table 4.7), and it under-predicted all observed data points. The A-D and tilted Gaussian both had regression slopes not significantly different from 1 and

intercepts not significantly different from 0 ($p > 0.05$). Overall the fit was much better for all models than that predicted with the previous three species; the over- and under-predictions for *A. rugosa* were much less, but the measured dispersal distance was also much less.

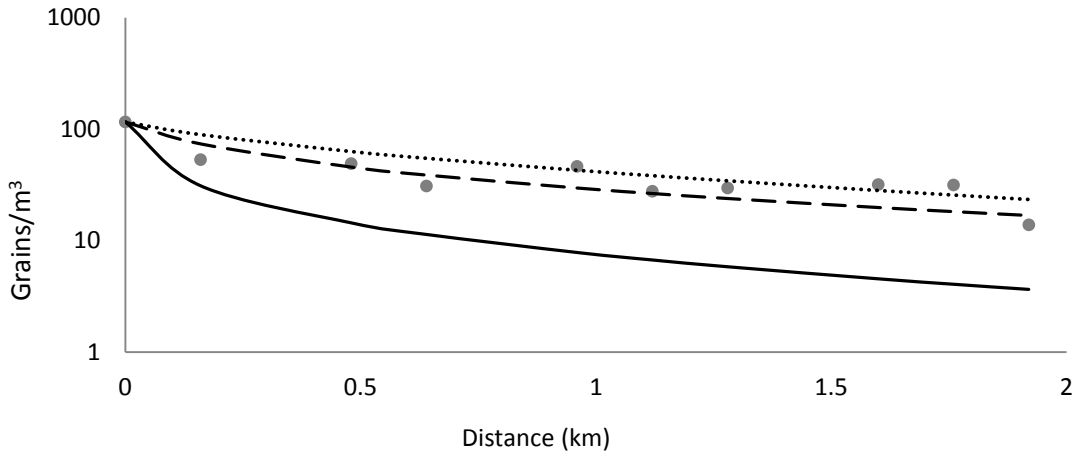


Figure 4.16: Observed (●) and Predicted grains/m³ for *Alnus rugosa*, $v_t=0.0195\text{m/s}$, $h=3.86\text{m}$. Predictions based on the WALD(—), advection-diffusion(---) and tilted Gaussian plume(⋯) models.

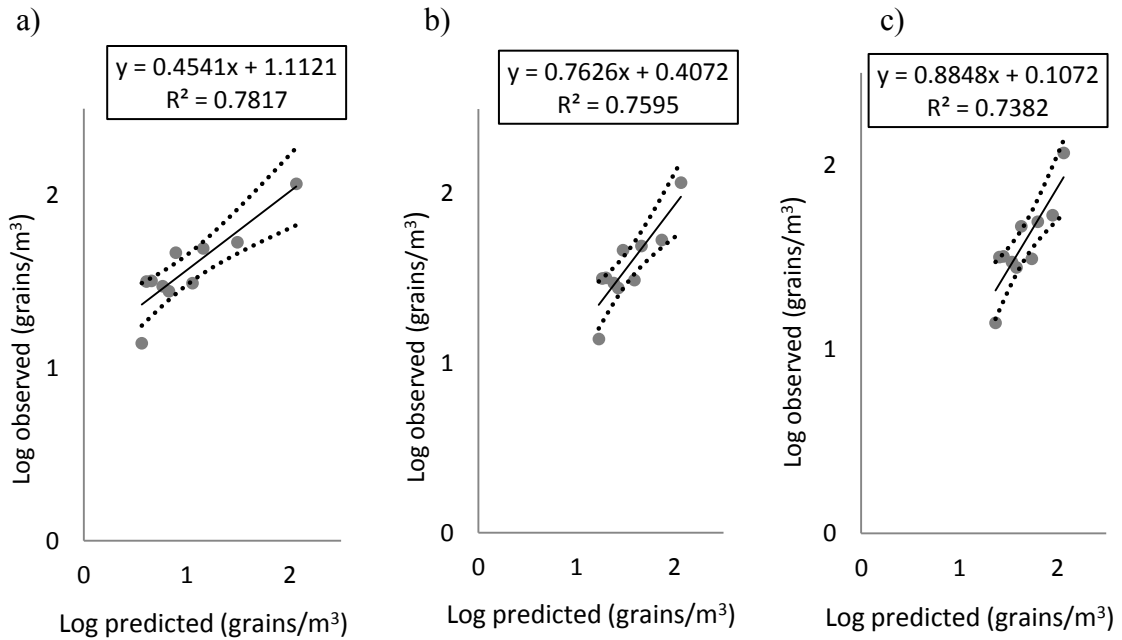


Figure 4.17: Linear regression of predicted versus observed pollen concentrations of *A. rugosa*, with associated 95% confidence intervals. Predicted values based on a) WALD b) advection-diffusion c) tilted Gaussian plume models.

Table 4.7: Statistical testing of *A.rugosa* with the three models. R^2 , slope (β) and y-intercept (α) of the associated best-fit line of the model predictions vs. observed concentration. 95% confidence intervals and the significance in the slope and y-intercept of the regression are also listed.

<i>A. rugosa</i>	R^2	β	α	95%		p(β)	p(α)
				(β)	(α)		
WALD	0.782	0.454	1.112	0.196	0.216	0.0002	2.3e-6
A-D	0.759	0.763	0.407	0.350	0.541	0.156	0.121
Tilted	0.738	0.885	0.107	0.430	0.717	0.553	0.739

For the *A. rugosa* sensitivity analysis of the WALD model (Figure 4.18), none of the parameter variations were able to improve the goodness-of-fit. Modifying ν_t or σ_w had virtually no effect on the curve. Changing x_r , and \bar{u} had more of an effect on the predicted curve, but only if the change was quite dramatic. Doubling x_r , or \bar{u} had little effect on either R^2 , or the slope and intercept of the regression, and still under-predicted all observed data. Increasing release height or horizontal wind velocity (Figure 4.18a,c) by 10 times the measured value improved the slope and intercept ($\beta=0.59$, $\alpha=0.77$) but did not reduce the WALD under-prediction. None of the parameter variations for the WALD model were able to improve R^2 or reduce the under-prediction enough to fit the observed data points.

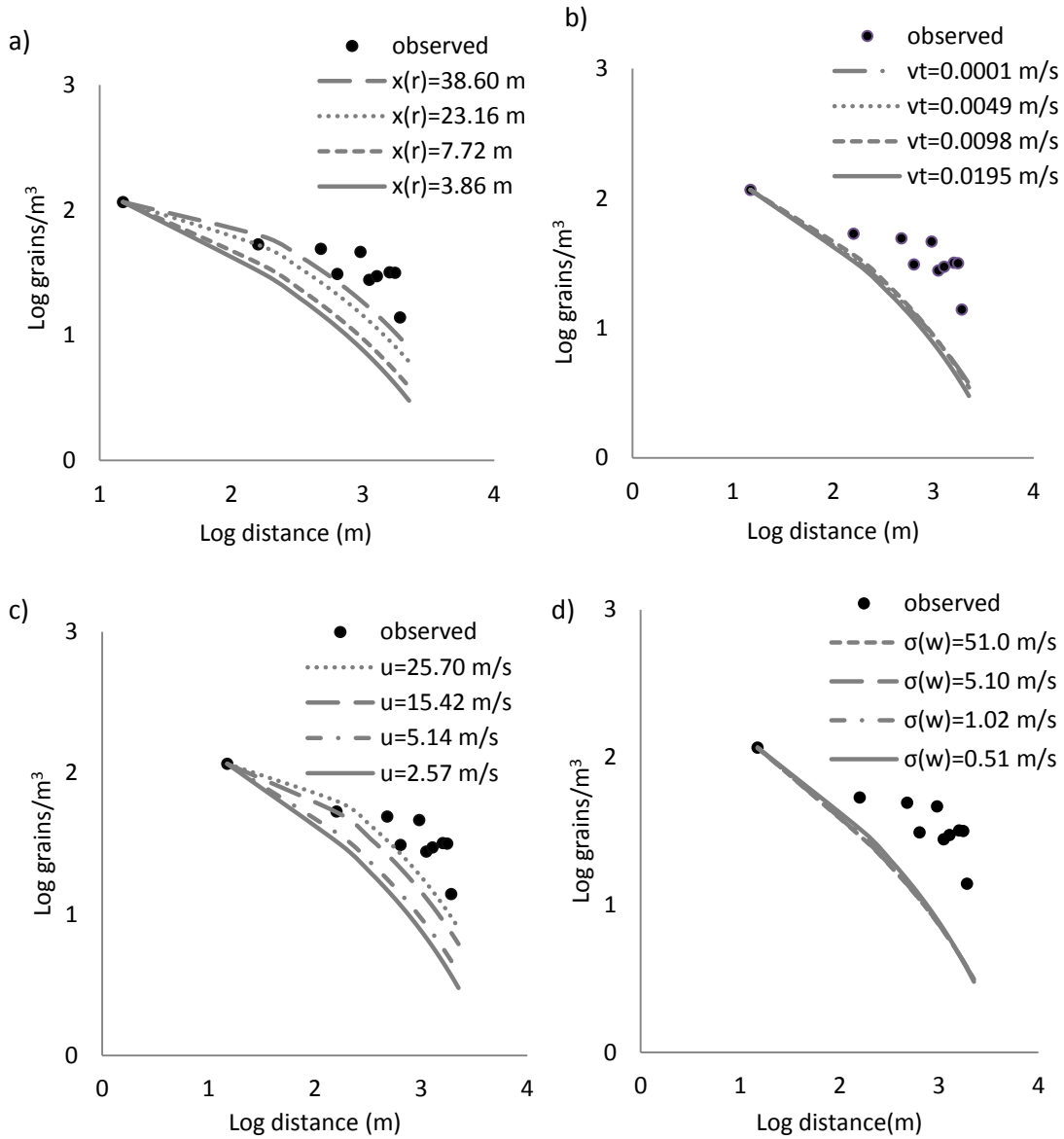


Figure 4.18: Observed *A. rugosa* pollen concentrations from 0 to 2 km (●), and pollen concentrations as predicted by the WALD model. Predicted curves reflect the sensitivity analysis performed by modifying a) release height b) terminal velocity c) horizontal wind velocity d) variance in vertical wind velocity (turbulence). Solid line indicates average measured value (as used in Figure 4.16).

For the *A. rugosa* sensitivity analysis of the Advection-Diffusion model (Figure 4.19), doubling v_t , or halving x_r , or \bar{u} resulted in a 0.01 increase in R^2 but worsened the regression slope and intercept. The best fit for the A-D model was obtained with the field-measured parameters; in particular, a regression slope not significantly different

from 1, and a regression intercept not significantly different from 0. Changing x_r , \bar{u} , or v_t only worsened the fit.

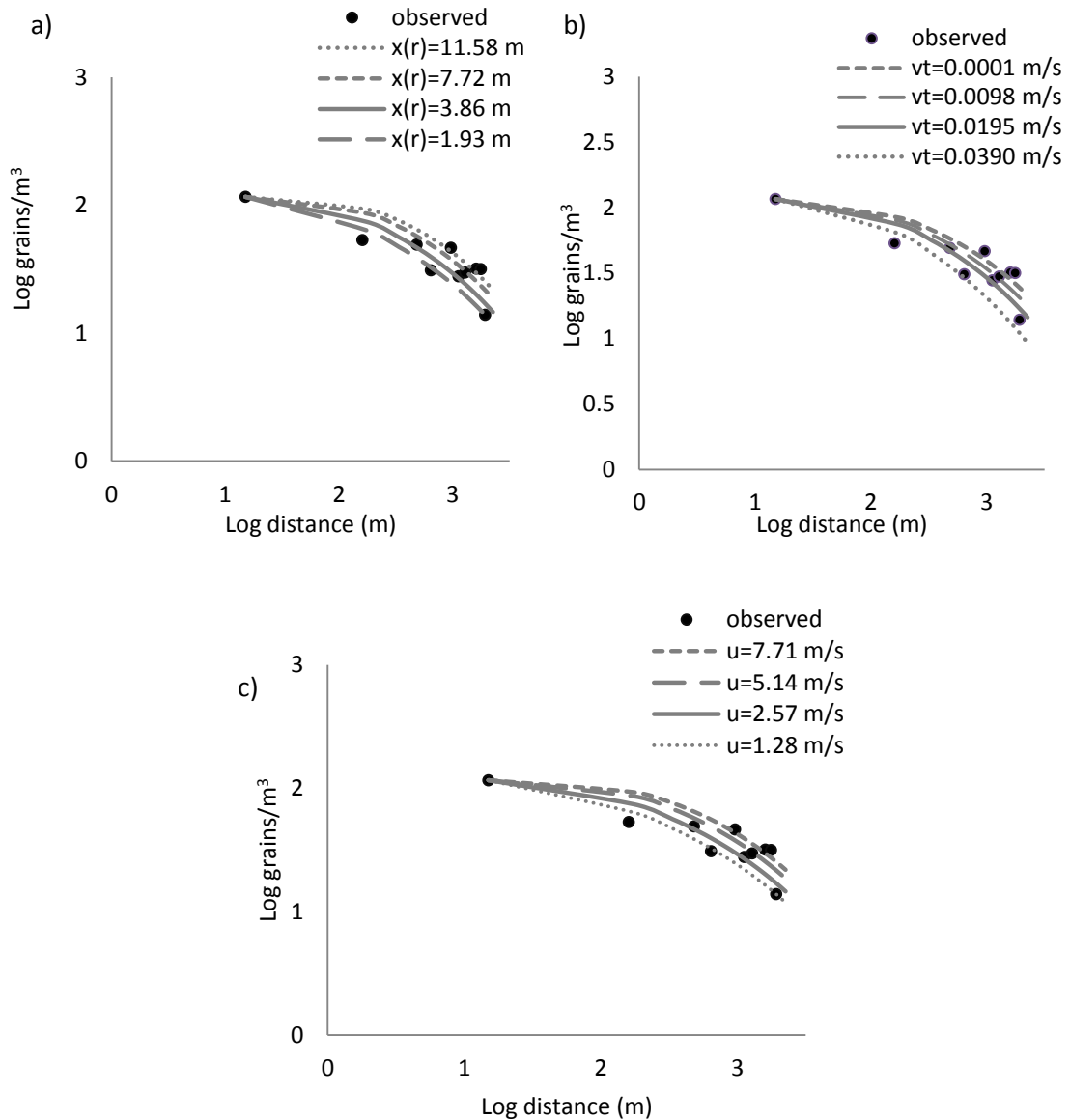


Figure 4.19: Observed *A.rugosa* pollen concentrations from 0 to 2 km (●), and pollen concentrations as predicted by the Advection-Diffusion model. Predicted curves reflect the sensitivity analysis performed by modifying a) release height b) terminal velocity c) horizontal wind velocity. Solid line indicates average measured value (as used in Figure 4.16).

For the sensitivity analysis of the tilted Gaussian plume model (Figure 4.20), slight modifications to x_r and \bar{u} improved R^2 , but did not bring the regression slope closer

to unity or the intercept closer to zero. Reducing x_r and \bar{u} by 25% of their field-measured values (to 2.89 m and 1.93 m/s) only brought R^2 up by 0.01 (Figure 4.20a,c). Modifying v_t did not improve the goodness-of-fit. As with the Advection-Diffusion, the field-measured parameters yielded the best predicted curve for *A. rugosa*.

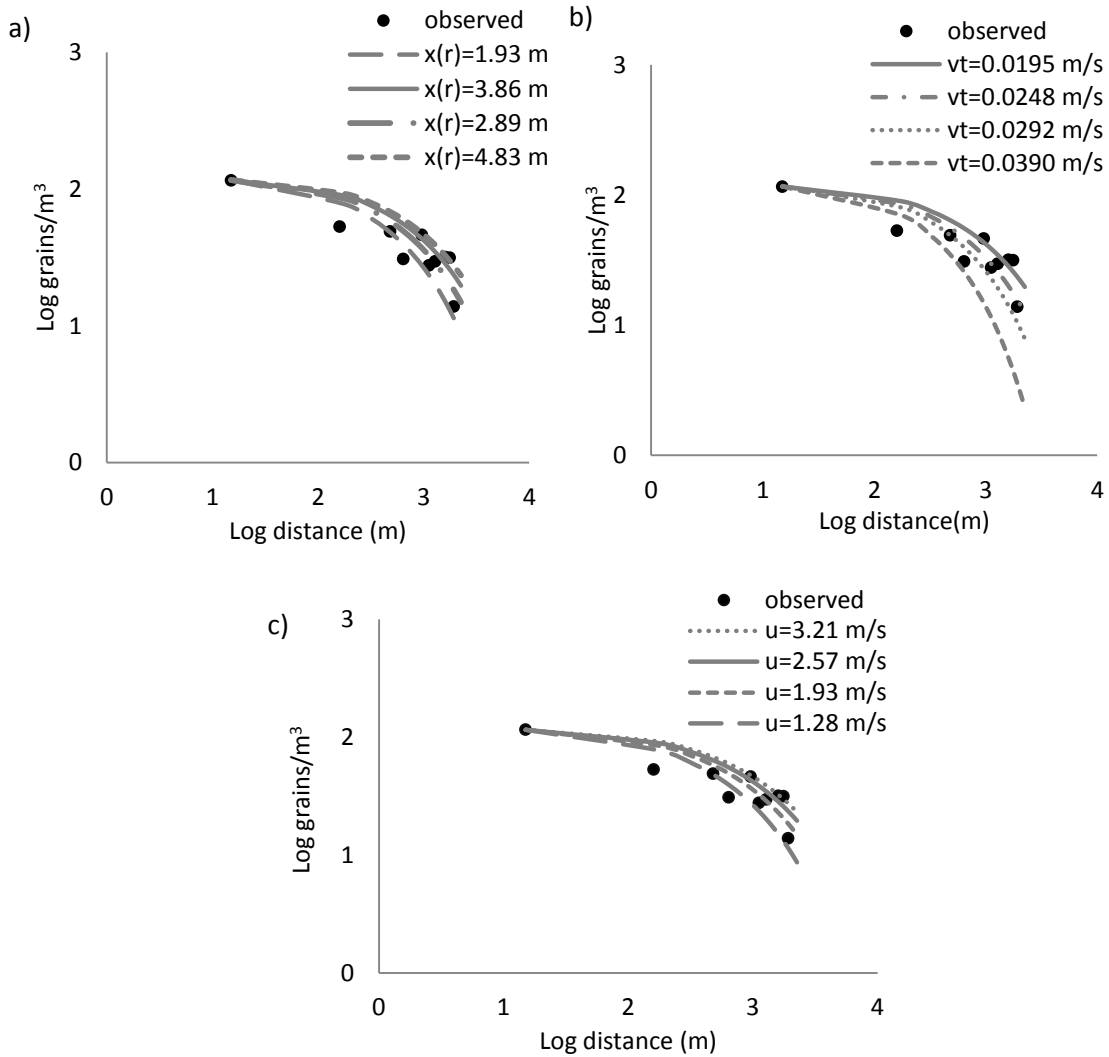


Figure 4.20: Observed *A. rugosa* pollen concentrations from 0 to 2 km (●), and pollen concentrations as predicted by the tilted Gaussian plume model. Predicted curves reflect the sensitivity analysis performed by modifying a) release height b) terminal velocity c) horizontal wind velocity. Solid line indicates average measured value (as used in Figure 4.16).

4.7 *Lycopodium clavatum* (point source)

For the *L. clavatum* point source experiment, the WALD, A-D and tilted Gaussian exhibited extreme over-predictions when using the actual number of spores released as the source strength (Q). The WALD model had the highest R^2 while the other two models had slightly lower R^2 values. The tilted Gaussian had the regression slope closest to 1 (Figure 4.22), but all three models had regression slopes statistically different from 1 (Table 4.8) and the regression intercepts were also all significantly different from 0 ($p \leq 0.05$).

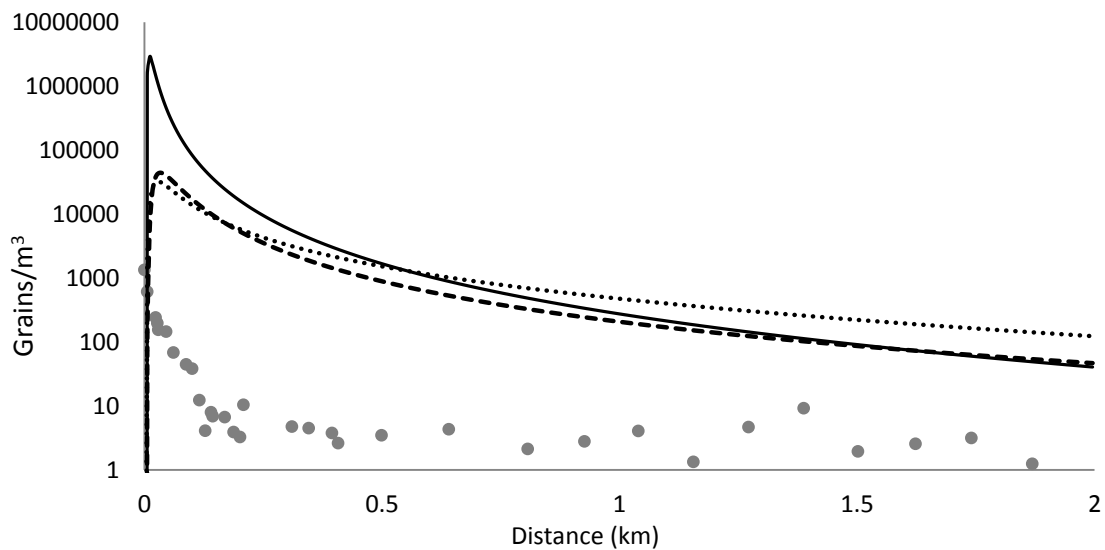


Figure 4.21: Observed (●) and Predicted grains/m³ for for *Lycopodium clavatum*, $v_t=0.0195\text{m/s}$, $h=2.0\text{ m}$. Predictions based on the WALD(—), advection-diffusion(---) and tilted Gaussian plume(•••) models.

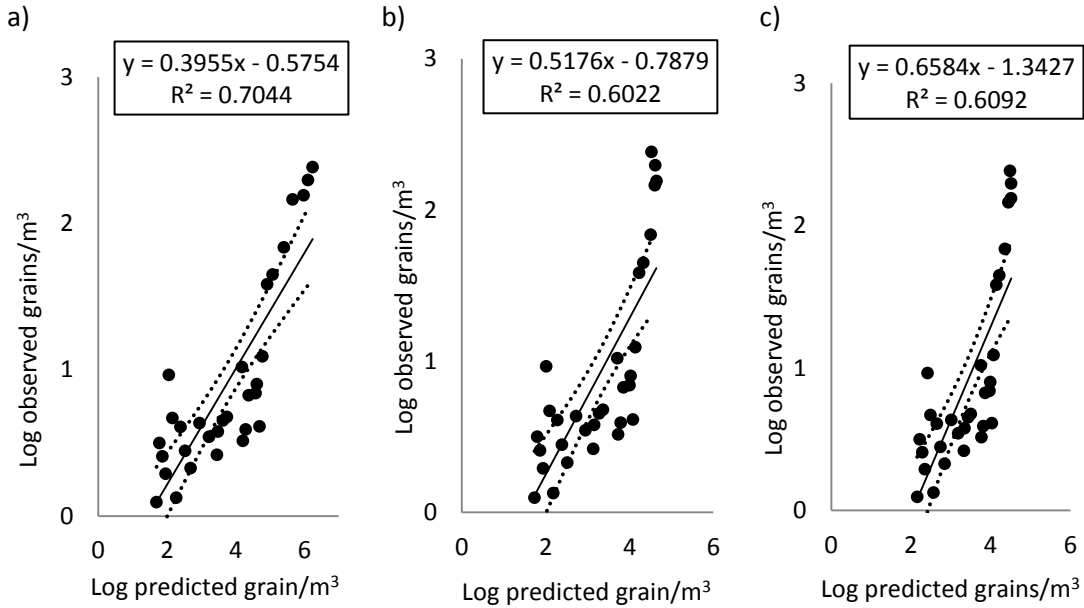


Figure 4.22: Linear regression of predicted versus observed pollen concentrations of *L. clavatum*, with associated 95% confidence intervals. Predicted values based on a) WALD b) advection-diffusion c) tilted Gaussian plume models.

Table 4.8: Statistical testing of *L.clavatum* with the three models. R^2 , slope (β) and y-intercept (α) of the associated best-fit line of the model predictions vs. observed concentration. 95% confidence intervals and the significance in the slope and y-intercept of the regression are also listed.

<i>L. clavatum</i>	R^2	β	α	95%		p(β)	p(α)
				(β)	(α)		
WALD	0.704	0.396	-0.575	0.097	0.391	2.23e-13	0.005
A-D	0.602	0.518	-0.788	0.159	0.549	9.88E-07	0.006
Tilted	0.609	0.658	-1.343	0.200	0.705	0.002	0.0005

For the sensitivity analysis of the WALD predicted dispersal distances, decreasing release height or horizontal wind velocity by 50% of the measured value (Figure 4.23 a,b), increased R^2 slightly, but the model still greatly over-predicted all observed data points. The WALD model was most sensitive to changes in x_r or v_t , and least sensitive to changes in σ_w ; even changing the latter by 100 times the measured value ($\sigma_w=20\text{m/s}$) had the little effect on the curve (Figure 4.23d). Increasing x_r or \bar{u} by 10 times, or v_t to 4 times the measured amount, better fit the far tail of the dispersal data, but not the near.

Virtually all of the parameter variations were unable to reduce the over-prediction enough to fit the majority of observed data.

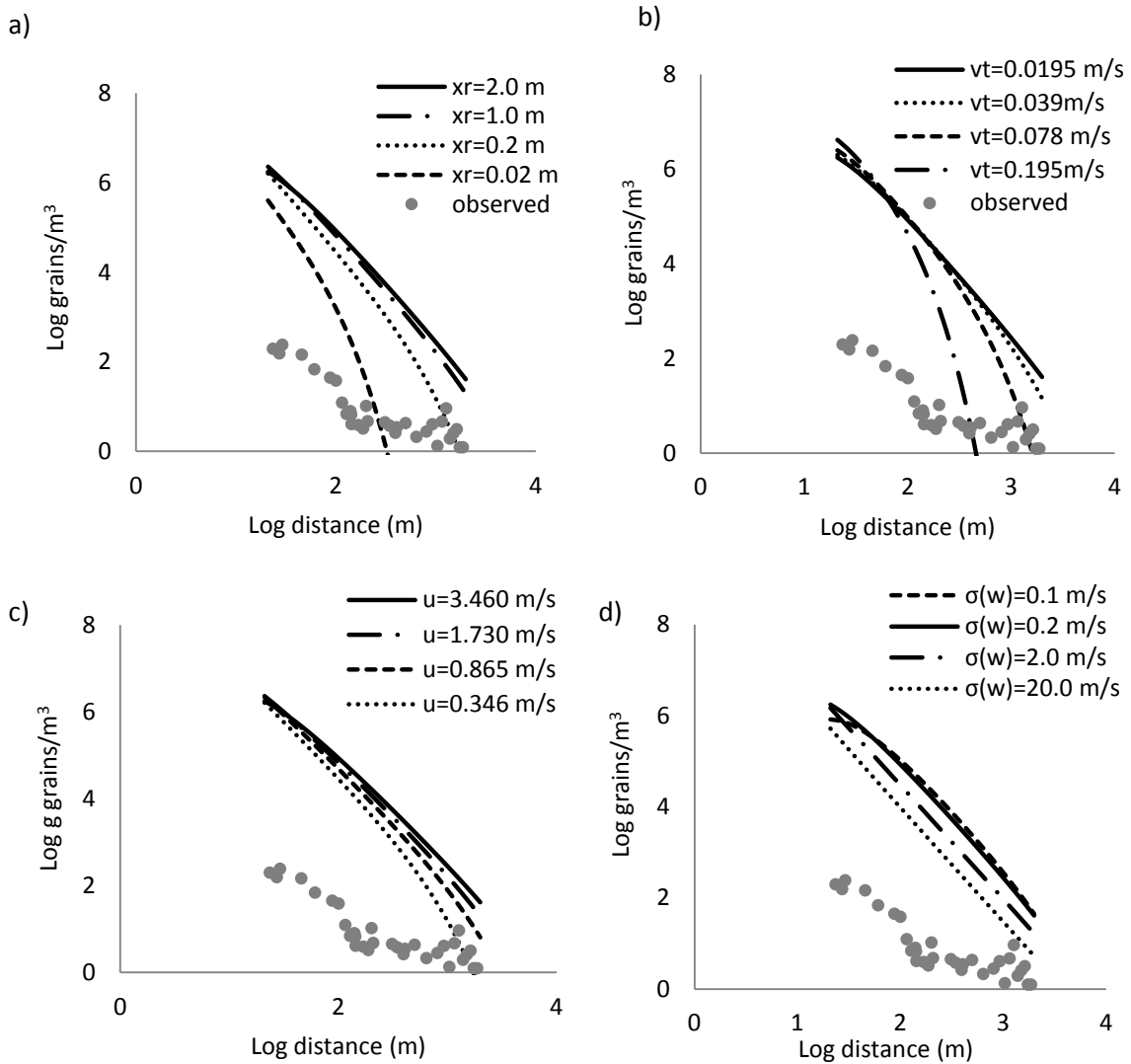


Figure 4.23: Observed *L. clavatum* pollen concentrations from 0 to 2 km (●), and pollen concentrations as predicted by the WALD model. Predicted curves reflect the sensitivity analysis performed by modifying a) release height b) terminal velocity c) horizontal wind velocity d) variance in vertical wind velocity (turbulence). Solid line indicates average measured value (as used in Figure 4.21).

The A-D model was most sensitive to modifications in terminal velocity. Changes in x_r or \bar{u} , even by unrealistic amounts, barely affected the curve (Figure 4.24a,c).

Increasing terminal velocity by 10 times the measured amount ($v_t = 0.195\text{m/s}$) increased

R^2 to 0.68 and fit some far tail points. However, like the WALD model, none of the parameter variations were able to improve the slope or intercept of a predicted versus observed regression, and parameter variations were unable to reduce the extreme over-prediction seen for *L. clavatum*.

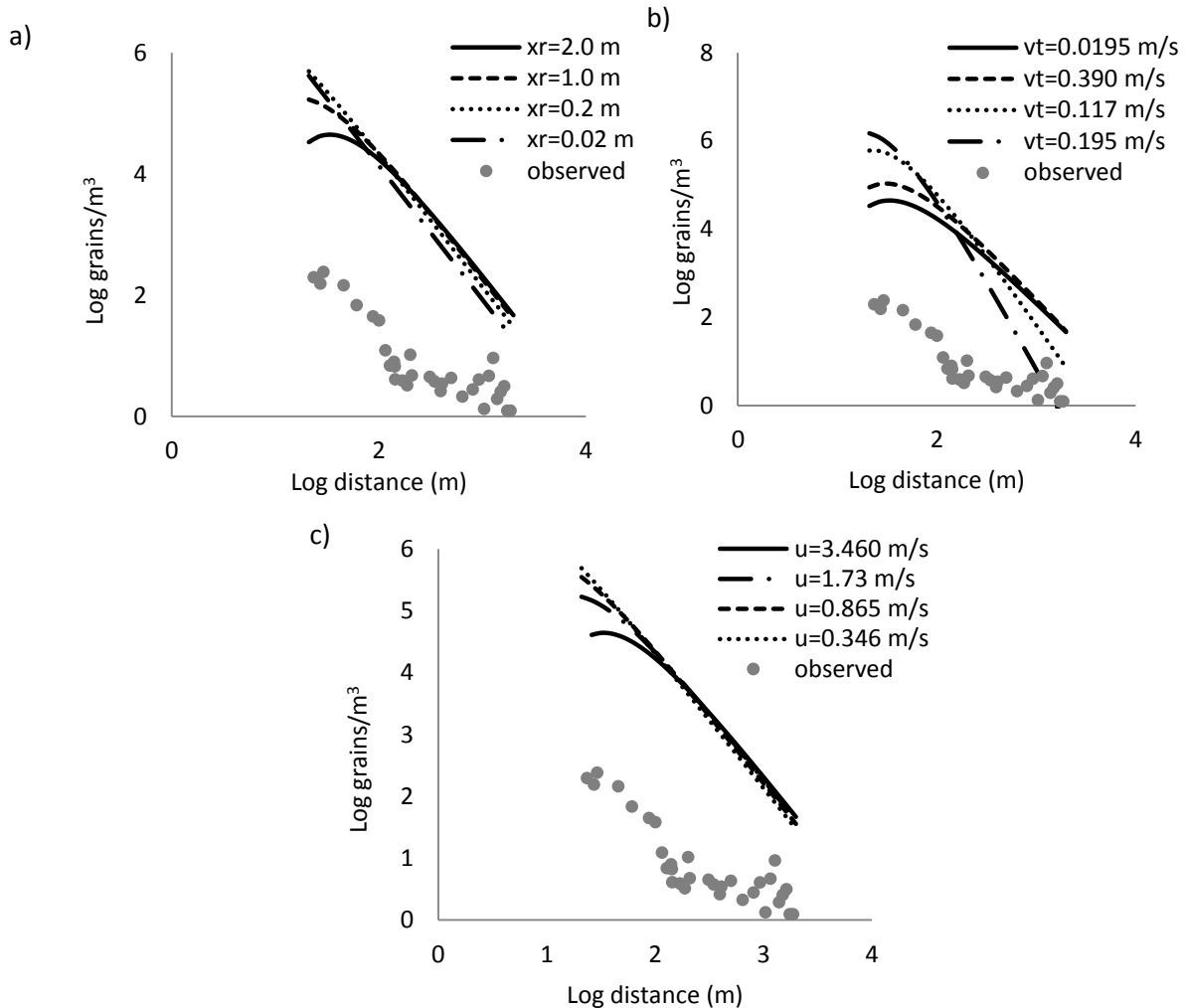


Figure 4.24: Observed *L. clavatum* pollen concentrations from 0 to 2 km (●), and pollen concentrations as predicted by the Advection-Diffusion model. Predicted curves reflect the sensitivity analysis performed by modifying a) release height b) terminal velocity c) horizontal wind velocity d) variance in vertical wind velocity (turbulence). Solid line indicates average measured value (as used in Figure 4.21).

The tilted Gaussian model was again more sensitive than the previous models to small changes in release height or terminal velocity. Like the WALD and A-D models,

horizontal wind velocity did not affect the curve at this shorter dispersal distance (>2 km). Reducing x_r by half improved R^2 , but the predicted curve still greatly over-predicted at all distances. Reducing x_r by 10 times or increasing v_t between 4 and 10 times the observed value, fit some of the far tail data points but did not improve the slope or intercept of the regression; and the drastic over-prediction remained (Figure 4.25 a,b).

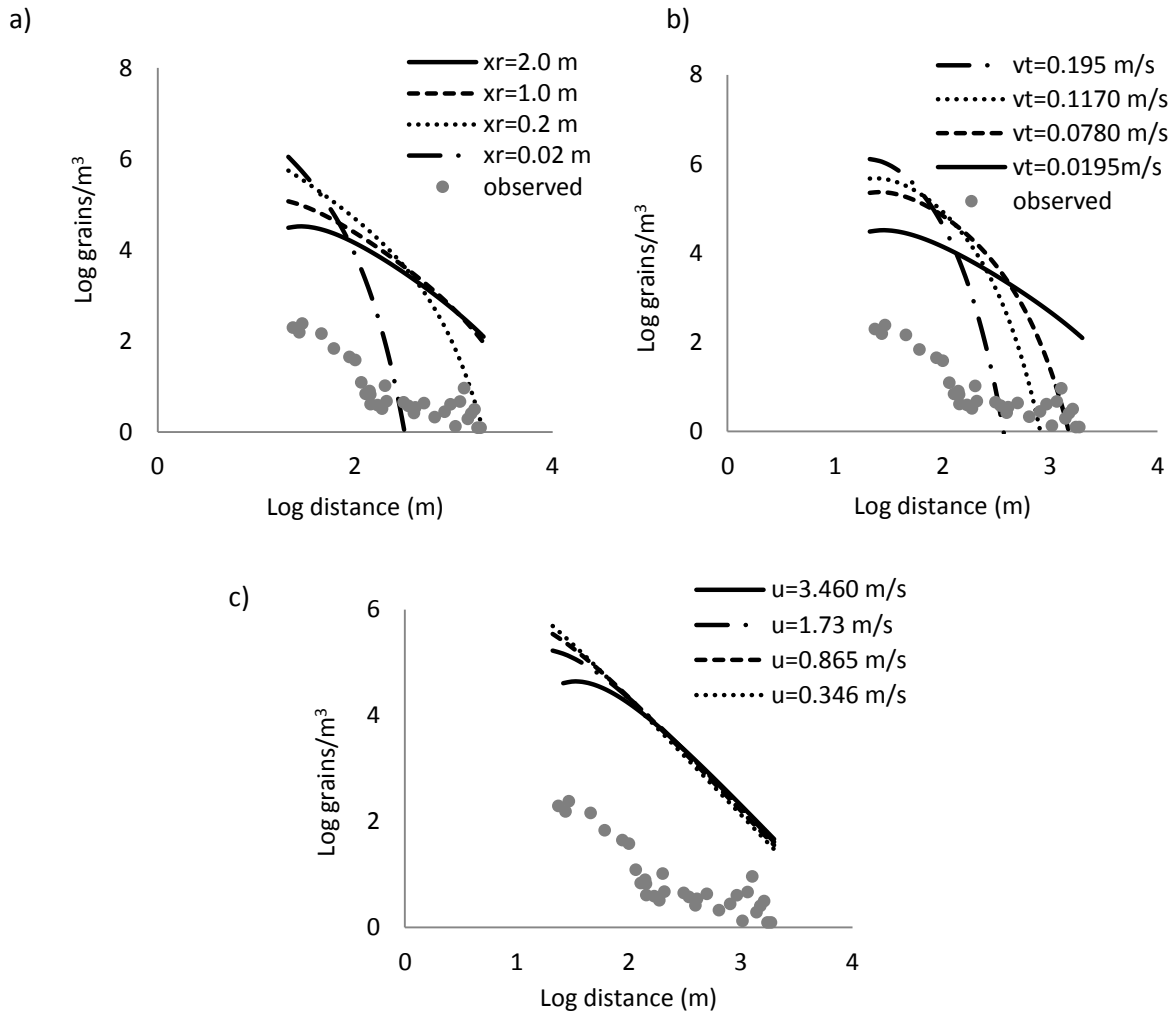


Figure 4.25: Observed *L. clavatum* pollen concentrations from 0 to 2 km (●), and pollen concentrations as predicted by the tilted Gaussian plume model. Predicted curves reflect the sensitivity analysis performed by modifying a) release height b) terminal velocity c) horizontal wind velocity d) variance in vertical wind velocity (turbulence). Solid line indicates average measured value (as used in Figure 4.21).

5 Discussion

5.1 General

This is the first dataset to measure airborne concentrations of biological particles out to very long distances (≤ 10 km). Greene and Calogeropoulos (2002) argued that it would be very costly to measure dispersal of pollen or seeds at great distances but we have demonstrated here that it is possible to do using a lake free of islands. (As is discussed below, however, using a lake generates some problems in parameterization of models).

5.2 Model Performance – Area Source

Empirically, all four species showed a sharp (semi-logarithmic) decline in concentration with distance from the forest edge out to about 2 km. At greater distances (> 2 km), the dispersal curve was quite flat. We refer to these as the near and far tail, or short-distance and long-distance dispersal, respectively. None of the models could simultaneously fit both the near and far tails. Indeed, with the exception of the heavier grains of *A. balsamea*, the A-D and tilted Gaussian models over-predicted the distance travelled by the pollen in the far tail, while the WALD model consistently under-predicted the far tail.

5.2.1 The WALD Model

The fit of the WALD model was, generally, poor at large distances but was adequate at distances less than 2 km. WALD under-predicted all observed data for every species except perhaps for *P. banksiana*, where the under-prediction was quite modest.

The sensitivity analysis showed that the WALD model was especially responsive to the magnitude of the release height and horizontal wind velocity. Terminal velocity, even when modified by a much larger proportional amount, was unable to lessen the under-prediction of the far tail, and only had a slight affect on the predicted dispersal curve. However, modifying the model parameters to better fit the near source data always resulted in an over-prediction at the far-tail, and trying to fit the far tail resulted in an under-prediction of the near source observed data.

The WALD model is the only one of the three models that formally incorporates turbulence and a three-dimensional wind profile, which are argued to be important determinants of long distance dispersal (Bullock & Clark, 2000; Nathan et al. 2002a, 2000b; Levin et al. 2003). The measured variation in vertical wind velocity can be input into the model and is assumed to increase with mean wind speed, whereas the other models in this study instead use a mean diffusivity constant determined from fluid dynamics. I.e., the other two models have both vertical and horizontal turbulence values included as a simple function of the magnitude of the horizontal wind speed. Changing σ_w within the WALD model did effectively alter the far tail of the dispersal curve without affecting the near tail (Figure 4.3d, 4.8d, 4.13d), but not significantly enough to counter the extreme under-prediction seen for three of four species at far distances.

5.2.2 The Advection-Diffusion Model

The A-D model over-predicted the observed data for *P. banksiana* and *P. mariana* but not for *A. balsamea*, and *A. rugosa*. It generally had a higher R^2 than the other two models. The most sensitive parameter for the A-D model was terminal velocity, as

changing the other parameters by similar proportions did not influence the predicted dispersal curve as much as modifying v_t . For all species except *A. balsamea*, using the field measured parameters resulted in the best fit. The model especially fit well the data for the shorter-dispersed pollen of *A. rugosa*. I.e., like WALD, this model is better suited to short-distance dispersal. *A. balsamea* was the only species where the A-D model under-predicted, but it was the least poor of the three model fits for these heavier pollen grains (Figure 4.6), most likely due to a higher sensitivity to changes in terminal velocity. As with the WALD model, fitting the far tail caused the predicted curve to under-predict at the near tail, and vice-versa.

As mentioned, there is also no formal mechanism within the model to account for variation in vertical or horizontal turbulence; instead, the model uses a value that is a simple function of the mean horizontal wind speed. Of course, vertical turbulence is indeed a positive function of horizontal wind speed because of the shearing effect of the wind.

5.2.3 The Tilted Gaussian Plume Model

The tilted Gaussian Plume model had a slight tendency to over-predict the majority of the measured data, and was unable to capture the flattening seen at far distances. The model was equally sensitive to changes in either v_t , x_r or \bar{u} , and was more sensitive to slight modifications of these three parameters than the previous two models. With the exception of *A. balsamea* (which all of the models fit poorly), using the field measured parameters for all species within the model yielded the best overall fit. In that sense, its performance was similar to that of the A-D model. Increasing or decreasing the

model parameters sometimes led to improvements in the fit of the near-source data but in those cases left the far tail of the dispersal curve poorly predicted, and vice versa.

5.3 Problems with Parameterizing Models for an Area Source

Ideally one would use the observed dispersal from a point source to test a dispersal model but it is essentially impossible to find a single tree so isolated from other conspecifics that the recoded pollen is deemed to be, unambiguously, from that source. Further, there would be the problem of insufficient recorded pollen at distances as great as 10 km from the single plant. Here, I discuss problems associated with using an area source, as well as more specific problems associated with an area source abutting a large lake.

The three point source models evaluated herein assume that the parameters are constant in time and space. The assumption of spatial homogeneity (at height, z) is especially problematic as the step change from forest to lake leads to a large increase in wind speed with distance out to an asymptote around 20 forest heights to the lee of the forest (Greene and Johnson, 1996). This would be approximately 300 m leeward from the beach. The same problem would obtain with any sharp change in the height of the vegetation (e.g. forest to clearing or shrubland to grassland). The three models studied here use mean wind speed values and do not allow for a change in wind speed across a varying terrain. Although there can be a mean horizontal speed at height z averaged across space, the models are not designed to deal with this change in wind regime at a scale of several kilometres. More specifically, in the far tail the grains experienced a higher mean wind speed than the parameter value we used, while in the near tail the

opposite is true. If pollen measurements were made deep inside the forest, pollen concentrations would certainly be under-predicted there, as our unduly high (for the forest) mean horizontal wind speed predicts grains should go farther than the real wind is permitting. On the other hand, there should be an over-prediction in deposition for the area where pollen concentrations were measured (lake edge to as much as 10 km distance over the lake), as fewer grains will have made it to the lake than expected. Then again, because the expected concentration was “pegged” to the actual observed concentration at the lake edge, this means that the over-prediction of deposition should only be seen at the very largest distances. Indeed, generally, two of the models—the A-D and tilted plume—consistently over-predicted at great distances from the lake edge.

Nonetheless, one cannot examine seed or pollen dispersal at large distances if there is not a dramatic step change, because it would be impossible to be sure where the sources were located. I.e. the change in landscape is an indication of a change in vegetation type, and thus there is spatial segregation of the sources for the species of interest. As in the Sharma & Khanduri (2007) study, one might examine pollen dispersal of conspecific trees from an area of continuous forest but one will not know whether the deposited pollen came from trees far away or from nearby. The only way to use homogenous terrain to study the far tail would be by relying on molecular markers for seeds (or the paternal contribution to a seed when one is focused upon pollen), but as pointed out by Greene and Calogeropoulos (2003), that is prohibitively expensive as one must sample tissue from all the potential parents at a spatial scale of many squared kilometres.

Terminal velocity could also be another parameter that may vary with the different conditions the pollen grains are exposed to during dispersal, although this is an idea that has not been well-explored experimentally. One study by Katifori et al. (2010) investigated the effect of dehydration on pollen grains and the ability of the pollen wall to alter its shape to prevent desiccation (and therefore death) while in transit. The grains then rehydrate when exposed to the humid environment near the stigma of a female flowers or micropyle of a female strobilus. This mechanism could, similarly, operate in the much more humid conditions above the lake surface than above or within the forest. The cellulosic intine of the pollen wall is water permeable, and so the environment above the lake could in theory cause the grain to take on extra water, causing an increase in terminal velocity. This hypothesis could also explain the over-prediction in the A-D and tilted Gaussian models, both shown in our analyses to be more sensitive to changes terminal velocity than the WALD model.

One of the biggest challenges in any study of pollen or seed dispersal is definitely knowing the source distance. However, using a large island-less lake poses a number of challenges in itself. Foremost, is the changing wind profile from forest edge to the centre of the lake, as described above. There are also several logistical issues as well, such as keeping the pollen-collection devices (Rotorods) afloat and operational in such a turbulent and unpredictable environment. This resulted in a higher abundance of near source data (0-2km), which was less difficult to obtain. This in turn posed analysis difficulties, especially when trying to measure goodness-of-fit of the observed versus predicted data, as there are many more dispersal points for less than 2 km, than beyond 2 km. Having more Rotorods at further distances and at closer intervals would have been

ideal to get a better idea of the entire dispersal curve out to 10 kilometres, but proved to be impossible on a large lake setting.

An alternative method for dealing with a step change and variability within parameters would be to switch from a closed-form model such as entertained here to a Lagrangian approach. Now, each pollen grain's trajectory can be simulated from source to deposition site in a three-dimensional space. Spatial (or temporal) changes in parameter values (e.g. wind speed or terminal velocity) would be easily incorporated.

5.4 Model Performance - Point Source

For the point-source experiment, the situation all the models tested were initially designed for, all three greatly over-predicted the measured data. Further, none of the three models exhibited slopes that conformed to the observed deposition.

Although Q for the *Lycopodium* experiment was known, as the number of spores released was calculated based on the spore size, density and weight, this may not be an accurate estimate of how many spores were available to be caught by the transects of Rotorods. Even though sampling was done only when the wind direction was relatively constant, there was a significant amount of lateral dispersion of spores after release, due to the inevitable deviation in the wind direction. We assume however that because we reduced the expected concentration accordingly, this should not be the explanation for the over-prediction

A more likely explanation for the over-prediction may lie in the estimate of the number of grains in the *L.clavatum* powder released for the point-source experiment. It was discovered that, along with the spores, the entire plant was also ground into the *L.*

clavatum powder used in this experiment. Therefore, the mass of powder released does not reflect the actual amount of spore thought to be released. We could only rely on an estimate (40%) of how many spores were contained in the powder released. (We suspect that the percentage of spores is actually much less than 40%; we await a new sample from the same company so that we can make a good estimate.)

Another discrepancy between the point source model predictions and the observed data is in the location of the peak pollen concentration. The three models studied here (and many other models) predict that the modal concentration would be some distance away from a point source due to the release height being well above the ground (Okubo & Levin, 1989; Di Giovanni & Kevan, 1991; Katul et al. 2005). For my study, the spores were released from a relatively low release height (2 metres above ground level) and so the peak concentration was not displaced from the release point. As can be seen in Figure 4.21, the predicted spore concentration was zero at $x=0$ m and the peak concentration is predicted to be between 20 – 30 m from the source, with a steady decline from that point forward. By contrast, the measured data peaks at the release point itself, and spore concentration steadily declined with distance to approximately 400 m and then a flattening is seen from this point out to 2 km.

5.5 Clumping

It has been observed that a large fraction of air-borne pollen grains often start as clusters shortly after abscission (Kuparinen et al. 2008, Di-Giovanni et al. 1995, Martin et al. 2009). Subsequently, they appear to disaggregate while in flight (perhaps because of drying), although this remains poorly studied. This could be an explanation for the

tendency of the A-D and tilted Gaussian models to over-predict, as these models were most sensitive to changes in v_t . The models assume each pollen grain is abscised as an individual particle and remains so from dispersal to deposition; thus it has a low terminal velocity. If instead, the pollen grains are clumped together over short distances before disaggregating, terminal velocity will be grains greatly increased. These clumped grains would fall faster than the model's prediction for a single grain. Thus, there would simply be fewer grains available at large distances and the models would tend to over-predict the fraction of the crop reaching great distances. Making the situation worse is that the disaggregation would cause the terminal velocity of each grain remaining in the clump to continuously decrease with distance until each airborne grain became solitary. Again though, a Lagrangian model could deal with this kind of change. (This explanation is highly speculative: clumping in *Alnus* and the *Pinaceae*, a family including our three conifers, has never been examined.)

5.6 Filtration

Another possible explanation for the over-prediction by some of the models is that there is a certain amount of filtration happening within the source forest, which is not accounted for in any of the models. Based on the Q estimates in section 4.2 the source forest could be filtering out a certain amount of pollen for each species. Despite this important aspect of dispersal, there is very little empirical data on filtration, and no known studies attempting to quantify the level of filtration within an entire forested area. Most of the limited amount of work on filtration has been with theoretical modelling (Bache, 1979a, 1979b; Slinn, 1982, Chamberlain & Wells, 1967). Only three instances

of empirical data on impaction and filtration were found, and these were at the individual leaf and branch level (Rosinski & Nagamoto, 1965; Langer, 1965; Tauber, 1967). The first two experiments attempted to quantify the number of particles collected on individual leaves in wind tunnel experiments; impaction was found to be nearly equal to re-entrainment, and filtration was deemed negligible (Rosinski & Nagamoto, 1965; Langer 1965). However the leaves were exposed to constant wind speeds over long periods of time with no other obstructing vegetation, conditions which would favour high levels of re-entrainment. Tauber (1967) on the other hand, found that as many as 10^6 pollen grains were accumulated on 20 individual twigs during a 12-day natural pollination period. This suggests that indeed there is a large amount of filtration for an entire forest.

Further, it is now clear that spider webs also trap a large amount of pollen. In a study done by Song et al. (2007), almost 3000 pollen grains were found on just 19 webs. It has been postulated that pollen may even serve as an important dietary component for some spiders who re-ingest their webbing (Peterson et al. 2010). Considering the very high total length of the spider webs present in an entire forest, this would result in a significant amount of pollen being removed from the air by spider webs.

Similar to Tauber (1967), I also observed large amount of vegetation impaction in an unpublished experiment in the Caxiuanã National Forest in Para, Brazil. I attempted to quantify the level of filtration seen in a natural environment by performing a filtration experiment in a tropical forest canopy. Approximately 10^9 pollen-sized particles were released from a 40 meter canopy tower in the humid tropical forest. At 40 meters from the source, 99.97% of the large ($75\mu\text{m}$) simulated pollen grains, and 99.6% of the small

grains (25 μm) released had been filtered out by the canopy (MacInnis & Straka, unpublished data). In that study, small and large particles experienced different levels of filtration and had to be analysed differently. The number of small grains remaining at each measured distance was at least an order of magnitude above that of large grains, and two orders of magnitude at the ground level. Past the 20 meter level the large particles exhibited a steeper decline than that of the smaller particles. It is apparent that the increase in foliage density had less of an effect on small grains, which showed a very little decline after 20 meters. Larger particles were filtered out more extensively because of larger impaction probability and their lesser ability to follow airflows around obstacles. This could be an explanation for the low apparent Q value (as pegged at the lake margin) for the larger grains of *A. balsamea* in the area-source experiment. Although *A. rugosa* showed a similar Q , even though its grains are smaller, its release height was also much smaller. *P. mariana* and *P. banksiana* both of approximately the same height as *A. balsamea* have inherently smaller grains and presumably much lower amounts of filtration. However, with the exception of this unpublished study, there is no appropriate field data available for 0.1-1 μm particles depositing on vegetation. Available data for total mass deposited are too coarse to provide estimates of the particle-size dependence of deposition velocity (Slinn, 1982).

The only one of the complication factors we have broached that might be incorporated in a closed-form model is filtration. One might develop a joint probability using the models and a constant rate of filtration with distance in the forest. Once this component is added into the models, it can be tested against the data collected here to

obtain a reliable estimate of how much filtration may be happening throughout a large forest area. Again, however, a Lagrangian approach could easily include filtration.

5.7 Long-distance vs. short distance dispersal

All our results indicate that modelling techniques have to be changed when trying to model dispersal over near and far distances, as the mechanisms involved between short and long distance dispersal are quite different. Turbulence is highly relevant for light particles dispersing over long distances, but may be less so for heavier particles. Our results with the tilted Gaussian and Advection-Diffusion model showed that the horizontal wind speed, terminal velocity, and release height are the key determinants of short-distance dispersal; and there is no need to increase model complexity if the goal is to predict near-source dispersal (Soons et al. 2004). Although this may be true, the ability of these models to be trusted for predictions of LDD is questionable. As mentioned above, they do not allow for the temporal variation of the horizontal wind speed (or perhaps terminal velocity) or a complex turbulence structure. As argued by Soons et al. (2004), more complex models (such as WALD) tend to predict short-distance dispersal more accurately, and, it was hoped, could be relied upon for accurate prediction of long-distance dispersal (Kuparinen et al. 2008; Soons et al. 2004). But as we saw, none of these models could be made to fit the long distance part of the curve without sacrificing their ability to accurately express the short distance dispersal.

It is becoming more apparent that a trustworthy, closed-form model of pollen (and seed) dispersal is not possible and any useful subsequent modelling attempt ought to be Lagrangian; i.e. following the individual movements of pollen grains in order to incorporate the timescales on which vertical eddies and turbulence occurs and the

extremely different wind conditions over varying terrain. Further, this approach could accommodate step changes in vegetation height (essentially a field measurement necessity) as well as changes in terminal velocity due to hydration or drying of pollen grains or disaggregation of initial clumps, and filtration.

6 Conclusion

As previously theorized by Higgins and Cain, 2002; Soons et al. 2004 and Kuperinen et al. 2008, and as seen in the observed data and the predictive ability (or lack thereof) of the models studied here, it is clear that there are two different mechanisms underlying short- and long-distance dispersal. All three closed-form models claim they can accurately account for these underlying processes, but we conclude that only Lagrangian modelling techniques can provide realistic prediction of particle dispersal. This latter approach can account for the high degree of stochasticity and variability in air currents and the rapid timescales on which changes are experienced by individual airborne particles.

The data I collected is unique in that it is certain that the pollen grains collected came from at least as far away as the shoreline. Initially it was thought that the problem in this discipline was primarily the dearth of empirical data rather than useful models, but we now think that these closed-form solutions must be regarded as failures. This is an unhappy conclusion as prediction of the rapid migration required of plant species by global warming means that we must have trustworthy models of long distance dispersal by seeds and pollen. It is hoped that the data collected in this study will be used to test new models, especially Lagrangian approaches, in addition, what was learned here proves that collecting truly LDD data is possible.

References

- Ackerman, J. D. (2000) Abiotic pollen and pollination: Ecological, functional, and evolutionary perspectives. *Plant Systematics and Evolution*, 222(1), 167-185.
- Andersen, M. (1991) Mechanistic models for the seed shadows of wind-dispersed plants. *American Naturalist*, 137(4), 476-497.
- Arritt, R. W., Clark, C. A., Goggi, A. S., Lopez Sanchez, H., Westgate, M. E., & Riese, J. M. (2007) Lagrangian numerical simulations of canopy air flow effects on maize pollen dispersal. *Field Crops Research*, 102(2), 151-162.
- Ashburner, G.R., Faure, M.G., James, E.A., Thompson, W.K. & Halloran, G.M. (2001) Pollination and breeding system of a population of tall coconut palms *Cocos nucifera* L. (Arecaceae) on the Gazelle Peninsula of Papua New Guinea. *Pacific Conservation Biology*, 6, 344-351.
- Ashman, T., Knight, T. M., Steets, J. A., Amarasekare, P., Burd, M., Campbell, D. R., (2004) Pollen Limitation of plant reproduction: Ecological and evolutionary causes and consequences. *Ecology*, 85(9), 2408-2421.
- Aylor, D. E. (1987) Deposition gradients of urediniospores of *Puccinia recondite* near a source. *Phytopathology*, 77, 1442-1448.
- Aylor, D.E., (1989) Aerial spore dispersal close to a focus of disease. *Agricultural and Forest Meteorology*, 47, 109
- Aylor, D.E., Flesh, T.K. (2001) Estimating spore release rates using a Lagrangian stochastic simulation model. *Journal of Applied Meteorology*, 40 (1), 196-1208.
- Aylor, D. E., Schultes, N. P., & Shields, E. J. (2003) An aerobiological framework for assessing cross-pollination in maize. *Agricultural and Forest Meteorology*, 119(3-4), 111-129.
- Bache, D. H. (1979a) Particle transport within plant canopies — I. A framework for analysis. *Atmospheric Environment*, 13, 1257-1262.
- Bache, D. H. (1979b) Particle transport within plant canopies — II. Prediction of deposition velocities. *Atmospheric Environment*, 13, 1681-1687.
- Banks, L., Di Giovanni, F. (1994) A wind tunnel comparison of the rotorod and samplair pollen samplers. *Aerobiologia*, 10(2), 141-145.
- Bateman, A.J. (1947) Contamination of seed crops. II. Wind Pollination. *Heredity*, 1, 235-246.

- Boehm, M.T. and Aylor, D.E. (2005) Lagrangian stochastic modeling of heavy particle transport in the convective boundary layer. *Atmospheric Environment*, 39, 4841–4850.
- Boyer, W. D. (1966) Longleaf pine pollen dispersal. *Forest Science*, 12, 367-368.
- Bullock, J.M., Clarke, R.T., (2000) Long distance dispersal by wind: measuring and modeling the tail of the curve. *Oecologia*, 124(4), 506-521.
- Burd, M., & Allen, T. F. H. (1988) Sexual allocation strategy in wind-pollinated plants. *Evolution*, 42(2), 403-407.
- Cain M.L., Milligan B.G., Strand A.E. (2000) Long-distance seed dispersal in plant populations. *American Journal of Botany*. 87, 1217-27.
- Chamberlain, A.C. (1967) Transport of lycopodium spores and other small particles to rough surfaces. *Proceedings of the Royal Society of London. Series A, Mathematical and Physical Sciences*, 296(1444), 45-70.
- Chamberlain, A.C., Wells, A.C. (1967) Transport of small particles to vertical surfaces. *British Journal of Applied Physics*, 18.
- Dafni, A., Kevan, P.G., Husband, B.C (eds.) (2005) *Practical Pollination Biology*. Enviroquest Ltd. Cambridge, ON, Canada.
- Davis, M. B. (2000) Palynology after Y2K—Understanding the source area of pollen in sediments. *Annual Review of Earth and Planetary Sciences*, 28(1), 1-18.
- Di-Giovanni, F., Beckett, P.M., Flenley, J.R. (1989) Modelling of dispersion and deposition of tree pollen within a forest canopy, *Grana* 28 (2), 129–139.
- Di-Giovanni, F. and Beckett, P.M. (1990) On the mathematical modeling of pollen dispersal and deposition. *Journal of Applied Meteorology*. 29, 1352–1357.
- Di-Giovanni, F., Kevan, P. (1991) Factors affecting pollen dynamics and its importance To pollen contamination: a review. *Canadian Journal of Forest Research*, 21(8), 1155-1170.
- Di-Giovanni, F. , Kevan, P. G., Nasr, M. E. (1995) The variability in settling velocities of some pollen and spores. *Grana*, 34(1): 39-44.
- Di-Giovanni, F., Kevan, P. G., & Arnold, J. (1996) Lower planetary boundary layer profiles of atmospheric conifer pollen above a seed orchard in northern ontario, canada. *Forest Ecology and Management*, 83(1-2), 87-97.

- Faegri, K.; Pijl, L. van der. (1979) *The principles of pollination ecology*. Ed. 3. Oxford, Pergamon Press.
- Farrar, J.L. (1995) *Trees in Canada*. Fitzhenry & Whiteside Limited; Markham, ON: Canadian Forest Service; Ottawa, ON: Natural Resources Canada.
- Frenz, David, A., Lince, Naomi, L. (1997) A comparison of pollen recovery by three models of the Rotorod Sampler. *Annals of Allergy, Asthma & Immunology*, 79, 256-258.
- Friedman J., Barrett S.C. (2009) Winds of change: new insights on the ecology and evolution of pollination and mating in wind-pollinated plants. *Annals of Botany*, 103 (9), 1515-1527.
- Giddings, G.D., Sackville Hamilton, N.R. (1997) The release of genetically modified grasses. Part 2: the influence of wind direction on pollen dispersal. *Theoretical and Applied Genetics* 94: 1007-1014.
- Greene, D. F., & Johnson, E. A. (1989) A model of wind dispersal of winged or plumed seeds. *Ecology*, 70(2), 339-347.
- Greene, D.F. Johnson, E.A.(1995) Long-distance wind dispersal of tree seeds, *Canadian Journal of Botany*, 73(7), 1036-1045.
- Greene, D.F. (1996) Wind dispersal of seeds from a forest into a clearing. *Ecology*, 77(2), 595-609.
- Greene, D. F, Calogeropoulos, C. (2003) Measuring and modeling seed dispersal of terrestrial plants. pp 3-23 in J. M. Bullock, R. E. Kenward, and R. S. Hails, editors. *Dispersal ecology*. Blackwell Press, Oxford, UK.
- Greene, D.F., Quesada, M., and C. Calogeropoulos. (2008) Dispersal of seeds by the tropical sea breeze. *Ecology* 89: 118-125.
- Higgins, S.I., Cain, M.L. (2002) Spatially realistic plant metapopulation models and the colonization-competition trade-off. *Journal of Ecology*. 90, 616-626.
- Hjelmroos, M.(1991) Evidence of long-distance transport of betula pollen', *Grana*, 30(1), 215-228
- Ho, R.H., Owens, J.N. (1973) Microstrobili of lodgepole pine. *Canadian Journal of Forestry Research*, 3, 453-465.

- Hoyle, M., & Cresswell, J. E. (2007) The effect of wind direction on cross-pollination in wind-pollinated GM crops. *Ecological Applications*, 17(4), 1234-1243.
- Jackson, S. T., & Wong, A. (1994) Using forest patchiness to determine pollen source areas of closed-canopy pollen assemblages. *Journal of Ecology*, 82(1), 89-99.
- Jackson, S. T., & Lyford, M. E. (1999) Pollen dispersal models in quaternary plant ecology: Assumptions, parameters, and prescriptions. *Botanical Review*, 65(1), 39-75.
- Jarosz, N., Loubet, B., Durand, B., McCartney, A., Foueillassar, X., Huber, L. (2003) Field measurements of airborne concentration and deposition rate of maize pollen. *Agricultural and Forest Meteorology*, 119, 37-51.
- Jarosz, N., Loubet, B., Huber, L. (2004) Modelling airborne concentration and deposition rate of maize pollen. *Atmospheric Environment* 38(33), 5555-5566.
- Katul, G., P.Wiberg, J. Albertson, and G. Hornberger. (2002) A mixing layer theory for flow resistance in shallow streams. *Water Resources Research*, 38, 1250.
- Katul,G.G., Porporato, A., Nathan, R., Siqueira, M., Soons, M.B., Poggi, D., Horn, H.S., Levin, S.A. (2005) Mechanistic models for long-distance seed dispersal by wind. *The American Naturalist*, 166(3), 368-381.
- Katul,G.G., Williams, C.G., Siqueira, M., Poggi, D., Porporato, A., McCarthy, H., Oren, R. (2006) Dispersal of Transgenic Conifer Pollen. In *Landscapes, Genomics and Transgenic Conifers* (121-146). Springer Netherlands.
- Kevan, P.G. (1993) Wind or insects: pollination of coconut (*Cocos nucifera*) in the Maldiv Islands. *Asian Apiculture* (ed. by L. T. Conner, T. Rinderer, H. A. Sylvester and S. Wongsiri), pp. 398-409. Wicwas Press, Cheshire, Connecticut, USA.
- Kuparinen, A. (2006) Mechanistic models for wind dispersal. *Trends in Plant Science*, 11(6), 296-301.
- Kuparinen, A., Markkanen,T., Riikonen, T., Vesala, T. (2008) Modeling air-mediated dispersal of spores, pollen and seeds in forested areas. *Ecological Modelling*,208, 177-188.
- Koenig, W. D., & Ashley, M. V. (2003) Is pollen limited? The answer is blowin' in the wind. *Trends in Ecology & Evolution*, 18(4), 157-159.
- Langer, G. (1965) Particle deposition on and reentrainment from coniferous trees. Part II: Experiments with individual leaves. *Colloid & Polymer Science* 204(1,2), 111-119.

- Lavigne, C., Godelle, B., Reboud, X., Gouyon, P.H. (1996) A method to determine the mean pollen dispersal of individual plants growing within a large pollen source. *Theoretical and Applied Genetics*, 93(8), 1319-1326.
- Levin, S.A., Muller-Landau, H.C., Nathan, R., Chave, J. (2003) The ecology and evolution of seed dispersal: A theoretical perspective. *Annual Review of Ecology, Evolution and Systematics*, 34, 575-604.
- Loos, C., Seppelt, R., Meier-Bethke, S.M. Schiemann, J., Richter, O. (2003) Spatially explicit modelling of transgenic maize pollen dispersal and cross-pollination. *Journal of Theoretical Biology*, 225, 241–255.
- Manitoba Conservation. (2001b) Five-year report on the status of forestry: April 1996 – March 2001. *Manitoba Conservation*. Winnipeg. MB.
- Martin, M.D., Chamecki, M., Brush, G.S., Meneveau, C., Parlange, M.B. (2009) Pollen clumping and wind dispersal in an invasive angiosperm. *American Journal of Botany*, 96(9), 1703-1711
- McCartney, H. A., & Lacey, M. E. (1991) Wind dispersal of pollen from crops of oilseed rape (*Brassica napus* L.). *Journal of Aerosol Science*, 22(4), 467-477.
- Mckibbin, R. (2006) Modelling pollen distribution by wind through a forest canopy. *JSME International Journal. Series B. Fluids and Thermal Engineering*, 49(3). 583-589.
- Michael D. Martin, M.D., Chamecki, M., Brush, G.,S., Meneveau, C., Parlange, M.B. (2009) Pollen clumping and wind dispersal in an invasive angiosperm. *American Journal of Botany* 96(9), 1703-1711.
- Meléndez-Ramírez, V., Parra-Tabla, V., Kevan, P.G., Ramírez-Morillo, I., Harries, H., Fernández-Barrera, M., Zizumbo-Villareal, D. (2004) Mixed mating strategies and pollination by insects and wind in coconut palm (*Cocos nucifera* L. (Arecaceae)): importance in production and selection. *Agricultural and Forest Entomology* 6, 155–163.
- Messeguer, J. (2003) Gene flow assessment in transgenic plants. *Plant Cell, Tissue and Organ Culture*, 73:201–212.
- Moen, J., K. Aune, L. Edenius, and A. Angerbjörn. (2004) Potential effects of climate change on treeline position in the Swedish mountains. *Ecology and Society* 9(1), 16.
- Nathan, R., Safriel, U.N., Noy-Meir, I. (2001) Validation and sensitivity analysis of a mechanistic model for tree seed dispersal by wind. *Ecological Society of America*, 82(2), 374-388.

- Nathan R., Horn H.S, Chave, J., Levin, S.A. (2002a) Mechanistic models for tree seed dispersal by wind in dense forests and open landscapes. *In Seed Dispersal and Frugivory: Ecology, Evolution and Conservation*; Levey, D.J., Silva, W.R., Galetti, M. CABI Publishing, 69-83.
- Nathan, R., Katul, G.G., Horn, H.S., Thomas, S.M., Oren, R., Avissar, R., Pacala, S.W., Levin, S.A. (2002b) Mechanisms of long-distance dispersal of seeds by wind. *Nature*, 418, 409-413.
- Nathan R., Perry, G., Cronin, J.T., Strand A.E., Cain M.L. (2003) Methods for estimating long-distance dispersal. *Oikos*. 103(2), 261-273.
- Nathan, R., Sapir, N., Trakhtenbrot, A., Katul, G. G., Bohrer, G., Otte, M., Avissar, R., Soons, M. B., Horn, H. S., Wikelski, M. and Levin, S. A. (2005) Long-distance biological transport processes through the air: can nature's complexity be unfolded *in silico*? *Diversity and Distributions*, 11, 131–137.
- Niklas, Karl J. (1985) The aerodynamics of wind pollination. *The Botanical Review* 51(3), 328-386
- Okubo, A., & Levin, S. A. (1989) A theoretical framework for data analysis of wind dispersal of seeds and pollen. *Ecology*, 70(2), 329-338.
- Owens, J. N., Takaso, T., & Runions, C. J. (1998) Pollination in conifers. *Trends in Plant Science*, 3(12), 479-485.
- Peterson, J.A., Romero, S.A., Harwood, J.D. (2010) Pollen interception by linyphiid spiders in a corn agroecosystem; implications for dietary diversification and risk-assessment. *Arthropod-Plant Interactions*, 4(4), 207-217.
- Portnoy, S., Willson, M.F. (1993) Seed dispersal curves: behavior of the tail of the distribution. *Evolutionary Ecology*, 7, 25-44.
- Proctor, M.C.F. Yeo, P. Lack, A. (1996) *The natural history of pollination*. Timber Press. London. 479 pp.
- Raynor, G.S., Hayes, J.V., Ogden, E.C. (1970) Dispersion and deposition of ragweed pollen from experimental sources. *Journal of Applied Meteorology*, 9, 885-895.
- Raynor, G.S., Hayes, J.V., Ogden, E.C. (1975) Particulate dispersion from sources within a forest. *Boundary-Layer Meteorology*, 9, 257-277.
- Rieger, M. A., Lamond, M., Preston, C., Powles, S. B., & Roush, R. T. (2002) Pollen-mediated movement of herbicide resistance between commercial canola fields. *Science*, 296(5577), 2386-2388.

- Rosinski, J., and C. T. Nagamoto. (1965) Particle deposition on and reentrainment from coniferous trees. *Colloid & Polymer Science* 204(1,2), 111–119.
- Roussey, A-M., Kevan, P.G. (2000) How accessible are receptive megastrobili to pollen? The example of jack pine (*Pinus banksiana*) *American Journal of Botany* 87(2), 215–220.
- Sampling Technologies Inc. (1989) *Operating Instructions for the Rotorod Sampler*. Los Altos Hills, CA.
- Sarvas, R. (1962) Investigation on the flowering and seed crop of *Pinus sylvestris*. *Communicationes Instituti Forestalis Fenniae*. 53.4, 1-198.
- Schuster, W. S. F., & Mitton, J. B. (2000) Paternity and gene dispersal in limber pine (*Pinus flexilis* James). *Heredity*, 84, 348–361.
- Schwendemann, A. B., Wang, G., Mertz, M. L., McWilliams, R. T., Thatcher, S. L., & Osborn, J. M. (2007) Aerodynamics of saccate pollen and its implications for wind pollination. *American Journal of Botany*, 94(8), 1371-1381.
- Sehmel, G. A. and Hodgson, W. H. (1976) Atmosphere-Surface Exchange of Particulate and Gaseous Pollutants, *ERDA Symposium Series* 38.
- Sharma, C.M., Khanduri, V.P. (2007) Pollen-mediated gene flow in Himalayan long needle pine (*Pinus roxburghii* Sargent). *Aerobiologia*, 23, 153-158.
- Silen, R. R. (1962) Pollen dispersal considerations for Douglas-fir. *Journal of Forestry*, 60, 790-795.
- Slinn, W. G. (1982) Predictions for particle deposition to vegetative canopies. *Atmospheric Environment* (1967) 16:1785–1794.
- Song X.-Y., Blackmore S., Bera S., Li C.-S. (2007) Pollen analysis of spider webs from Yunnan, China. *Review of Palaeobotany and Palynology*, 145 (3-4), 325-333.
- Soons, M.B., Heil, G. W., Nathan, R., Katul, G.G. (2004) Determinants of long-distance seed dispersal by wind in grasslands. *Ecology* 85, 3056–3068
- Sreeramula, T., Ramalingam, A. (1961) Experiments on the dispersion of *Lycopodium* and *Podaxis* spores in the air. *Annals of Applied Biology*, 49, 426-436.
- Tackenberg, O. (2003a) Modeling long-distance dispersal of plant diaspores by wind. *Ecological Monographs* 73, 173-189.
- Tackenberg, O., Poschlod, P., Bonn, S. (2003b) Assessment of wind dispersal potential in plant species. *Ecological Monographs*, 73(2), 191-205.

- Tackenberg, O., Poschlod, P., Kahmen, S. (2003c) Dandelion Seed Dispersal: The horizontal wind speed does not matter for Long-distance dispersal – it is updraft! *Plant Biology*, 5(5), 451-454.
- Tauber, H. (1967) Investigations of the mode of pollen transfer in forested areas. *Review of Palaeobotany and Palynology*, 3(1-4), 277-286.
- Timmons, A.M., O'Brien, E.T., Charters, Y.M., Dubbels, S.J., Wilkinson, M.J. (1995) Assessing the risks of wind pollination from fields of genetically modified *Brassica napus ssp. oleifera*. *Euphytica*, 85(1), 417-423
- Tufto J., Engen S., Hindar K. (1997) Stochastic dispersal processes in plant populations. *Theoretical Population Biology*. 52, 16-26.
- Turchin, P. (1998) Quantitative analysis of movement: measuring and modeling population redistribution in animals and plants. Sunderland, MA: Sinauer.
- Vogel, S. (1981) Life in Moving Fluids: The Physical Biology of Flow. Boston, Mass: Willard Grant.
- Weisstein, Eric W. Circular Sector. From *MathWorld-A Wolfram Web Resource*. <http://mathworld.wolfram.com/CircularSector.html>. Accessed 2011.
- Whitehead, D. R. (1969) Wind pollination in the angiosperms: evolutionary and environmental considerations. *Evolution*, 23(1), 28-35.
- Whitehead, D. R. (1983) Wind pollination: some ecological and evolutionary perspectives. In: L. Real, Editor, *Pollination Biology*, Academic Press, 97-108.
- Xie, C. Y., & Knowles, P. (1994) Mating system and effective pollen immigration in a Norway spruce (*Picea abies* (L.) Karst) plantation. *Silvae Genetica*, 43, 48–52.
- Yamartino, R.J. (1984) A comparison of several "single-pass" estimators of the standard deviation of wind direction". *Journal of Climate and Applied Meteorology* 23 (9): 1362–1366.